TECHNISCHE UNIVERSITÄT MÜNCHEN

Lehrstuhl für Phytopathologie

Analysis of the role of potential phytohormone and light-signalling components in photosynthetic organisms

Manti Christiana Schwarzkopf

Vollständiger Abdruck der von der Fakultät Wissenschaftszentrum Weihenstephan für Ernährung, Landnutzung und Umwelt der Technischen Universität München zur Erlangung des akademischen Grades eines

Doktors der Naturwissenschaften

genehmigten Dissertation.

Vorsitzender: Univ.-Prof. R. F. Vogel
Prüfer der Dissertation: 1. Univ.-Prof. R. Hückelhoven
                          2. Univ.-Prof. W. Liebl

Die Dissertation wurde am 23.07.2012 bei der Technischen Universität München eingereicht und durch die Fakultät Wissenschaftszentrum Weihenstephan für Ernährung, Landnutzung und Umwelt am 14.11.2012 angenommen.

Content

Abbreviations

AHK	*Arabidopsis* histidine kinase
AHP	histidine phosphotransfer protein
Asp	aspartate
At, Arabidopsis	*Arabidopsis thaliana*
ATP	adenosine-5'-triphosphateadenosine-5'-triphosphate
Bgh	*Blumeria graminis* f. sp*. hordei*
bp	basepairs
CaMV	cauliflower mosaic virus
CCM	CO_2 concentrating mechanism
c-di-GMP	bis-(3'-5')-cyclic dimeric guanosine monophosphate
cfu	colony forming units
CHASE	cyclase/histidine kinase associated sensory extracellular
Chl	chlorophyll
CKX	cytokinin oxidase
Cyt b_6f	cytochrome b_6f complex
dai	days after inoculation
DBMIB	dibromothymoquinone
DCMU	3-(3',4'-dichlorophenyl)-1,1-dimethylurea
DGC	diguanylate cyclase
DNA	deoxyribunucleic acid
cDNA	complementary DNA
mRNA	messenger RNA
t-DNA	transferred DNA
dNTPs	2' deoxynucleoside 5' triphosphate
ER	endoplasmatic reticulum
f.sp.	forma specialis
GAF	cGMP phosphodiesterase adenylate cyclase/FhlA
G6PDH	glucose-6-phosphate dehydrogenase
GFP	green fluorescing protein
h	hour
k	rate constant *k*
Hik	histidine kinase
HKD	histidine kinase domain

HKRD	histidine kinase-related domain
IPT	isopenthenyltransferase
KO	knockout
LAHG	light-activated heterotrophic growth
MASE	membrane associated sensor
Mb	mega base pairs
NAD^+	nicotinamide adenine dinucleotide (reduced form)
$NADP^+$	nicotinamide adenine dinucleotide phosphate (reduced form)
NDH-1	NADPH type-1 dehydrogenase
OE	overexpression
OD	optical density
OPPP	oxidative pentosephosphate pathway
PAS	Per/Arnt/Sim; period circadian protein/aryl hydrocarbon receptor nuclear translocator protein/single-minded protein
PAM	Pulse Amplitude Modulation
PAR	photosynthetic active radiation
PCC	Pasteur Culture Collection
PDE	phosphodiesterase
Pst	*Pseudomonas syringae* pv. *tomato* DC3000
PS I, PS II	photosystem I, II
PQ	plastoquinone
pv.	pathovar
TCA	tricarboxylic acid cycle
$t_{1/2}$	half-life
ROS	reactive oxygen species
RR	response regulator
RT	room temperature
SA	salicylic acid
SDH	succinate dehydrogenase
V	Volt
WT	wildtype
w/v	weight per volume
v/v	volume per volume

1 Introduction

For all living organisms it is critically important to adapt quickly and efficiently to changes in their physical and chemical environment. In bacteria, adaptational processes can occur at different levels, at the level of individual genes and proteins, via altered gene expression and allosteric regulation of enzyme activity, the whole-cell level via cellular motility and the multicellular level via cell aggregation and biofilm formation (Galperin, 2010). The ability to mediate these adaptive responses is conferred by sophisticated signal transduction systems, the so-called two-component signalling systems, which are found ubiquitously in prokaryotes and archae, fungi, yeast and certain plants and have been shown to regulate physiological and molecular processes at each level of adaptation (Galperin, 2010; Perry *et al.*, 2011). Considerable effort has been made in the past years to elucidate these signal transduction processes and the functions of the associated proteins (Stock *et al.*, 2000; Laub & Goulian, 2007; Schaller *et al.*, 2008; Gao & Stock, 2009; Wuichet *et al.,* 2010; Schaller *et al.*, 2011; Jung *et al.,* 2012). However, a thorough under-standing of these complex signalling networks remains elusive. Considering the involvement of signal transduction systems in essential processes and the concomitant far-ranging effects, it is of great importance to contribute to the under-standing of the underlying molecular mechanisms.

1.1 *Synechocystis* sp. PCC 6803

Cyanobacteria are considered to be among the evolutionarily oldest organisms on earth since the discovery of 3.5 billion year old putative stromatolites and microfossils, attributed to cyanobacteria (Schopf, 1993). With their ability to perform oxygenic photosynthesis, cyanobacteria played a significant role in the history of earth and the evolution of life as primary producers of atmospheric oxygen (Nakao *et al.*, 2010). Even today, these prokaryotic microorganisms contribute substantially to maintain the biosphere, as they are important primary producers at a global scale with a relevant role in the carbon and nitrogen cycles (Herreiro & Flores, 2008). Considering their long evolutionary history, cyanobacteria are among the most successful groups of microorganisms on earth. One of the main reasons for their evolutionary success can be related to their adaptability to a broad range of environmental conditions, resulting in an almost ubiquitous distribution in marine and terrestrial ecosystems, ranging from fresh and salt water to even more extreme

habitats such as thermal springs, alkaline lakes, glaciers and deserts (van den Hoek *et al.,* 1993; Whitton & Potts, 2000; Koksharova, 2009). According to the endo-symbiont theory (Margulis, 1970), chloroplasts in plants and eukaryotic algae have evolved from cyanobacterial ancestors via endosymbiosis (Nakamura *et al.,* 2000). Cyanobacteria and especially the unicellular cyanobacterium *Synechocystis* sp. PCC 6803 (order *Chroococcales*) have become important model organisms for research of photosynthesis, respiration, carbon metabolism and its regulation, as well as in signal transduction processes and stress responses. The ability to perform oxygenic photosynthesis with a complete gene set similar to higher plants (Nakamura *et al.,* 2000) and to grow and survive in a wide range of conditions, made *Synechocystis* sp. PCC 6803 (hereafter *Synechocystis*) one of the most intensely studied cyano-bacteria. The original *Synechocystis* strain was isolated from a fresh-water lake and was deposited in the Pasteur Culture Collection (PCC) in 1968 (Rippka *et al.,* 1979). In the early 1980s, the strain was recognised to be spontaneously transformable by integration of exogenous DNA into its genome via double homologous recombination (Grigorieva & Shestakov, 1982). Their natural transformation competence can be used for analysing functions of unknown genes through gene disruption and insertion mutational analysis (Nakamura *et al.,* 2000).

Synechocystis cells can either live as single planktonic organisms or in sessile communities, the so-called called biofilms or biomats. Biofilms are generally defined as microbial communities adhered to a substratum and embedded in an extracellular polymeric matrix produced by the microbial cells itself (Costerton *et al.,* 1987, 1994). In its natural habitat, *Synechocystis* grows photoautotrophically. Besides photoauto-trophic growth, certain strains of *Synechocystis* are able to utilise organic com-pounds, e.g. glucose as a carbon source concomitant with photosynthetic CO_2 fixation (Rippka *et al.,* 1979; Stal & Moezelaar, 1997; Gomez-Baena *et al.,* 2008). Accordingly, the glucose-tolerant wildtype strain of *Synechocystis* is capable of photoautotrophic and photomixotrophic growth under light conditions and of hetero-trophic growth in darkness in glucose-supplemented media (Williams, 1988; Anderson & McIntosh, 1991). However, light irradiation is still required for hetero-trophic growth, which occurs even with a low light intensity at which photosynthesis can scarcely proceed (Tabei *et al.,* 2009), as *Synechocystis* cells are unable to grow in complete darkness. Occasional light pulses (e.g. for 5 min every 24 h) are sufficient to enable growth and survival of the cells in darkness. This phenomenon is referred to as light-activated heterotrophic growth (LAHG; Anderson & McIntosh, 1991). The ability to carry out heterotrophic growth without loss of viability made

Synechocystis a useful model organism in photosynthesis research by enabling the disruption of photosynthesis-related genes to investigate functions and contributions to the photosynthetic pathway (Nakamura *et al.,* 2000). Its role as model organism became even more important after *Synechocystis* was the first photosynthetic organism to be completely sequenced (Kaneko *et al.,* 1996). The availability of the entire genomic nucleotide sequence provides the possibility to study gene functions and regulatory mechanisms on a genome-wide level. To summarize, *Synechocystis* has become an extremely versatile model organism in research of signal trans-duction processes and stress responses, as well as in carbon metabolism and especially in oxygenic photosynthesis.

1.2 The primary energy metabolism in *Synechocystis*

The primary energy metabolism in cyanobacteria consists of anabolic and catabolic processes, including photosynthesis, CO_2 fixation, glycogen formation, gluconeo-genesis and glucose degradation processes, such as glycolysis, the oxidative pentose phosphate pathway (OPPP) and the incomplete tricarboxylic acid (TCA) cycle, respectively. Cyanobacteria constitute a unique case where the anabolic and catabolic carbohydrate mechanisms function in the same compartment of the cell (Yang *et al.,* 2002; Shastri & Morgan, 2005, 2007; Takahashi *et al.,* 2008; Haimo-vich-Dayan *et al.,* 2011). Accordingly, this requires strict regulation of the direction of reactions in response to environmental conditions (Tabei *et al.*, 2009).

Light is one of the most important environmental factors for photosynthetic organisms. They use light energy to produce chemical energy and reducing power for the fixation of atmospheric carbon and the assimilation of other nutrients. Reduced carbon provides energy, as well as building blocks in metabolic reactions required for growth and development. In their natural habitat, cyanobacteria are exposed to changing light conditions, such as the diurnal light-dark cycle or daily changes in light quality and quantity. In order to maintain their metabolic homeo-stasis, it is of critical importance to adapt to changing light conditions, either by switching between metabolic modes during the light-dark cycle or by using mechanisms to adjust the distribution of light energy for maximal energy utilisation and protection against photodamage. Changing light conditions can cause redox im-balances and an excessive production of damaging reactive oxygen species (ROS), when the perceived light is not fully utilised by downstream processes (Apel & Hirt, 2004; Scheibe *et al*., 2005; Muramatsu & Hihara, 2012). It has been suggested that photosynthetic organisms integrate nutrient-specific pathways by tightly connecting

photosynthetic processes with other principal metabolic pathways to survive under constantly changing environmental and metabolic cues (Wang *et al*., 2003; Forchhammer, 2004; Gutierrez *et al.*, 2007; Singh *et al.,* 2010). Furthermore, the tight connection between the activity of photosynthetic processes and metabolic pathways becomes apparent as photosynthesis represents the sole source to generate chemical energy for photosynthetic organisms under photoautotrophic conditions (Singh *et al.*, 2010). When light is available, cyanobacteria assimilate inorganic carbon via the Calvin cycle, using ATP and NADPH generated through photosynthesis. The fixed carbon enters the glycolytic pathway and is subsequently utilised to generate reducing equivalents, cofactors and building blocks for biosynthetic pathways. Besides, excess carbon can be assimilated in the form of glycogen and stored as reserve carbohydrate. Under non-photosynthetic conditions respiration releases the energy stored in those carbon compounds. Glucose residues, derived from glycogen, are catabolized via the OPPP, the lower energy-conserving phase of glycolysis and the TCA cycle, resulting in the production of NAD(P)H and biosynthetic intermediates required for maintenance and growth (Stal & Moezelaar, 1997; Knowles & Plaxton, 2003; Singh & Sherman, 2005; Tabei *et al.,* 2009). The following two sections will give a detailed overview on the primary metabolism and its concomitant processes, beginning with photosynthesis and respiration, followed by the central carbon metabolism.

1.2.1 Photosynthesis and respiration

In cyanobacteria, both metabolic processes, oxygenic photosynthesis and aerobic respiration, are located in the same compartment (Schmetterer*,* 1994). Unlike in plants, where photosynthesis and respiration are separated in different organelles, cyanobacteria possess, due to the lack of compartmentalization, a highly differentiated membrane system, which harbors the electron transport chains required for photosynthesis and respiration (Vermaas *et al.,* 1994; Mullineaux, 2008b; Nickelsen *et al.,* 2010). This internal membrane system, the thylakoid membrane, which separates the cytoplasm from the lumen, contains a photosynthetic electron transport chain including the two photosystems (PS II and PS I) and a respiratory electron transport chain, including among others, NADPH type-1 dehydrogenase (NDH-1), succinate dehydrogenase (SDH) and a cytochrome aa_3-type terminal oxidase (cytochrome *c* oxidase) (Tanaka *et al.,* 1997; Cooley *et al.,* 2000). In the thylakoid membrane both electron transport chains intersect and share electron carriers, such as the cytochrome b_6f complex, the plastoquinone pool (PQ) and soluble redox active proteins (Schmetterer, 1994; Vermaas, 2001). In contrast,

the cytoplasmatic membrane, which forms the inner boundary of the periplasmatic space, harbors solely components associated with the respiratory electron transport chain. Therefore, in most cyanobacteria, photosynthetic electron transport occurs solely in the thylakoids, while the respiratory electron flow takes place in both, the thylakoid and the cytoplasmatic membrane systems (reviewed by Vermaas, 2001).
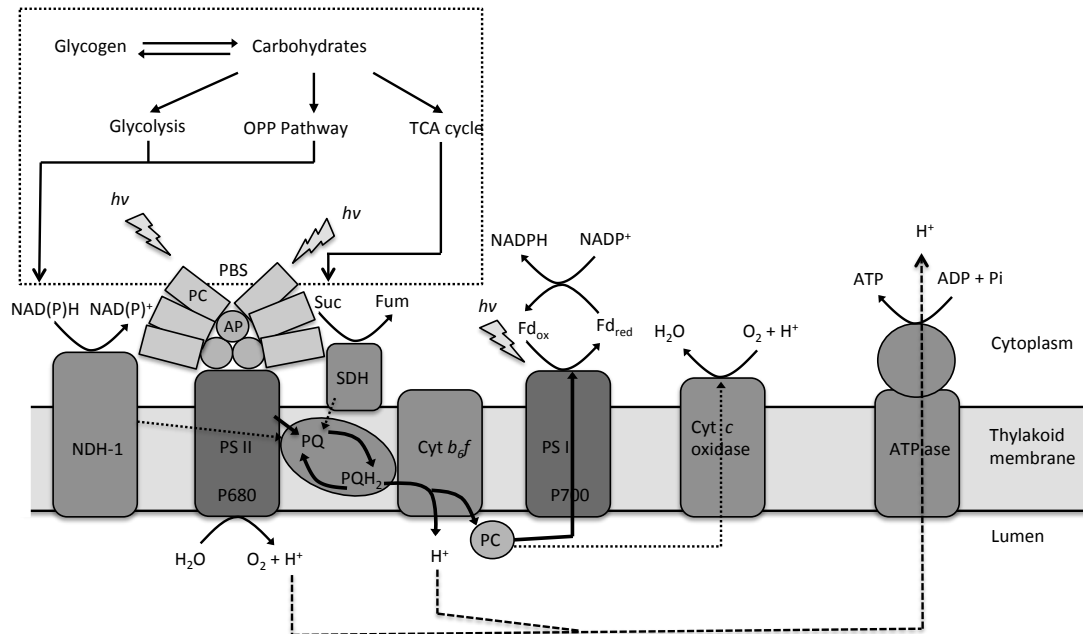
Figure 1: Schematic illustration of the intersecting photosynthetic and respiratory electron transport pathways in the thylakoid membrane of *Synechocystis* sp. PCC 6803 (modified after Campbell *et al.,* 1998; Vermaas, 2001; Singh *et al.,* 2009)

Bolts designate light energy, starting the redox reactions in both photosystems. Arrows indicate photosynthetic and respiratory electron transfer reactions. Linear photosynthetic electron transport: from water to $NADP^+$ via PS II and PS I (thick solid arrows); respiratory electron transport: from NADPH and succinate to cytochrome *c* oxidase (dotted arrows) and cyclic electron transport: around PS I via Fd and/or NDH-1 (not indicated). Dashed arrows indicate protons released into the lumen, thereby establishing a proton gradient (ΔpH) across the thylakoid membrane, which powers ATP synthase.
Abbreviations: NDH-1, type I NADPH dehydrogenase; SDH, succinate dehydrogenase; Suc, succinate; Fum, fumarate; PS I and II; photosystem I and II; P680, P700, reaction center chlorophyll molecules of PS II and I, respectively; PQ/PQH_2, plastoquinone pool; cyt b_6f, cytochrome b_6f complex; PC, plastocyanin; cyt *c* oxidase, cytochrome *aa3*-type cytochrome *c* oxidase; ATPase, ATP synthase complex; ATP, adenosine-5'-triphosphate; NADP(H), nicotinamide-adenine dinucleotide phosphate (reduced form); PBS, phycobilisome; PC, phycocyanin; AP, allophycocyanin; *hv*, photons; Fd_{ox}/Fd_{red}, ferredoxin in oxidized and reduced forms, respectively; OPP Pathway, oxidative pentosephosphate pathway.

Electron input in the transport system in cyanobacterial thylakoid membranes is a complex process due to the existence of converging metabolic pathways, feeding electrons into the system. Under light conditions, there is net input of electrons into the transport system from water-splitting activity of PS II (Campbell *et al.,* 1998). Under light or dark conditions, variable electron fluxes from NAD(P)H, which is oxidized by one or more thylakoid-bound dehydrogenases (Scherer *et al.,* 1982; Mi

et al., 1992, 1995; Herbert *et al.,* 1995; Tanaka *et al.,* 1997; Ogawa & Mi, 2007; Battchikova & Aro, 2007; Battchikova *et al.,* 2011) feed into the electron transport system (Campbell *et al.,* 1998). In this electron transport network, three intersecting pathways have been found dominant in *Synechocystis* thylakoid membranes: linear photosynthetic electron transport from water to $NADP^+$ via PS II and PS I, cyclic electron transport around PS I and respiratory transport from NADPH and succinate to cytochrome *c* oxidase (Cooley & Vermaas, 2001), which will be described in detail in the following section.

Photosynthetic electron transport

Photosynthetic light reactions establish an electron flow in the thylakoid membranes, comprising of linear and cyclic electron transport, leading to the production of NADPH and ATP used for carbon fixation (Iwai *et al.,* 2010). The primary reactions of oxygenic photosynthesis are catalyzed by two large protein complexes, PS II and I, acting in series to drive light-dependent electron transfer reactions (Pakrasi, 1995; Singh *et al.,* 2009). The photosynthetic reaction is initiated by the absorption of light, captured by specialized antennae structures. These antennae transfer the excitation energy to specialized chlorophyll molecules (P680 and P700), the reaction centers in both photosystems, which in turn catalyze light-induced electron transfer across the thylakoid membrane (Pakrasi, 1995). In cyanobacteria, the prevalent antenna pigments for the absorbtion of light energy are chlorophyll (Chl) and bilin (Glazer, 1977; MacColl, 1998; Mullineaux, 2008a). Chls are mainly associated with PS I and absorb light with maximum absorbance wavelengths (λ_{max}) of 435 and 680 nm, while bilins are covalently attached to light-harvesting proteins, the phycobili-proteins, and are mainly associated with PS II (Singh *et al.,* 2009). The specific combination of apoproteins and bilins in a phycobilisome (PBS) determines its light absorption profile. The two main phycobiliproteins in cyanobacterial PBS are the red light-absorbing allophycocyanin (AP) with λ_{max} ~ 650 nm and phycocyanin (PC) with λ_{max} ~ 620 nm (Singh *et al.,* 2009). Structurally, APs form together with their specific linker polypeptides the "core" of a PBS, whereas PCs (sometimes also phycoerythrins and other phycobiliproteins) represent together with their associated linker polypeptides the "rod" elements, radiating out from the core. PBS are mobile light-harvesting complexes that are located peripheral to the thylakoid membrane (Grossman *et al.,* 1993; MacColl, 1998) and transfer energy directly to the PS (Mullineaux, 2008a). After absorption of excitation energy via the light-harvesting complexes, the photochemical reaction starts with the transfer of the excitation energy to the reaction center molecules of the photosystems. During linear electron transport, PS

II catalyzes the light-driven oxidation of water and the reduction of plastoquinone (PQ). In each charge separation event, one electron is extracted from the Mn-containing oxygen-evolving complex. After accumulation of four positive charges, oxygen is evolved and four H^+ are released into the lumen of the thylakoids. The electron is transferred from P680* to plastoquinone (PQ). After two charge separation events, PQ is double reduced, takes up two protons from the cytoplasm and leaves PS II as PQH_2. PQH_2 diffuses through the membrane to the cytochrome b_6f complex, which reduces a soluble electron carrier in the thylakoid. This electron carrier can either be plastocyanin (PC) or cytochrome c_{553} (cyt c_{553}), depending on the species and the availability of copper, as plastocyanin is a copper-containing enzyme (Vermaas, 2001). The two protons of PQH_2 are released into the lumen and two additional protons are pumped across the membrane by the cyt b_6f complex. The reduced PC translocates from the cyt b_6f complex to PS I. Light energy, captured by the antenna system of PS I, is transferred to the reaction center of the complex. When the excitation energy reaches P700, P700* is formed. An electron is ejected and transferred across the membrane to the final acceptor ferredoxin (Fd) at the cytoplasmatic side of the PS I complex. The reduced ferredoxin is subsequently used for NADPH production, which provides the reducing power for the conversion of carbon dioxide to organic molecules via the Calvin cycle. During linear photosynthetic electron transfer, protons are released into the lumen upon water splitting at PS II and plastoquinol oxidation by the cytochrome b_6f complex, thereby establishing a proton gradient (ΔpH) across the thylakoid membrane. This ΔpH is used for ATP generation by powering the membrane-bound ATP-synthase. In addition to the linear electron transport, an alternate pathway, the cyclic electron transport, contributes to the ΔpH. This electron transport is driven solely by PS I (Fork & Herbert, 1993; Bendall & Manasse, 1995; Munekage & Shikanai, 2005; Iwai *et al.,* 2010) and allows the generation of ATP without the accumulation of reducing equivalents (Singh *et al.,* 2009). Cyclic electron transport describes electron flows around PS I, from PS I via ferredoxin (Fd) and/or NAD(P)H (Herbert *et al.,* 1995; Mi *et al.,* 1995) directly back to the intersystem transport chain (Campbell *et al.,* 1998). Two possible electron transport pathways have been proposed for cyclic electron transport, an Fd-dependent pathway and an NDH-1-dependent pathway (reviewed by Shikanai, 2007). In the NDH-1-dependent pathway, NDH-1 mediates NADPH oxidation and PQ pool reduction similar to complex I in mitochondria (Okhawa *et al.,* 2000), while it remains elusive how electrons on Fd are transferred to the PQ pool in the Fd-dependent cyclic electron transport (Iwai *et al.*, 2010). Hence, linear photosynthetic electron transport leads to NADPH and ATP production and to the

generation of a ΔpH across the thylakoid membranes, whereas cyclic electron flow results only in establishing a ΔpH, which is subsequently used for ATP generation (Tsunoyama *et al.,* 2009).

Depending on environmental or physiological conditions, the ratio between ATP and NADPH can be adjusted by fine-tuning the ratio of cyclic and linear electron transport (Tsunoyama *et al.,* 2009). Cyclic/linear electron transport ratio adjustments support a redox poise of the PQ pool, which is essential for maximal light energy utilisation and protection against photodamage or other types of stress (Fork & Herbert, 1993; Bukhov & Carpentier, 2004; Munekage *et al.,* 2004; Joliot & Joliot, 2006; Shikanai, 2007; Rumeau *et al.,* 2007; Iwai *et al.,* 2010). For example, changes in the spectral composition of light can lead to imbalanced excitation of the photosystems, which in turn leads to reduced photosynthetic efficiency and damages of the photosynthetic apparatus (Anderson *et al.,* 1995; Dietzel *et al.,* 2008; Singh *et al.,* 2009; Muramatsu & Hihara, 2012). In order to cope with such imbalances and to ensure efficient photosynthesis, cyanobacteria, algae and plants have developed adaptation mechanisms, that act on different time-scales, the so-called short-term and long-term mechanisms (Manodori & Melis, 1986; Chow *et al.,* 1990; Anderson *et al.,* 1995; Fujita, 1997; Allen, 2003; Dietzel *et al.,* 2008). Within the range of seconds to minutes, a short-term mechanism, known as state transition, controls the distribution of excitation energy transfer between the two photosystems (Bonaventura & Myers, 1969; Murata, 1969). Accordingly, two states, state I and state II, have been defined, in which the photosynthetic apparatus gives an optimal quantum yield of photo-synthesis in light, having a composition favouring its absorption by PS I or PS II, respectively (Wollman, 2001; Allen, 2003). In cells adapted to state I, PBS transfer energy primarily to PS II (Mullineaux, 2008a), resulting in a predominance of the linear electron transport. In cells adapted to state II a significant proportion of PBS transfer energy to PS I instead (van Thor *et al*., 1998; McConnell *et al*., 2002; Mullineaux, 2008a), resulting in a predominance of cyclic electron transport. In contrast to higher plants and green algae, cyanobacteria are in state I upon illumination and in state II in the dark or in very low light due to the respiratory electron flow reducing the PQ pool (Mullineaux & Allen, 1986; Mao *et al*., 2002; Tsunoyama *et al*., 2009). State transitions are triggered by the redox state of the PQ pool or a closely located electron carrier (Mullineaux, 2008a). Hence, they allow the regulation of light-harvesting in response to the photosynthetic electron transport chain (Mullineaux & Allen, 1990; Mullineaux, 2008a). State transitions require PBS diffusion (Joshua & Mullineaux, 2004) and are assumed to be involved in covalent

modification of PBS, thereby changing their binding properties for PS II or PS I (Allen *et al*., 1985). Nevertheless, the signal transduction pathway that connects a change in PQ redox state to a change in the binding properties of PBS remains elusive (Mullineaux, 2008a). During prolonged changes in light quality, cyanobacteria utilise long-term mechanisms that occur within hours and days to circumvent reduced photosynthetic efficiency and to protect cells from photodamage. In contrast to the antenna movement during state transitions, the long-term mechanism requires the adjustment of the photosystem stoichiometry to regulate the balance of electron flow between two reaction centers (Chow *et al.,* 1990; Anderson *et al.,* 1995; Dietzel *et al.,* 2008). Hence, cyanobacteria cope with changing light quality by modulating the composition, structure and functions of the photosynthetic apparatus, thereby ensuring an effective balance of electron transfer rates between the two photo-systems (Singh *et al*., 2009).

Respiratory electron transport

Electron input into the transport system in the cyanobacterial thylakoid membrane either results from photosynthetic activity or from catabolic pathways providing the respiratory substrates in the absence of light. In the respiratory pathway, electrons from NAD(P)H and succinate enter the electron transport chain via NADPH dehydrogenase 1 (NDH-1) (Mi *et al.,* 1992; Ryu *et al.,* 2003) and succinate dehydro-genase (SDH) (Cooley & Vermaas, 2001). Despite many studies of the respiratory electron transport pathways in cyanobacterial thylakoid membranes, controversy still remains about whether SDH, rather than NDH-1, is the major pathway of electron flow into the PQ pool (Mi *et al.,* 1995; Cooley *et al.,* 2000; Ryu *et al.,* 2003). Besides its function as electron acceptor, the PQ pool serves as electron donor for the respiratory oxidases. The respiratory oxidases function as terminal components of the respiratory electron transport chain, where the electrons are finally transferred to molecular oxygen. So far, three terminal oxidases have been identified in *Synechocystis* (Hart *et al.,* 2005), cytochrome *aa3*-type cytochrome *c* oxidase and cytochrome *bd*-type quinol oxidase (Schmetterer, 1994; Howitt & Vermaas, 1998; Berry *et al.,* 2002) used for respiration and a third terminal oxidase, for which its *in vitro* oxidase activity is still in dispute (Howitt & Vermaas, 1998; Pils & Schmetterer, 2001; Berry *et al.,* 2002; Mogi & Miyoshi, 2009). Electrons are either transferred directly to cytochrome *bd*-type oxidase or via plastocyanin/cyt$_{553}$ to a cytochrome *aa3*-type cytochrome *c* oxidase (Schmetterer, 1994; Howitt & Vermaas, 1998; Berry *et al.,* 2002; Mogi & Myoshi, 2009). The latter functions as the main oxidase for the NADPH-driven electron transport in the thylakoid membrane (Berry *et al.,* 2002).

This electron transport establishes a ΔpH across the thylakoid membrane, which is subsequently utilised for ATP generation through ATP-synthase.

1.2.2 Central carbon metabolism

Besides nitrogen, sulphur and phosphorus, reduced carbon is an essential macro-nutrient required for growth and development of all organisms. Photosynthetic organisms produce reduced carbon through photosynthesis by using light energy to generate chemical energy and reducing power for the fixation of atmospheric carbon and the assimilation of other nutrients (Singh *et al*., 2008).
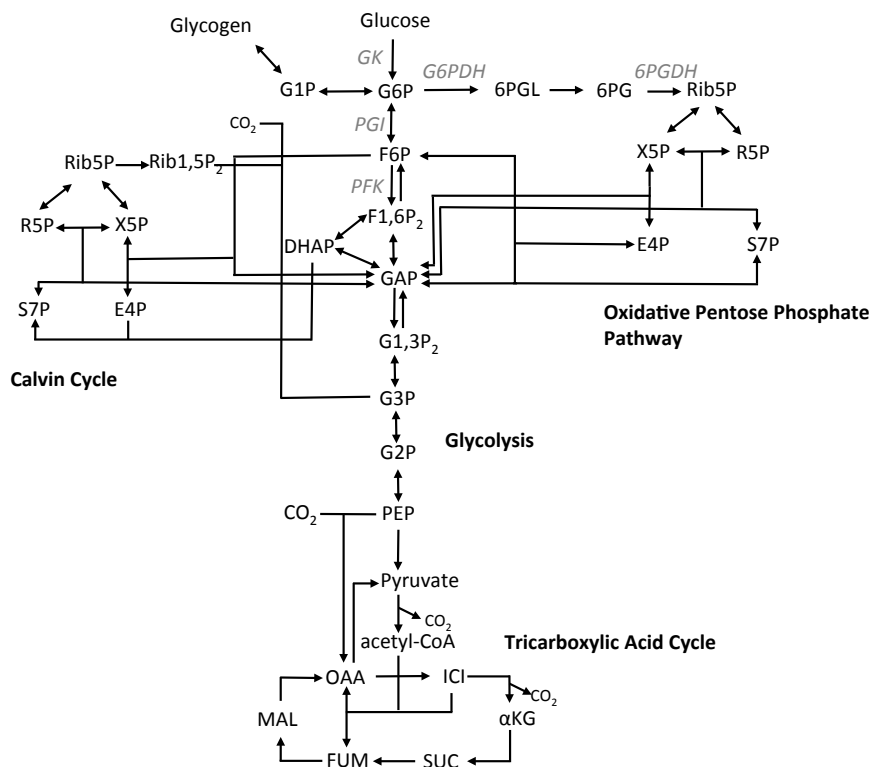
Figure 2: Schematic metabolic map of the central carbon metabolism in *Synechocystis* sp. PCC 6803, including the Calvin cycle, glycolysis, the oxidative pentose phosphate pathway and the (incomplete) tricarboxylic acid cycle (modified after Yang *et al*., 2002).

Abbreviations: G1P, glucose-1-phosphate; G6P, glucose-6-phosphate; 6PGL, 6-phospho-gluconolactone; 6PG, 6-phosphogluconate; Rib5P, ribulose-5-phosphate; R5P, ribose-5-phosphate; S7P, sedoheptulose-7-phosphate; X5P, xylulose-5-phosphate; E4P, erythrose-4-phosphate; Rib1,5P$_2$, ribulose-1,5-bisphosphate; F6P, fructose-6-phosphate; F1,6P$_2$, fructose-1,6-bisphosphate; GAP, glyceraldehyde-3-phosphate; DHAP, dihydroxyacetone-phosphate; G1,3P$_2$, 1,3-bisphosphoglycerate; G3P, 3-phosphoglycerate; G2P, 2-phospho-glycerate; PEP, phosphoenolpyruvate; acetyl-CoA, acetyl coenzyme A; ICI, isocitrate; αKG, α-ketoglutarate; SUC, succinate; FUM, fumarate; MAL, malate, OAA, oxalacetate; Enzymes (italic, grey font): G6PDH, glucose-6-phosphate dehydrogenase; 6PGDH, 6-phospho-gluconate dehydrogenase; GK, glucokinase; PGI, phosphoglucose isomerase; PFK, phosphofructokinase.

In the absence of light, they must switch to heterotrophic energy generation, which includes the degradation of stored carbon compounds via the OPPP, the lower energy-conserving phase of glycolysis and the TCA cycle (Stal & Moezelaar, 1997; Knowles & Plaxton, 2003; Takahashi *et al.,* 2008). Figure 2 presents a schematic overview of these metabolic pathways and their involvement in the formation and degradation of carbohydrates.

Photosynthetic light reactions provide energy in the form of ATP and NADPH, which is subsequently used for carbon fixation in the Calvin cycle and in the production of hexosephosphates via gluconeogenesis. The first step of the Calvin cycle, the carboxylation of ribulose-1,5-bisphosphate ($Rib1,5P_2$), is catalyzed by the enzyme ribulose-1,5-bisphosphate carboxylase/oxygenase (Rubisco). Due to the relatively low affinity of Rubisco for its substrate, *Synechocystis* utilises a CO_2-concentrating mechanism (CCM) that is upregulated when the cells are exposed to a limiting CO_2 level, resulting in an increase of the CO_2 concentration in close proximity to Rubisco within the carboxysomes (Kaplan & Reinhold, 1999; Giordano *et al*., 2005; Badger *et al*., 2006; Kaplan *et al.,* 2008; Price *et al.,* 2008). The resulting sugar products enter the glycolytic pathway and are subsequently utilised in many biosynthetic pathways or converted into glycogen, the main carbohydrate storage compound in cyano-bacteria (Preiss & Sivak, 1998a, 1998b; Knoop *et al.,* 2010), which serves as metabolic energy source under non-photosynthetic conditions/during periods of dark-ness. The degradation of glycogen provides glucose, which is catabolized via the lower energy-conserving phase of glycolysis, an incomplete TCA cycle and the OPPP (Stal & Moezelaar, 1997; Knowles & Plaxton, 2003; Takahashi *et al.,* 2008).

In the glycolytic pathway glucose is converted into pyruvate by generating small amounts of ATP and reducing power in the form of NADH. Glycolysis is a central pathway that produces important precursor metabolites, including the six-carbon compounds glucose-6-phosphate (G6P), fructose-6-phosphate (F6P) and three-carbon compounds of glyceraldehyde-3P (GAP), 1,3-bisphosphoglycerate ($G1,3P_2$), 3-phosphoglycerate (G3P), phosphoenol-pyruvate (PEP) and pyruvate. The oxidative decarboxylation of pyruvate produces acetyl coenzyme A (acetyl-CoA), the activated form of acetate, which is the starting molecule of the TCA cycle. The two-carbon acetyl group in acetyl-CoA is transferred to the four-carbon compound of oxalacetate (OAA) to form the six-carbon compound of citrate. In a series of reactions, two carbons in citrate are oxidized to CO_2 and the reaction pathway supplies NADH for the use in the oxidative phosphorylation and other metabolic processes. At the end of the cycle, the remaining four-carbon part is transformed

back to OAA. The TCA cycle is an important pathway for the final steps of carbohydrate oxidation and also supplies important precursor metabolites, such as 2-oxoglutarate. In cyanobacteria, the TCA cycle was assumed to be non-functional due to the absence of the key enzyme 2-oxoglutarate dehydrogenase, which converts 2-oxoglutarate to succinyl-coenzyme A (Pearce *et al.*, 1969; Stanier & Cohen-Bazire, 1977). Consistently, sequence analyses revealed that no fully sequenced cyanobacterial genome encodes the genes for 2-oxoglutarate dehydro-genase (Wood *et al.,* 2004). However, *Synechocystis* is able to convert 2-oxo-glutarate to succinate despite the absence of a 2-oxoglutarate dehydrogenase complex, which indicates the use of an alternate pathway (Cooley *et al.*, 2000; Vermaas, 2001). Only recently, Zhang and Bryant (2011) identified genes encoding a novel 2-oxoglutarate decarboxylase and succinic semialdehyde dehydrogenase in *Synechococcus* sp. PCC 7002. They demonstrated that these two enzymes convert 2-oxoglutarate to succinate and thus functionally replace 2-oxoglutarate dehydro-genase and succinyl-CoA synthetase in the TCA cycle (Zhang & Bryant, 2011).

In the OPPP, glucose-6-phosphate (G6P) is first converted to 6-phosphoglucono-lactone (6PGL), catalyzed by the enzyme glucose-6-phosphate dehydrogenase (G6PDH) and further catabolized to glyceraldehyde-3-phosphate (GAP). The catabolic processes of the OPPP provide reducing power in the form of NADPH, as well as metabolic precursors for anabolic processes, such as the biosynthesis of amino acids or nucleic acids (Kruger & von Schaewen, 2003; Osanai *et al.,* 2007). The OPPP is widely accepted to be the main route of glucose catabolism in cyano-bacteria, both for the breakdown of glycogen or exogenously supplied glucose (Hagen & Meeks, 2001; Yang *et al*., 2002). Hence, the enzyme G6PDH (encoded by *Zwf*, *slr1843*) is of particular importance, as it catalyzes the initial step of glucose degradation, thereby controlling the carbon flow into the OPPP. The regulation of G6PDH is complex and still not fully understood. Metabolites, including NADPH, ATP, G6P, glutamine and $Rib1,5P_2$ have been implicated in its regulation (Schaeffer & Stanier, 1978; Cossar *et al.,* 1984), as has thioredoxin, which may reductively inactivate and oxidatively reactivate the enzyme in the light and dark, respectively, to prevent futile cycling, which would occur if the Calvin and OPP cycles operated simultaneously (Cossar *et al.,* 1984; Udvardy *et al.,* 1984; Gleason, 1996; Hagen & Meeks, 2001). Biochemical analyses indicated that G6PDH exists in various aggregation states that show different kinetic properties (Schaeffer & Stanier, 1978; Gleason, 1996; Sundaram *et al*., 1998; Kahlon *et al*., 2006), however, the biological significance of the aggregation states remains elusive. Besides, a role in regulating

G6PDH activity has been suggested for OPCA (OPP cycle protein A), as this protein is assumed to be involved in the assembly of G6PDH, its oligomerization and activation in various cyanobacteria (Sundaram *et al*., 1998; Min & Golden, 2000; Hagen & Meeks, 2001; Kahlon *et al*., 2006).

Variations in the ability of cyanobacteria to consume carbon from their surroundings have been reported. In addition to photoautotrophic growth, where carbon dioxide represents the sole carbon source, some cyanobacteria are also capable of photo-mixotrophic and heterotrophic growth by utilising exogenous organic carbon (Rippka *et al.*, 1979; Stal & Moezelaar, 1997). It is known that the presence of exogenous glucose affects many physiological and biochemical parameters in *Synechocystis,* including growth and carbon metabolism (Yang *et al.*, 2002; Knowles & Plaxton, 2003; Lee *et al.,* 2005; Osanai *et al*., 2005; Singh & Sherman, 2005) and photo-synthesis and respiration (Ryu *et al.,* 2004, Lee *et al.,* 2005; Kurian *et al.,* 2006). In contrast to the numerous responses to glucose, the profiles of transcript abundance and protein levels remain almost unaltered in photoautotrophic and photomixotrophic cultures (Yang *et al.,* 2002; Knowles & Plaxton, 2003; Tu *et al.*, 2004; Singh & Sherman, 2005; Kahlon *et al.,* 2006), indicating that the response to glucose is mainly accomplished on alterations at the post-translational level (Kahlon *et al.,* 2006). However, the mechanism by which cyanobacteria sense and respond to the presence of glucose in their environment is still unclear. So far, only a small number of corresponding regulators are known in cyanobacteria. In *Synechocystis*, several sensors have been identified that are involved in glucose-induced signalling of several glycolytic and OPPP genes under photoautotrophic, photomixotrophic and heterotrophic growth conditions (Lee *et al*., 2007). Among these sensors are histidine kinases, the sensory components of the so-called two component signalling systems, which are described in detail in Section 1.4. The histidine kinase 8 (HIK8) has been reported to play an important role in glucose metabolism (Singh & Sherman, 2005). HIK8 has significant protein sequence similarity to SASA from *Synechococcus* sp. strain PCC 7942 (*Synechococcus* adaptive sensor A), a histidine kinase that interacts with KAIC (Iwasaki *et al.*, 2000), one of the three circadian clock proteins responsible for circadian control in *Synechococcus* (Golden & Canales, 2003). HIK8 was found to enable cells to grow under heterotrophic growth conditions, probably via transcriptional regulation of *Gap1*, which encodes one of the two glyceraldehyde-3-phosphate dehydrogenases, catalyzing the catabolic reaction (Singh & Sherman, 2005; Lee *et al.,* 2007). Furthermore, it has been reported that the histidine kinase 31 (HIK31) is involved in the regulation of glucose catabolism in

Synechocystis, either via transcriptional regulation of the *lcfG* gene, which encodes a protein serine phosphatase (Shi *et al.,* 1999) or by modulation of glukokinase activity (Kahlon *et al.,* 2006). In addition to two-component signalling regulatory proteins, sigma factors represent another group of important regulators determining transcript profiles by directly interacting with the promotor sequence (Paget & Helmann, 2003; Lee *et al.,* 2007). Among the nine sigma factors (SIG) existing in *Synechocystis*, SIGE has been reported to positively regulate the expression of sugar catabolic genes (Osanai *et al.,* 2005, 2007; Lee *et al.,* 2007).

1.3 Phytochrome signalling in plants and cyanobacteria

Light is an important environmental factor for all photosynthetic organisms. Not only does it provide the radiant energy for photosynthesis and hence for growth and metabolism, but also the sensory information for adaptive and developmental processes. Accordingly, photosynthetic organisms possess various photosensors, which enable them to perceive environmental light signals and to respond by regulating the gene expression through signal transduction pathways (Quail, 1994). One such group of photosensors is the red/far-red sensitive phytochrome family. Phytochromes were first discovered in higher plants in the 1950s (Butler *et al.,* 1959), based on the ability to measure the ratio of red light (R) and far-red light (FR) to control plant morphogenesis (Quail, 2002; Smith, 2000). Although originally thought to be restricted to plants, similar genes have been found more recently in several cyanobacteria (Hughes *et al.,* 1997; Yeh *et al.*, 1997; Wu & Lagarias, 2000; Park *et al.*, 2000), in bacteria (Jiang *et al.*, 1999; Bhoo *et al.*, 2001) and even in fungi (Montgomery & Lagarias, 2002; Lamparter *et al.,* 2002; Karniol & Vierstra, 2003; Blumenstein *et al.,* 2005).

Signalling mediated by most phytochromes involves absorption of R light (650-660 nm) and FR light (700-730 nm), which leads to two stable conformations Pr and Pfr, respectively (Figure 3 A) (Smith, 1994; Quail *et al.,* 1995). In most phytochromes, the photoproduct is metastable and can slowly return to the thermally stable dark state in the so-called dark reversion process (Rockwell & Lagarias, 2010). Figure 3 B displays the absorption spectra of Pfr and Pr and their partial overlap. Light establishes a Pr/Pfr photoequilibrium, reflecting environmental light conditions. Changes in the ratio between Pfr and Pr lead to changes in the equilibrium, therefore making phytochromes useful as sensors of critical changes in light quality (Sharrock, 2008). The ability to absorb light is conferred to the phytochrome by a covalently attached tetrapyrrole (bilin) chromophore, which typically absorbs light at 665 nm

(Quail, 1997; Fankhauser, 2001). This bilin chromophore, produced by the oxidative cleavage of heme, differs slightly among various organisms (Rockwell *et al.,* 2006), ranging from phytochromobilin utilised by plant phytochromes to phytocyanobilins in cyanobacteria (Yeh *et al*., 1997; Hughes *et al*., 1997) and biliverdin, which is used by eubacterial and fungal phytochromes (Rockwell & Lagarias, 2010 and references therein). The chromophore is bound autocatalytically to a conserved cysteine residue within the cGMP phosphodiesterase/adenylcyclase/FhlA (GAF) domain of the photo-sensory unit of the apoprotein. Upon light absorption, the chromophore undergoes a conformational change comprising of a Z/E photoisomerization (Rockwell *et al*., 2009).
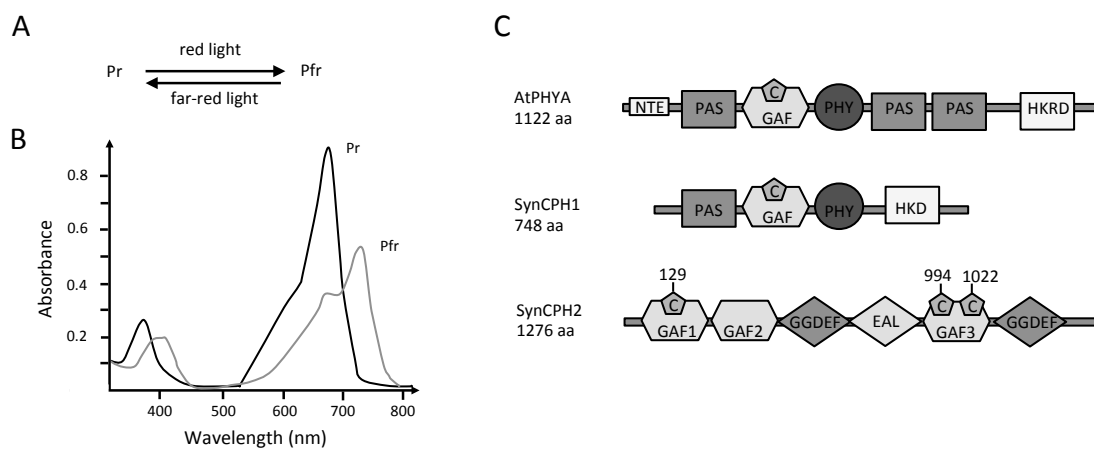
Figure 3: Overview of phytochrome properties and domain structures.

(A) Phytochromes exist in two photointerconvertible forms, Pr and Pfr. (B) Absorption spectra of Pr and Pfr (modified after Elich & Chory, 1997). (C) Schematic representation of phyto-chrome domain organisation in plants (e.g. AtPHYA) and in the cyanobacterium *Synecho-cystis* (SynCPH1 and SynCPH2) (modified after Nagatani, 2010; Anders *et al*., 2011; Savakis *et al.,* 2012). The chromophores are covalently linked to the conserved cysteine residues (denoted C) at position 129 and 1022 in the GAF1 and GAF3 domain, respectively.
Abbreviations: aa, amino acids; NTE, N-terminal extension domain; GAF, domain present in vertebrate cGMP-specific phosphodiesterases, in cyanobacterial adenylate cyclases and in the formate lyase transcription activator FhlA; PHY, phytochrome-associated domain; PAS, domain found in family members including the period clock (PER) protein, the aromatic hydrocarbon receptor nuclear translocator (ARNT) and the single minded (SIM) of *Droso-phila*; HKRD, histidine kinase-related domain; HKD, histidine kinase domain; GGDEF and EAL, domains with conserved sequence motifs, Gly-Gly-Asp-Glu-Phe and Glu-Ala-Leu, respectively, both domains, which are known to be involved in turnover of the second messenger c-di-GMP.

The conformational change of the chromophor triggers a subsequent conformational change in the protein, which initiates a signal transduction cascade (Quail, 1997; Fankhauser, 2001). Thus, by interconverting between the two photochemically distinct forms, phytochromes act as Pr/Pfr-regulated photosensory switches in various controlling processes, ranging from phototaxis, re-setting of the circadian clock, chromatic adaptation and pigmentation in cyanobacteria, to seed germination,

photomorphogenesis, shade avoidance and flowering time in higher plants (reviewed by Ulijasz & Vierstra, 2011; Chen & Chory, 2011). Phytochromes are encoded by multigene families (Elich & Chory, 1997). In the model plant system *Arabidopsis thaliana*, the phytochrome family consists of five members, designated PHY A to E (Mathews & Sharrock, 1997), which fall into two classes: light-labile (PHY A) and light-stable (PHY B-E) phytochromes (Furuya, 1993). The first prokaryotic genes encoding phytochrome-like proteins have been detected in cyanobacteria (Kehoe & Grossman, 1996; Wilde *et al*., 1997). The chromosome of *Synechocystis* sp. PCC 6803 contains a number of open reading frames, exhibiting different degrees of similarity to plant genes encoding putative phytochrome-like proteins (Kaneko *et al.,* 1996). These proteins contain one or several putative chromophore binding domains fused to various signal-transmitting domains, but the red/far red photoconversion of a covalently attached bilin chromophore, typical for plant phytochromes, has only been shown for two *Synechocystis* proteins: CPH1 (Hughes *et al.,* 1997; Yeh *et al*., 1997; Hübschmann *et al.,* 2001) and CPH2 (Wu & Lagarias, 2000; Park *et al.,* 2000). The domain architecture of phytochromes (Figure 3 C) implies conserved sequences and domains that are either ubiquitous among phytochromes or conserved in different subfamilies (Rockwell *et al*., 2009). Plant phytochromes, the cyanobacterial phytochrome CPH1 and most bacterial phytochromes (BphPs) share a common architecture, consisting of an N-terminal photosensory region with three conserved PAS (PER/ARNT/SIM), GAF (cGMP phosphodiesterase adenylate cyclase/FhlA) and PHY (phytochrome-associated) domains and a C-terminal regulatory histidine kinase or histidine kinase-related domain (HKRD) (Quail, 1997). Histidine kinases are involved in signal transduction in prokaryotes and eukaryotes and are best studied as sensors of two-component signal transduction systems that are widely distributed among bacteria (Wilde *et al.,* 2002). Light-regulated protein kinase activity was first reported for the cyanobacterial phytochrome CPH1 from *Synechocystis* (Yeh *et al.,* 1997). CPH1 was shown to be a true phytochrome by analysing recombinant CPH1 apoprotein from *Escherichia coli* (Hughes *et al.,* 1997; Yeh *et al*., 1997; Lamparter *et al*., 1997), as well as the native holoprotein isolated from *Synechocystis* (Hübschmann *et al.,* 2001). Once assembled with the chromophore, CPH1 was shown to undergo classic red/far-red reversibility *in vitro* (Hughes *et al.,* 1997; Yeh *et al*., 1997). Moreover, CPH1 was found to autophosphorylate at a histidine kinase residue and to transfer the phosphate to the downstream response regulator RCP1 (Yeh *et al.,* 1997). In earlier studies it has been proposed that plant phytochromes also act as light-regulated histidine kinases, based on limited sequence similarity of their C-termini to the histidine kinase domain present in

bacterial two-component histidine kinases (Schneider-Poetsch, 1992; Yeh *et al.*, 1997; Karniol *et al.,* 2005). However, the histidine kinase-related sequence of plant phytochromes lacks several important residues characteristic for two-component histidine kinases, indicating that plant phytochromes work by an alternative mechanism. More recently, plant phytochromes were shown to be light-regulated serine/threonine kinases (Yeh & Lagarias, 1998). In contrast to CPH1, the second cyanobacterial phytochrome CPH2 lacks a histidine kinase domain in the C-terminal module and has a different domain organisation (Figure 3 C). In addition to the two N-terminal GAF domains (GAF1 and GAF2), which form the Pr/Pfr-reversible photosensory module, CPH2 possesses a third C-terminal GAF domain (GAF3). GAF1 and GAF3 contain the bilin-binding sites, two conserved cysteine residues at position 129 and 1022 (cysteine-129 and cysteine-1022) (Park *et al.,* 2000), which have been shown capable of ligating bilin chromophores autocatalytically (Wu & Lagarias, 2000; Anders *et al.,* 2011). Spectroscopic analyses of bilin attachment to the recombinant N-terminal GAF domain showed the typical red/far-red reversibility, while the phycocyanobilin adduct of the recombinant C-terminal part absorbed blue light stronger than red light (Wu & Lagarias, 2000; Moon *et al.,* 2011). Furthermore, GAF3 shows homology to the cyanobacteriochromes (Ikeuchi & Ishizuka, 2008), phytochrome-like proteins that are capable to photointerconvert between green and red (Terauchi *et al.,* 2004; Narikawa *et al.,* 2008; Hirose *et al.,* 2008, 2010), blue and green (Yoshihara *et al.,* 2004; Ishizuka *et al.,* 2006, Rockwell *et al.,* 2008), UV and blue, or violet and orange (Rockwell *et al.,* 2011) absorbing states. This led to the assumption that CPH2 additionally acts as a blue light receptor (Wilde *et al.,* 2002; Fiedler *et al.,* 2005), which was recently confirmed by Savakis and co-workers (2012). They demonstrated that CPH2 undergoes photoconversion between blue and green light absorbing photostates, like other cyanobacteriochromes, e.g. TePixJ (Ishizuka *et al.,* 2006, 2007, 2011; Ulijasz *et al.,* 2009) and Tlr0924 (Rockwell *et al.,* 2009), thereby utilising the same photochemistry including the double tethering of the bilin chromophore by two cysteines, cysteine-994 and cysteine-1022 (Savakis *et al.,* 2012). Thus, based on its molecular architecture, CPH2 can be considered as a hybrid photoreceptor that comprises an N-terminal Pr/Pfr photosensory module and a C-terminal blue/green light-absorbing cyanobacteriochrome module (Savakis *et al.,* 2012).

Following the two N-terminal GAF domains, CPH2 possesses GGDEF and EAL domains. GGDEF and EAL domains are known to be involved in regulating intracellular levels of bis-(3'-5')-cyclic dimeric guanosine monophosphate (c-di-GMP),

a second messenger that is known to regulate motility and biofilm formation in bacteria (Römling *et al*., 2005; Jenal & Malone, 2006; Cotter & Stibitz, 2007; Yan & Chen, 2010). The cellular c-di-GMP concentration is regulated by GGDEF domains acting as c-di-GMP cyclases to increase the cellular c-di-GMP concentration and by EAL domains, acting as phosphodiesterases to decrease the c-di-GMP content (Yan & Chen, 2010; Anders *et al.,* 2011). Increasing concentrations of c-di-GMP promote the production of extracellular polysaccharides, the matrix that maintains the structural integrity of biofilms, and result in multicellular behaviour and biofilm formation, while low c-di-GMP concentrations promote motility (reviewed by Jenal & Malone, 2006). Furthermore, c-di-GMP also regulates biofilm formation through other multiple factors/signalling pathways, such as quorum sensing, chemotaxis and twitching motility (Tamayo *et al.,* 2007; Yan & Chen, 2010). In *Synechocystis*, the cells display a flagellar-independent twitching or gliding motility that allows bacteria to move over moist surfaces using type IV pili (Bhaya *et al.,* 1999; Fiedler *et al*., 2005). Interestingly, it has been reported on the photomovement that CPH2 controls phototaxis by inhibiting positive phototaxis towards blue light (Wilde *et al*., 2002; Fiedler *et al.,* 2005; Moon *et al.,* 2011).

1.4 Histidine kinase signalling

Acclimation to fluctuations in environmental conditions is critically important for the survival of all living organisms. Adaptational processes require the ability to perceive changes in the physical and/or chemical environment in order to adapt by regulating the gene expression and protein synthesis appropriately. In particular unicellular organisms are routinely challenged by changes in their extracellular environment, which makes adaptive responses to altered conditions indispensable for successful competition and survival. The ability to mediate these adaptive responses is conferred by sophisticated signal transduction systems, which represent a funda-mental strategy in information processing in both prokaryotes and eukaryotes (reviewed by Schaller *et al.,* 2011). Signal-induced protein phosphorylation is a common regulatory mechanism to transduce intracellular or extracellular signals in both prokaryotes and eukaryotes (Kakimoto, 2003; Schaller *et al.,* 2008). In eukaryotes, regulatory protein phosphorylation predominantly occurs at serine, threonine and tyrosine residues (Hunter, 1995; Hunter & Plowman, 1997; Plowman *et al*., 1999), while many signal transduction pathways in bacteria use the so-called two-component systems that rely upon phosphorylation of histidine and aspartic residues (Mizuno, 1997; Schaller *et al.,* 2008). However, both phosphorylation

schemes (His→Asp and Ser/Thr/Tyr) can function in prokaryotes and eukaryotes, as His→Asp phosphotransfer systems have been found in several eukaryotic organisms (Wurgler-Murphy & Saito, 1997; Chang & Stewart, 1998; Loomis *et al.*, 1997, 1998) and Ser/Thr and Tyr kinases and phosphatases have been identified in bacteria (Zhang, 1996). Notably, plants also make use of two-component systems, which are involved in important cellular processes, such as the responses to cytokinin, ethylene, red light and osmosensing (Mizuno, 2005, Schaller *et al.,* 2008; Tsai *et al.,* 2012).

The core of two-component signalling pathways is a phosphotransfer reaction between two conserved components, a histidine kinase (Hik) and a cognate response regulator (RR) (Stock *et al.,* 1995; 2000; Gao & Stock, 2009; Bourret & Silversmith, 2010; Jung *et al.,* 2012). The Hik is typically the input component of the pathway, which senses stimuli and correspondingly regulates the signalling pathway, while the RR represents the output component of the system, which is regulated by the Hik and finally affects the cellular response (Gao & Stock, 2009). Structurally, Hiks are generally homodimeric integral membrane proteins with a N-terminal signal-sensing (input) domain, which is located in the extracellular space and a C-terminal cytoplasmatic signal-transducing (transmitter) domain (Stock, 1999; Kakimoto, 2003). Signalling is initiated upon ligand binding to the histidine kinase sensory component. Most frequently, the signal is sensed by an extracellular loop formed between two membrane-spanning regions (Gao & Stock, 2009). However, depending on the corresponding signal, the sensor domains of some Hiks can also be located within the membrane or completely within the cytoplasm (Gao & Stock, 2009). Upon ligand binding, the C-terminal kinase domain is activated, which is followed by autophosphorylation at a specific histidine residue (the H-box) using ATP as phosphate donor (Stock & Da Re, 2000). In prototypical Hiks, the cytoplasmatic kinase core consists of two distinct domains: a well-conserved C-terminal catalytic and ATP-binding domain and a less-conserved dimerization and histidine phosphotransfer domain (Gao & Stock, 2009). Several characteristic sequence motifs are conserved across the kinase core domains in both eukaryotic and prokaryotic Hiks (Stock *et al.,* 1989; Parkinson & Kofoid, 1992; Alex & Simon, 1994). On the basis of specific sequences, they are referred to as H, N, G1, F and G2 boxes, with the H-box containing the phosphorylation site in the dimerization domain and the nucleotide binding pocket in N, G1, F and G2 boxes, located in the catalytic domain (Gao & Stock, 2009). After autophosphorylation of the Hik at its His residue, a high-energy phosphoryl group is created that is transferred from the Hik to an

aspartate residue in the conserved receiver domain of the cognate RR. This phosphorylation event leads to a conformational change that activates an attached output domain of the RR, triggering the cellular response. Response regulatory proteins possess various outputs, which include transcriptional, post-transcriptional, post-translational controls and protein-protein interactions (Perry *et al.,* 2011). Most frequently, output domains are DNA-binding domains so that phosphorylation of the RR is coupled directly to changes in transcription (Laub & Goulian, 2007). However, many other output domains have enzymatic activities, for example the regulation of the c-di-GMP concentration (Hengge, 2009), while other RRs even lack a distinct output domain, concomitant with their regulatory function residing within the receiver domain (Ulrich & Zhulin, 2009). One of those RRs is the chemotaxis protein CheY, which controls the rotational direction of the bacterial flagellar motor (Wadhams & Armitage, 2004).

Besides the typical two-component pathway, involving a single HK and a single RR that participate in an onestep His→Asp phosphotransfer, more complex variants exist (reviewed by Jung *et al.,* 2012). These so-called multistep phosphorelays involve multiple His-containing and Asp-containing domains and a multistep His→Asp→His→Asp phosphotransfer (Appleby *et al.,* 1996; Goulian, 2010; Wuichet *et al.,* 2010). In many cases, Hiks are bifunctional and can catalyze both the phosphory-lation and dephosphorylation of their cognate RR (Keener & Kustu, 1988; Aiba *et al.,* 1989; Lois *et al.,* 1993). For bifunctional Hiks, input stimuli can regulate either the kinase or phosphatase activity (Laub & Goulian, 2007). These phosphorelays are usually initiated by a hybrid histidine kinase that autophosphorylates and transfers its phosphoryl group intramolecularly to an RR-like receiver domain. The phosphoryl group is then transferred to a signalling intermediate, a histidine phosphotransfer (HP) protein. HP domains can often be found fused to hybrid histidine kinases or as independent proteins that facilitate the phosphotransfer process (Appleby *et al*., 1996; Stock *et al.,* 2000). Due to their ability to both receive and transmit phosphoryl groups, HP proteins subsequently transfer them to the receiver domains of a terminal RR, which can induce the corresponding response (Kato *et al.,* 1997; Laub & Goulian, 2007). Phosphotransfer pathways are the most common pathway architecture in prokaryotes, while phosphorelays, which provide a greater number of steps for regulation, are predominant in eukaryotes (Robinson *et al*., 2000).

1.4.1 Histidine kinase signalling in cyanobacteria

The cyanobacterium *Synechocystis* sp. PCC 6803 contains a total of 47 genes for Hiks and 45 genes for RR on its chromosome and plasmids (Kaneko *et al.*, 1996; Mizuno *et al.*, 1996; Kaneko *et al.,* 2003; Los *et al.,* 2008). There are 44 genes for Hiks on the chromosome, two genes on the plasmid pSYSX and one gene on the plasmid pSYSM (Murata & Suzuki, 2006). The 44 genes for Hiks on the chromo-some have been named *Hik1* through *Hik44.* Among them, the three putative Hiks, HIK11, HIK17 and HIK37 are supposed to be inactive as histidine kinases because they lack the conserved histidine residue in the Hik domain (Murata & Suzuki, 2006). The genes for the Hiks on the plasmids have been designated *Hik45-Hik47*. Likewise, the 42 genes for RRs on the chromosome have been designated *Rr1* through *Rr42*, while *Rr43-Rr45* are located on the plasmids.

In *Synechocystis*, all putative *Hik* genes have been inactivated by insertion of a spectinomycine-resistance gene cassette in order to create a gene-knockout library (Suzuki *et al.,* 2000). The characterisation of these knockout mutants led to the identification of histidine kinases involved in sensing environmental stimuli, including high light, cold and oxidative stress (HIK33), heat (HIK34), salt stress and hyperosmotic stress (HIK33, HIK34, HIK2, HIK41, HIK16 and HIK10), and phosphate limitation (HIK7) (Hirani *et al*., 2001; Mikami *et al.,* 2002; Hsiao *et al.,* 2004; Paithoonrangsarid *et al*., 2004; Shoumskaya *et al.,* 2005; Suzuki *et al.,* 2005; Kanesaki *et al.,* 2007), indicating that a single histidine kinase may respond to more than one stimulus and that multiple histidine kinases may respond to any specific environmental cue (Summerfield *et al.,* 2011). One of these histidine kinases, HIK12, encodes a hybrid histidine kinase and a cognate RR (Cyanobase, 2012), which displays structural homologies to the *Arabidopsis* cytokinin receptors AHK2, AHK3 and AHK4, thereby suggesting a putative role for HIK12 as cyanobacterial cytokinin receptor. In addition to the structural homologies, HIK12 possesses a threonine residue within its MASE (membrane associated sensor) domain, which is conserved in all three *Arabidopsis* cytokinin receptors and was found to be one of the five amino acid positions within the ligand binding domain of AHK4, relevant for cytokinin binding (Heyl *et al.,* 2007). First evidence of cyanobacteria responding to cytokinin was observed by Selivankina and co-workers (2006) who demonstrated that the cytokinin *trans*-zeatin affects the transcriptional activity in *Synechocystis*, leading to the conclusion that cyanobacteria possess the molecular targets for cytokinin signal recognition. During the endosymbiotic event many cyanobacterial genes have been transferred to the plant nucleus (Wuichet *et al.,* 2010; Kieber & Schaller, 2010).

Accordingly, the cytokinin signalling system in plants might also be an inheritage of their cyanobacterial ancestors.

1.4.2 Cytokinin signalling in plants

In *Arabidopsis*, two-component elements are encoded by multigene families (Schaller *et al.,* 2002; Heyl & Schmülling, 2003; Kakimoto, 2003; Ferreira & Kieber, 2005; Maxwell & Kieber, 2005), which fall into three major clades, phytochromes, ethylene receptors and cytokinin receptors (Schaller *et al.*, 2008). The cytokinin receptor family in *Arabidopsis* consists of three histidine kinases, AHK2, AHK3 and AHK4 (Inoue *et al.*, 2001; Suzuki *et al.,* 2001; Ueguchi *et al.,* 2001; Yamada *et al.,* 2001). AHK4, which is also known as WOL1 or CRE1, was originally identified in two independent screens for *woodenleg* (*wol*) mutants with short roots in *Arabidopsis* (Mähönen *et al.,* 2000) and for *cytokinin response* (*cre*) mutants that were defective in cytokinin induction of shoots in tissue culture (Inoue *et al.,* 2001). Different studies have shown that AHK4 and its paralogs AHK2 and AHK3 act as cytokinin sensors and are capable of mediating cytokinin-dependent histidine kinase activity in heterologous bacterial and yeast systems (Inoue *et al.,* 2001; Suzuki *et al.,* 2001; Ueguchi *et al.,* 2001; Yamada *et al.,* 2001).

The cytokinin receptors AHK2, AHK3 and AHK4 are hybrid Hiks, displaying a common primary structure consisting of a cyclase/histidine kinase associated sensory extracellular (CHASE) domain, predicted to be extracytosolic, which binds cytokinin (Anantharaman & Aravind, 2001; Heyl *et al.,* 2007) and two flanking N-terminal transmembrane domains. The CHASE domain is followed towards the C-terminus by a Hik and an RR domain in the predicted cytoplasmic part (Heyl & Schmülling, 2003). Functional evidence for cytokinin binding to the CHASE domain was obtained in *in vivo* binding assays (Romanov *et al.,* 2005; Heyl *et al.*, 2007; Wulfetange *et al.,* 2011b). In addition, Heyl and co-workers (2007) identified four amino acid positions within the CHASE domain of AHK4, relevant for cytokinin binding. It was proposed that plants might have acquired the CHASE domain via lateral transfer through their chloroplasts, which have a cyanobacterial ancestry (Anantharaman & Aravind, 2001; Mougel & Zhulin, 2001).

Cytokinin binding to the CHASE domain triggers autophosphorylation of the Hik at a conserved His residue. The phosphoryl group is subsequently transferred from the Hik to a conserved aspartate (Asp) residue in the receptor's receiver domain. The C-terminal receiver domains of all three receptors interact redundantly with histidine phosphotransfer proteins (AHPs), which transmit the signal to the nucleus (Hwang &

Sheen, 2001; Punwani *et al.,* 2010), where the phosphoryl group is transferred to a conserved Asp residue in the receiver domain of an RR protein (Müller & Sheen, 2007), resulting in the activation of the RR protein. In *Arabidopsis*, there are two types of RRs: type-A and type-B ARRs. Type-B ARRs directly regulate gene expression, including the transcriptional induction of type-A response regulator genes (Mason *et al.,* 2005; Heyl & Schmülling, 2006; Argyros *et al.,* 2008; Ishida *et al.,* 2008). Type-A ARRs mediate downstream responses to cytokinin and function as negative feedback regulators of the initial cytokinin signalling (Sakai *et al.,* 2001; Hwang *et al.,* 2002; Heyl & Schmülling, 2003; To *et al.,* 2004; Ferreira & Kieber, 2005; Hirose *et al.,* 2007; To & Kieber, 2008; Cheng *et al.,* 2010).

Until recently, models of cytokinin signalling predicted a localization of cytokinin receptors to the plasma membrane (Heyl & Schmülling, 2003; Hwang & Sakakibara, 2006; Müller & Sheen, 2007; To & Kieber, 2008; Pils & Heyl, 2009), based on bioinformatic analysis of the protein sequence and analogy with sensor His kinase localization in bacteria and yeast (Inoue *et al.,* 2001; Ueguchi *et al.,* 2001). Furthermore, the localization to the plasma membrane was experimentally supported by the localization of overexpressed AHK3-GFP fusion proteins to the plasma membrane of *Arabidopsis* protoplasts (Kim *et al.,* 2006). However, recent findings revealed that cytokinin receptors in monocots and dicots are predominantly located to the endoplasmatic reticulum (ER; Wulfetange *et al.,* 2011a; Caesar *et al.,* 2011; Lomin *et al.,* 2011) and not as previously assumed to the plasma membrane. The novel predominant ER localization makes it necessary to revise the concept of cytokinin perception and signalling. According to these findings, the ligand-binding CHASE domain is not oriented to the apoplast as previously assumed, but exposed to the ER lumen, while the C-terminal his kinase domain is exposed to the cytoplasm. Cytokinin receptors located on the ER membrane could transmit the cytokinin signal via AHP to the nucleus, similar as it was proposed for signal transmission from the plasma membrane (Schaller *et al.,* 1995; Hwang & Sheen, 2001; Heyl & Schmülling, 2003; Kakimoto, 2003; Bishopp *et al.,* 2006). This topology of the receptors is further supported by biochemical studies, revealing an optimal cytokinin binding at pH values of ~6.5 (Romanov *et al.,* 2006), which corresponds to conditions found in the ER lumen (Kim *et al.,* 1998). At pH values of ~5.5, as it has been reported for the apoplast (Li *et al.,* 2005), cytokinin binding activity is almost abolished (Caesar *et al.,* 2011). Cytokinin receptor localization in the ER offers new opportunities for cross talk, as numerous other plant receptor proteins, including the structurally related ethylene receptors (Chen *et al.,* 2002), auxin signalling-related

proteins and specific metabolic enzymes, such as cytokinin oxidases are also located at the ER (Werner *et al.,* 2003; Geldner & Robatzek, 2008; Irani & Russinova, 2009; Friml & Jones, 2010; Wulfetange *et al.,* 2011a).

In *Arabidopsis,* the genes encoding the cytokinin receptors are expressed in almost all tissues, although with different abundance (Riefler *et al.,* 2006; reviewed by Shi & Rashotte, 2012). AHK4 is predominantly expressed in the root, while AHK2 and especially AHK3 transcripts are more abundant in the aerial parts of *Arabidopsis* plants (Mähönen *et al.,* 2000; Ueguchi *et al.,* 2001; Higuchi *et al.,* 2004; Nishimura *et al.,* 2004; Stolz *et al.,* 2011). Promoter:β-glucuronidase (GUS) fusions revealed that the receptor genes have overlapping, but partly distinct expression domains and are transcribed in almost all cells in the different organs although with different strength (Higuchi *et al.,* 2004; Nishimura *et al.,* 2004; Mähönen *et al.,* 2006). Analyses of T-DNA insertional mutations in AHK2, AHK3 and AHK4 have shown that there is a considerable degree of redundancy of these three receptors (Higuchi *et al.,* 2004; Nishimura *et al.,* 2004; Riefler *et al.,* 2006; Stolz *et al.,* 2011; Shi & Rashotte, 2012). Loss-of-function mutation of single receptors displayed no or only minor effects on most of the phenotypes studied, while double *ahk2ahk3* mutants show marked developmental impairments and triple *ahk2,3,4* mutants displayed near complete insensitivity to cytokinins and severe developmental defects, indicating a key regulatory role of cytokinins in plant growth and development (Higuchi *et al.,* 2004; Nishimura *et al.,* 2004; Riefler *et al.,* 2006; To *et al.*, 2007; Kieber & Schaller, 2010; Stolz *et al.,* 2011). However, individual receptors were shown to possess distinct functions and to mediate specific cytokinin activities. These functions include a role for AHK4 in regulating the sensitivity to cytokinin in root elongation and a major role for AHK3 (together with AHK2) in regulating leaf senescence (Inoue *et al.,* 2001; Riefler *et al.,* 2006; Kim *et al.,* 2006; Werner & Schmülling, 2009; Müller *et al.,* 2011). Furthermore, AHK3 appears to be the main regulator of cell differentiation in the transition zone of the root meristem (Dello Ioio *et al.,* 2007), while AHK4 regulates embryonic root patterning (Mähönen *et al.,* 2000; Müller & Sheen, 2007), the phosphate starvation response (Franco-Zorrilla *et al.,* 2002, 2005) and sulphate assimilation (Maruyama-Nakashita *et al.,* 2004). For AHK2, no specific function has been assigned so far, although AHK2 alone was shown to be sufficient to maintain normal plant growth under standard growth conditions (Higuchi *et al.,* 2004; Nishimura *et al.,* 2004; Riefler *et al.,* 2006).

1.5   Cytokinin function in plants

Cytokinins are a class of plant hormones that have been discovered more than 50 years ago, based on their ability to strongly stimulate growth and cell division in tobacco tissue culture (Miller *et al.,* 1955; Amasino, 1955). Cytokinins are involved in numerous developmental and physiological processes, including cell division, shoot meristem initiation, leaf and root differentiation, chloroplast biogenesis, stress tolerance, delay of senescence and also in pathogen resistance (Mok & Mok, 2001; Hwang *et al*., 2002; Heyl & Schmülling, 2003; Mizuno, 2004; Ferreira & Kieber, 2005; Walters & McRoberts, 2006; Argueso *et al.,* 2009; Choi *et al.,* 2010; Großkinsky *et al.,* 2011). Cytokinins control essential developmental processes in plants by interacting with other plant hormones, including salicylic acid, auxin, gibberellic acid, brassinosteroids, ethylene and abscisic acid (Bishopp *et al.,* 2006; Bari & Jones, 2009; Argueso *et al.,* 2010). These interactions include the reciprocal control of hormone biosynthesis, the expression of components in other signal transduction pathways and cross talk of signal transduction intermediates directly downstream of the receptors (reviewed by Bishopp *et al.,* 2006). Although considerable progress has been made, the understanding of this complex signalling network is still at an early stage.

1.5.1 Cytokinin occurrence and homeostasis

Cytokinins consist of a large array of natural adenine derivatives, which can either be produced by plants and some bacteria through specific enzymatic pathways and degradation of nucleic acids, or can be artificially generated by chemical synthesis (Mok & Mok, 2001; Sakakibara, 2006; Miyawaki *et al.,* 2006). Naturally occurring cytokinins are either isoprenoid or aromatic cytokinins, depending on the con-figuration of their N^6-side chain (Mok & Mok, 2001). Isoprenoid cytokinins occur more often and in greater abundance in plants than aromatic cytokinins (Sakakibara, 2006). Common natural isoprenoid cytokinins are N^6-(Δ^2-isopentenyl)-adenine (iP), *trans*-zeatin, *cis*-zeatin and dihydrozeatin. The major derivatives are usually *trans*-zeatin, iP and their sugar conjugates, whereas their distinct abundancy varies depending on plant species, tissue, and developmental stage (Sakakibara, 2006). Cytokinin homeostasis in cells is regulated by the rate of *de novo* synthesis, import, synthesis and breakdown of cytokinin conjugates and finally, the rate of export and breakdown (Mok & Mok, 2001; Schmülling *et al.,* 2003). Key enzymes for cytokinin homeostasis are adenosine phosphate-isopentenyl-transferases (IPT) and cytokinin oxidase/dehydrogenases (CKX), which are involved in cytokinin synthesis and

degradation, respectively (Sakakibara, 2006; Kamada-Nobusada & Sakakibara, 2009; Frébort *et al.,* 2011). In *Arabidopsis*, both gene families encompass seven members (AtIPT1, AtIPT3-8 and AtCKX1-7) (Takei *et al.,* 2001; Werner *et al.,* 2003; Schmülling *et al.,* 2003; Miyawaki *et al.,* 2006; Kamada-Nobusada & Sakakibara, 2009). Both display differential expression patterns during plant development with highest activities in regions of active growth (Werner *et al.,* 2003).

1.5.2 Cytokinin function in defense reactions

A further function of cytokinin has been suggested that directly links cytokinin effects and plant responses to biotrophic pathogens, due to a striking similarity between several well-established cytokinin functions and changes in host physiology during plant-pathogen interactions (Walters & McRoberts, 2006; Walters *et al.,* 2008). Biotrophic fungal or bacterial pathogens utilise cytokinins to form so-called green islands, sites of green living tissues surrounding the sites of active pathogen growth, which leads to delayed senescence and enhancement of sink activity (Walters & McRoberts, 2006; Walters *et al.*, 2008; Argueso *et al.,* 2009; Choi *et al.,* 2011). It has been assumed that the cytokinin-mediated growth response suppresses plant basal defense mechanisms (Robert-Seilaniantz *et al.*, 2007). However, recent research revealed that plant-originated cytokinins increase plant immunity together with salicylic acid (SA) (Choi *et al.*, 2010). SA is known to play a crucial role in plant defense and is generally involved in the activation of defense responses, such as the induction of pathogenesis-related (PR) genes and in the establishment of systemic acquired resistance (SAR; Grant & Lamb, 2006; Bari & Jones, 2009, Choi *et al.,* 2011). Interplay between SA and cytokinin in plant immunity has been suggested based on phenotypic and genetic data, however, the underlying molecular mechanism remains elusive. In *Arabidopsis,* the cytokinin receptors and in particular AHK3, are able to recognise both plant- and pathogen-derived cytokinins, but elicit different outputs, either the activation of a defense response or the development of pathogenic symptoms (Pertry *et al.,* 2009; Choi *et al.,* 2011). Together, cytokinins are involved in a variety of plant developmental and physiological processes. In particular, cytokinins have emerged as major factors in plant-pathogen interactions, where they play an essential role in maintaining plant viability by simultaneously enhancing cell division activity and resistance to biotic and abiotic stresses (Choi *et al.,* 2011). Recent findings on the molecular mechanisms underlying the cytokinin-mediated signal transduction network contribute to the understanding of the cytokinin function in plant defense responses. Nevertheless, a thorough understanding of cytokinin receptor function is still at an early stage.

1.6 Objectives

The ability to perceive environmental changes and to respond by adapting appropriately is critically important for the survival and successful competition of all living organisms. Although considerable effort has been made in the past years to elucidate signal transduction processes and the underlying molecular mechanisms, a thorough understanding remains elusive. In the first part of the present study, a cyanobacterial phytochrome, CPH2, and a cyanobacterial histidine kinase of yet unknown function, HIK12, were analyzed with a special focus on their function in the regulation of the central carbon metabolism. For this purpose, knockout and overexpression mutants were used to analyse the function of the respective proteins in the cyanobacterial model organism *Synechocystis* sp. PCC 6803. The mutants were analysed under distinct growth conditions, with particular interest in the transition from exponential growth to a sessile lifestyle in biomats. During the endosymbiotic event, many cyanobacterial genes have been transferred to the plant nucleus. In particular, genes coding for proteins involved in signal transduction are highly conserved among cyanobacteria and plants, e.g. the cyanobacterial histidine kinase HIK12, which shows sequence homologies to the cytokinin receptor family in *Arabidopsis*. Therefore, the goal of this study was to contribute to the understanding of signalling mechanisms in cyanobacteria and to gain new ideas of potentially similar signalling processes in plants.

Besides being involved in essential developmental and physiological processes, cytokinins have recently emerged as important factors in plant-pathogen interactions. The second part of this study focused on the function of cytokinin in regulating plant susceptibility or basal resistance during the interaction with biotrophic/hemibiotrophic pathogens. For this purpose, transiently transformed barley leaves, overexpressing cytokinin-degrading enzymes, were analysed during the interaction with the biotrophic powdery mildew fungus *Blumeria graminis* f. sp. *hordei.* Furthermore, a T-DNA insertion line of the *Arabidopsis* cytokinin receptor AHK3 was analysed during the interaction with the hemibiotrophic pathogen *Pseudomonas syringae* pv. *tomato.*

2 Materials and methods

2.1 *Synechocystis* sp. PCC 6803

Synechocystis sp. PCC 6803 strains

All experiments were performed with the unicellular, photoautotrophic, facultative photoheterotrophic freshwater cyanobacterium *Synechocystis* sp. PCC 6803 (order *Chroococcales)*. For our analyses, two independent *cph2* knockout lines (*cph2-1* and *cph2-2* KO*; locus *sll0821*) and the corresponding glucose-tolerant, parental wildtype strain were provided by Dr. Young Mok Park (Korea Basic Science Institute, Daejeon, South Korea). *Hik12* (locus *sll1672*) knockout line (*hik12* KO) and the corresponding wildtype were obtained from Dr. Iwane Suzuki (Graduate School of Life and Environmental Sciences, University of Tsukuba, Tsukuba, Japan). Both knockout lines (*cph2* KO and *hik12* KO) were generated by inserting a spectinomycine resistance cassette into the coding regions of *cph2* and *hik12*, thereby disrupting the functionality of the corresponding gene (Moon *et al.,* 2011; Suzuki *et al.,* 2000). In this study, *hik12* and *cph2* overexpression lines (*hik12* OE and *cph2* OE) were generated in the *hik12* and *cph2-2* background for functional complementation of the knockout lines with a full-length wildtype coding sequence (*hik12* and *cph2,* respectively) under the control of the constitutive petJ promoter. Furthermore, a second independent knockout line of *hik12* (*hik12* KO_2) was generated in this study. The parental wildtype strain used for transfomation with *hik12* knockout_2 construct was provided by Kay Marin (University of Cologne, Cologne, Germany).

Cultivation of *Synechocystis* sp. PCC 6803

Synechocystis cells were cultivated in BG-11 (Blue-Green) medium, prepared as described in Stanier *et al*., (1971).

BG-11 medium (10x)	$NaNO_3$	15	g
	K_2HPO_4	0.4	g
	$MgSO_4 * 7 H_2O$	0.75	g
	$CaCl_2 * 2 H_2O$	0.36	g
	Citric acid	0.06	g
	Ferric ammonium citrate (III+)	0.06	g
	EDTA Na_2	0.01	g

	Na$_2$CO$_3$	0.2 g
	Trace metal solution	10 ml
	ad H$_2$O$_{dest.}$	1 l
Trace metal solution	H$_3$BO$_3$	2.86 g
	MnCl$_2$* 4 H$_2$O	1.81 g
	ZnSO$_4$* 7 H$_2$O	0.22 g
	Na MoO$_4$*5 H$_2$O	0.39 g
	CuSO$_4$* 5 H$_2$O	0.08 g
	Co(NO$_3$)$_2$* 6 H$_2$O	0.05 g
	ad H$_2$O$_{dest..}$	1 l

BG-11 medium was prepared in ten-fold concentration, autoclaved at 121°C for 12 min and stored at 4°C. Before use, the ten-fold medium was diluted 1:10 with H$_2$O$_{dest}$ and autoclaved. For solid medium BG-11 was supplemented with 1.5% (w/v) agar, 0.3% sodium thiosulfate (Na$_2$S$_2$O$_3$*5 H$_2$O) and where appropriate, filter-sterilized antibiotics were added. For cultivation of *cph2* and *hik12* knockout lines BG-11 medium was supplemented with spectinomycine (Sigma-Aldrich, Hannover, Germany), overexpression lines were cultivated in BG-11 medium containing spectinomycine and chloramphenicole (Merck, Darmstadt, Germany). The second independent knockout line of *hik12* was cultivated in BG-11 containing kanamycine (Duchefa, Haarlem, Netherlands). All antibiotics (in liquid and solid medium) were used at a final concentration of 10 µg/ml.

For cultivation and maintenance, the cells were grown under constant light irradiance (NARVA LT 36W/760-010 daylight, Brand-Erbisdorf, Germany) with a light intensity of 20 µmol photons m^{-2} s^{-1} and streaked out at regular 3-week intervals on BG-11 agar plates, supplemented with the appropriate antibiotics. For cultivation in liquid cultures, pre-cultures were inoculated with a sterile inoculation loop directly from the specific cultures, grown on BG-11 agar plates. The cultures were supplemented with 5 mM TES-NaOH (*N*-tris-(hydroxymethyl)methyl-2-aminoethanesulfonic acid) buffer (pH 8) to maintain a stable pH value. Appropriate antibiotics were added to the pre-cultures of the mutant lines, while the experiments were conducted in BG-11 medium without antibiotics. For acclimatization, cell cultures were grown photoautotrophically on a rotary shaker (Rack-Shaker, A. Kühner GmbH, Birsfelden, Switzerland) at 135 rpm, 28°C and under constant white light (L13W/840 ACTIVE daywhite, Osram, Augsburg, Germany). After 3 to 4 days of acclimatization, the cultures were trans-

ferred to a shaker (Certomat®, Sartorius Stedim Biotech, Aubagne Cedex, France) and grown photoautotrophically at 140 rpm, 28°C and under constant light irradiance (Gro-Lux, F-36W/GRO-T8, Havells Sylvania Germany GmbH, Erlangen, Germany) of 20 µmol photons m^{-2} s^{-1}, enriched with red spectrum.

Determination of the optical density

Growth of the cell cultures was monitored by measuring the optical density at a wavelength of 750 nm (OD_{750}) in a spectrophotometer (Amersham Pharmacia ULTROSPEC III spectralphotometer, Hertfordshire, GB). H_2O_{dest} was used as blank.

Enduring culture stocks

5 ml of *Synechocystis* cell culture in mid-exponential growth phase were centrifuged (3 min, RT, 2000 rpm, Rotor A-4-62, Eppendorf 5810 R). After resuspension of the pellet in 10% dimethyl sulfoxide (w/v) (DMSO, in BG-11), the stocks were stored at -20°C.

2.1.1 General molecularbiological and cloning methods

Polymerase Chain Reaction (PCR)

Standard PCRs and colony PCRs were performed with SupraTherm™ *Taq* DNA polymerase (Genecraft, Münster, Germany) in a thermocycler (Biometra TPersonal or TProfessional Basic Gradient, Biometra GmbH, Göttingen, Germany). For colony PCRs single colonies of *E. coli* or *Synechocystis* were used as template. For the amplification of coding regions, subsequently used for cloning, PCRs were performed with Phusion® proof-reading *Taq*-polymerase (Finnzymes, New England Biolabs, Ipswich, UK).

Table 1: Standard PCR reaction mix and standard PCR program.

Components	Volume		Temp.	Time	Cycles
Buffer (10x)	2.5 µl	Initial denaturation	95°C	5 min	1
dNTPs (2 mM)	2.5 µl	Denaturation	95°C	30 sec	
Primer 1 (10 pmol)	1.5 µl	Annealing	x°C [1]	30 sec	33
Primer 2 (10 pmol)	1.5 µl	Elongation	72°C	x min [2]	
Template DNA	150-1000 ng	Final Elongation	72°C	5 min	1
Taq-DNA-Polymerase	0.2 µl	[1] Annealing temperature depends on the melting temperatures of the specific primers.			
$H_2O_{bidest.}$	ad 25 µl	[2] Elongation time depends on the estimated fragment size			

Agarose gel electrophoresis

To separate DNA fragments, horizontal gel electrophoresis (Sambrook *et al.,* 1989) was used. Due to their intrinsic negative charge, DNA molecules can be separated according to their size by applying an electric field to move the charged molecules through an agarose matrix. 0.8-2% agarose (w/v) in 1x TBE buffer was heated in a microwave until the agarose was melted completely. Before polymerization, ethidium bromide (final concentration 0.5 µg/ml) was added. Ethidium bromide intercalates with double-strand DNA, allowing visualization of the DNA molecules under UV light. The samples, supplemented with DNA loading dye (6x Orange DNA loading dye, Fermentas, St. Leon-Rot, Germany), were loaded on the gel in a gel chamber with 1x TBE. GeneRuler™ 100 bp DNA ladder plus (Fermentas, St. Leon-Rot, Germany) was used as standard. Depending on the size of the DNA fragments and the gel, voltage application was set to 90-120 V for 40-60 min. For documentation DeVision G camera and software (Decon, Hohengandern, Germany) was used.

TBE buffer (10x)	Tris	0.9	M
	Boric acid	0.9	M
	EDTA pH 6.8	0.025	M
	ad H_2O_{dest}	1	l

TBE buffer was autoclaved at 121°C for 20 min.

Elution of DNA fragments from agarose gels

QUIAquick® Gel Extraction Kit (Quiagen, Hilden, Germany) was used according to the manufacturer's instructions to isolate and purify DNA fragments from excised agarose gel blocks.

DNA restriction

For cleaving of double-stranded DNA by restriction endonucleases, restriction enzymes and corresponding buffers from Fermentas (St. Leon-Rot, Germany) were used according to the manufacturer's instructions. To prevent recircularization during ligation, an alkaline phosphatase (CIAP, *calf intestine alkaline phosphatase*, Fermentas, St. Leon-Rot, Germany) was used to dephosphorylate vector DNA, according to the manufacturer's instructions.

Ligation

Single DNA fragments can be ligated by linking terminal 3' OH groups with 5' phosphate groups in an ATP-dependent reaction via T4-DNA polymerase. Complement ends as well as blunt ends can be ligated. DNA and linearized vector fragments were mixed in a molar ratio of 3:1. The reaction was carried out in a total volume of 10 µl, containing 1 µl of 10 x ligase buffer, 1-2 U T4-DNA ligase (Fermentas, St. Leon-Rot, Germany). After incubation for 2 h at RT for sticky-end ligation or overnight at 4°C for blunt-end ligation, the ligation mix was used for transformation of competent *E. coli* cells.

Escherichia coli **- cultivation, transformation and plasmid isolation**

Escherichia coli (*E. coli*) bacteria cells grown in Luria broth (LB) medium were used for plasmid construction and replication. *E. coli* were either cultivated in overnight cultures in liquid LB medium at 230 rpm and 37°C or on solid LB agar plates at 37°C. When required, filter-sterilized antibiotics, ampicilline (Roth, Karlsruhe, Germany; at a final concentration of 100 µg/ml) or kanamycine (Duchefa, Haarlem, Netherlands; at a final concentration of 50 µg/ml) were added.

LB medium	Peptone	10 g
	Yeast extract	5 g
	NaCl	10 g
	Agar (for plates only)	15 g
	ad H_2O_{dest} and autoclave	1 l

LB medium was autoclaved at 121°C for 20 min. Antibiotics were added after autoclaving.

For transformation of *E. coli,* the strains K12 Dh5α, provided by Clontech (Heidelberg, Germany) and the more efficient *E. coli* strain XL1-blue, purchased from Stratagene (Amsterdam, Netherlands) were used. $CaCl_2$ competent *E. coli* cells were prepared as described previously (Sambrook *et al.,* 1989). For transformation, 80-100 µl of competent *E. coli* cells were supplemented with the ligation mix and incubated for 30 min on ice. After a heat shock at 42°C for 90 sec, the cells were supplemented with 0.8 ml LB medium and incubated at 37°C and 230 rpm for 1 h. After brief centrifugation, the supernatant was discarded, cells were resuspended in the reflux and plated out on LB agar plates, containing appropriate antibiotics. For blue/white selection LB agar plates were supplemented with 40 µl X-Gal (20 µg/ml in DMF) and 4 µl IPTG (20 µg/ml in H_2O_{bidest}). The plates were incubated over night at

37°C. Colonies were picked and cells were grown in LB medium, supplemented with the appropriate antibiotics at 130 rpm, 37°C over night. The isolation of plasmid DNA was achieved by using the NucleoSpin® Plasmid-Kit and the NucleoBond® Xtra Midi Kit from Macherey-Nagel (Düren, Germany) according to the manufacturer's instructions.

Isolation of genomic DNA from *Synechocystis* sp. PCC 6803

For genomic DNA isolation 15 ml of mid-exponential cell cultures (OD_{750} = 0.5-0.8) were harvested by centrifugation (10 min, 4°C, 4000 rpm, Rotor A-4-62, Eppendorf 5810 R). The pellet was resuspended in 200 µl TEN buffer (10 mM Tris/HCL, pH 7.6, 150 mM NaCl, 10 mM EDTA). After addition of 10 µl lysozyme (20 mg/ml; SERVA Electrophoresis GmbH, Heidelberg, Germany), the samples were mixed and incubated for 15 min at 37°C. 5 µl of 10% sodium dodecyl sulfate (SDS) was added and mixed by inverting the tube. After addition of 5 µl protease K (20 mg/ml; Fermentas, St. Leon-Rot, Germany), the samples were incubated for 1 h at 60°C. 200 µl TEN buffer and 400 µl phenol (pH 8; Sigma-Aldrich, Hannover, Germany) were added and mixed by inverting continuously for 5 min. Phase separation was carried out by centrifugation (3 min, RT, 13 000 rpm). The supernatant was transferred to a new tube and mixed with 300 µl of phenol/chloroform/IAA (25:24:1) by inverting continuously for 5 min. After centrifugation, the DNA containing supernatant was transferred to a new tube and mixed with 1/10 of sodium acetate (3 M, pH 5) and 400 µl EtOH (98%, -20°C) and left over night at -20°C for precipitation. After centrifugation the DNA pellet was washed twice with EtOH (70%, -20°C), dried at RT and resuspended in 30 µl H_2O_{bidest}.

Isolation of genomic DNA from *Arabidopsis thaliana*

Genomic DNA was isolated from 4-week-old *Arabidopsis* leaves. Plant material (1 leaf per plant) was frozen in liquid nitrogen and stored at -80°C. Prior to DNA isolation, plant material was ground under liquid nitrogen and supplied with 0.5 ml of DNA extraction buffer (200 mM Tris, pH 7.5, 250 mM NaCl, 25 mM EDTA, 0.5% SDS). Samples were thoroughly mixed by vortexing and incubated for 10 min at RT. The samples were supplied with 0.5 ml chloroform and mixed. After centrifugation (10 min, 4°C, 13 000 rpm), the DNA-containing supernatant was transferred to a new 1.5 reaction tube and supplied with 0.5 ml isopropanol and mixed. After centrifugation (10 min, 4°C, 13 000 rpm), the supernatant was discarded. The pellet was washed with ethanol (70%) before air-drying. Finally, the pellets were resuspended in 50 µl H_2O_{bidest} and stored at 4° C until further analysis.

2.1.2 Oligonucleotide primers

All oligonucleotide primers used in this study were purchased from Eurofins MWG Operon (Ebersberg, Germany).

Table 2: Names, stocknumbers and sequences of all primers used.

Primername	Stock No.	Sequence
Oligonucleotides used for cloning of *cph2* OE		
Cph2 OX-L	857	ACATATGAACCCTAATCGATCC
Cph2 OX-R	858	TAGATCTTGTGGCGACAACTACAC
Oligonucleotides used for cloning of *hik12* OE		
Hik12 OX-LB_neu	1008	AATCGATGCAAATCAATAACCATGTT
Hik12 OX-term	991	AAAACGCCCGGCGGCAACCGAGCGTTCATCGGTATTTTC CATAAT
Oligonucleotides used for cloning of *hik12* KO_2		
Hik12-L	441	GCTTTATTGGCTACAATG
L-KM	977	AGATTTTGAGACACAACGTGGCTTTCCCTTAAATCAC GGTCTGAG
Hik12-R	443	CTTTGAATGGTAAACTGAC
R-KM	978	GATGCTCGATGAGTTTTTCTAATTGAGCCGCTATCATAG
KM-F	850	GGAAAGCCACGTTGTGTCT
KM-R	851	TTAGAAAAACTCATCGAGCATCAAATG
Oligonucleotides used for semi-quantitative RT-PCR		
RnpB-1fw	768	TGTCACAGGGAATCTGAGGA
RnpB-2rv	769	AAGGGCGGTATTTTTCTGTG
G6PDH-1fw	766	GCAAAATCTGATGGTGTTCC
G6PDH-2rv	767	AATAACCGGCTCGTTCTTCT
CtaDI-1fw	1413	CTGGGGGCGATTAATTTTGT
CtaDI-2rv	1414	GATGCTAACACTGGGGTGGA
PsaA-1fw	772	GCACCTGCCAAGTATCTGGT
PsaA-2rv	773	GTACCC CAAACATCGGATTG
PsbA3-1fw	770	CTGAGCTTGAGGCCAAATCCTT
PsbA3-2rv	771	CTGTTCCCACAATGAAGCGCT
Cph2-qPCR-1	1850	TGCGGCTGTATCGAGAAGGT
Cph2-qPCR-2	1851	CATTCATGGGCAATGAGCAA
Hik12-qPCR-1	1852	AAACTCCTCGCTCCCTTTGG
Hik12-qPCR-2	1853	GCATTGCCTTTGACCTGACC

Other oligonucleotides used for sequencing, screenings and cloning

Psk9-fw-seq	1068	GACCGCAACTTTGACAGAT
Cph2-OX-L1	872	ACCTGGGGTTGGAAGTAG
psk9_fwfw_seq	1087	CTG TTG GTG TTA ATT CTT GCC
psk9_fw_3	1120	ACAGGAAGTGATTAACC
psk9-cph2-seq2	1166	CTG TTG CCC AGC ATT AC
Psk9_cph2-seq3	1171	AAGACTGTTGAGCACCT
psk9_cph2-Seqfw_4	1186	GACAGTGGTGCTGCTC
psk9_cph2_4.1	1205	TGGTGACGGAATCCCAC
Psk9_cph2_Seq5	1121	CACAAGGAGTTACTGCG
Hik12 SDM1	1223	GTAGTCCTAGCTAGCAACTTTAGAAATGC
Hik12 SDM2	1224	GCATTTCTAAAGTTGCTAGCTAGGACTAC
KO_Check_1	1233	CTGACCATCTCATCTGTA
KO_Check_2	1234	CAGACCGATACCAGGATC
Hik12 KOCheck_fw	1241	CATTGAACCAACTCATTA
Hik12 KOCheck_rev	1242	GGATATCCTGTAATTCTTC
M13 fw	324	GTTTTCCCAGTCACGAC
M13 rev	323	AACAGCTATGACCATGA
PGY1-fwd	262	TGACGCACAATCCCACTAT
PGY1-rev	271	AGAGAGACTGGTGATTTCAGC
CKX1-1	582	GTAGTCTGTCCAGGACTTTG
CKX2-1	583	CTCCTAACACTCCATAGAAC
CKX2 seqfw_2	859	CTTGAACCGTGTACATGTCG
CKX2 seqrev_3	860	TACTAACAAGAGGACCGTTTCG
TDNA	356	ATATTGACCATCATACTCATTC
AHK3-7 rev	907	CGTAACCATCTAACTCTGTGTC

2.1.3 Generation of mutant lines in *Synechocystis* PCC 6803

Transformation of *Synechocytis* is achieved via the uptake of DNA by type IV pili and incorporation into the host genome by homologous double recombination. *Synechocystis* cells were transformed with psk9 vector-based constructs. The psk9 vector was provided by Annegret Wilde (Justus-Liebig University, Giessen, Germany) and with pGEM-T® vector-based constructs (Promega GmbH, Mannheim, Germany).

Table 3: Overview of constructs, cloning strategies and genetic background.

Construct	Cloning strategy	Transformed in
psK9-*cph2* OE	Amplification of full length *cph2* (4015 bp) by Cph2 OX-L (857)/Cph2 OX-R (858), *Nde*I/*Bgl*II in psK9	*cph2* KO (obtained from Y. Mok Park, Korea Basic Science Institute, Daejeon, South Korea)
psk9-*hik12* OE	Amplification of full length *hik12* (2561 bp) by Hik12 OX-LB (1008)/Hik12 Ox-term (991), *Cla*I in psK9	*hik12* KO (obtained from I. Suzuki, Univ. of Tsukuba, Tsukuba, Japan)
pGEM-T-*hik12* KO_2	Amplification of flanking regions left border (436 bp, 441/977)/right border (414 bp, 978/443) and Km[R] (928 bp, 850/851) from pIGA, fusion (441/44) and ligation into pGEM-T®	Wildtype strain (obtained from K. Marin, Univ. of Cologne, Cologne, Germany)

Construction of overexpression lines

For complementation of the knockout lines, overexpression constructs of *hik12* and *cph2* were generated. Therefore, full-length coding sequences of *Synechocystis hik12* and *cph2* genes were amplified from genomic DNA of *Synechocystis* by PCR, using a proof-reading Taq-polymerase (Phusion® Taq-polymerase, Finnzymes, New England Biolabs, Ipswich, UK) and the following primers: Cph2 OX-L (857)/Cph2 OX-R (858) and Hik12 OX-LB_neu (1008)/Hik12 OX-term (991). Primer sequences are listed in Table 2, fragment sizes in Table 3. For subsequent cloning, restriction sites were introduced by oligonucleotides. *Cla*I sites were introduced at the 5' and the 3' of *hik12* coding sequence by forward and reverse primers. An *Nde*I site that overlaps with the ATG start codon of *cph2* gene was introduced by the forward primer, while *Bgl*II was introduced at the 3' end by the reverse primer. The PCR products were isolated and purified by gel extraction. Using the distinct restriction sites (*Nde*I/*Bgl*II or *Cla*I), the PCR products were ligated in the vector psk9 for chromosomal integration under the control of the petJ promotor. The ligation mixes were used for transformation of competent *E. coli* cells. The correct integration of constructs was checked by restriction analysis and DNA sequencing, prior to *Synechocystis* transformation. DNA sequencing was performed by the Agowa sequencing service (Berlin, Germany). To generate complementation lines, the *Synechocystis* knockout lines of *hik12* and *cph2* were used as parental strains for transformation with the corresponding overexpression constructs. Positive *Synecho-*

cystis transformants were selected on BG-11 agar plates containing 10 µg/ml chloramphenicole and 10 µg/ml spectinomycine as resistance marker.

Construction of knockout lines

For the analysis of the *Synechocystis* histidine kinase 12 (*hik12*, locus *sll1672*) a second independent knockout line, besides the *hik12* knockout line obtained from Dr. Iwane Suzuki (Graduate School of Life and Environmental Sciences, University of Tsukuba, Tsukuba, Japan) was generated in this study. For this purpose, a deletion mutant was generated by inserting a kanamycine resistance cassette (KM^R) as resistance gene marker, which disrupts the functionality of the corresponding gene. Chromosomal integration was accomplished by homologous recombination, by replacing the wildtype alleles with the mutated copies via double crossover. For generation of the construct, two fragments with the sizes of 436 and 414 bp, corresponding to the 5' and 3' flanking regions of the *hik12* gene, were amplified by PCR using the following primers: Hik12-L (441)/L-KM (977) and R-KM (978)/Hik12-R (443). The kanamycine resistance cassette was amplified by PCR with the primers KM-F (850)/KM-R (851) using the vector pIGA as template. pIGA contains the gene *AhpII*, coding for kanamycine resistance and was obtained from Martin Hagemann (University of Rostock, Rostock, Germany). In a fusion PCR, using the outer primers Hik12-L (441)/Hik12-R (443), all three fragments (5' flanking region, kanamycine resistance cassette and 3' flanking region) were combined by 3-fragment-PCR, resulting in one assembled construct. After isolation and purification of the assembled PCR product, the construct was ligated into the vector pGEM-T® (Promega GmbH, Mannheim, Germany) according to the manufacturer's instruction and transformed into *E. coli.* Positive transformants were identified by blue/white selection and verified by restriction analysis and DNA sequencing, prior to *Synechocystis* transformation. DNA sequencing was performed by the Agowa sequencing service (Berlin, Germany). For transformation, the *Synechocystis* wildtype strain, obtained from Kay Marin (University of Cologne, Cologne, Germany) was used. Positive *Synechocystis* transformants were selected on BG-11 agar plates containing 10 µg/ml kanamycine as resistance marker.

Stable transformation of *Synechocystis* sp. PCC 6803

Stable transformation of *Synechocystis* was performed according to Grigorieva and Shestakov (1982) with modifications. Cells were grown photoautotrophically in liquid cultures to an OD$_{750}$ of 0.5. 10 ml of the cultures were centrifuged (5 min, 28°C, 3000 rpm, Rotor A-4-62, Eppendorf 5810). The pellet was resuspended in 5 ml BG-11

medium and distributed to 5 sterile reaction tubes. DNA (3 to 5 µg of plasmid DNA) was added and the cells were incubated in darkness (wrapped in aluminium foil) at 28°C over night. 200 µl of the cell cultures were plated on BG-11 agar plates lacking any antibiotics. After 2 days of incubation under constant light with a light intensity of 20 µmol photons m^{-2} s^{-1}, the agar layer was lifted with a sterile spatula and the selection marker (1 ml of a solution containing the appropriate antibiotics at a final concentration of 15 µg/ml) was applied beneath the agar layer. Plates were incubated under continuous illumination with a light intensity of 20 µmol photons m^{-2} s^{-1}. Colonies appear after 2 to 3 weeks. Single colonies were picked and streaked out on BG-11 agar plates containing the appropriate antibiotics. For segregation of the transformants, restreaks were performed in weekly intervals for 3 to 4 weeks (successive streak purification). To verify the transformants for the presence of the overexpression construct or the absence of the WT genomic sequence in the knockout, colony PCR and PCR on isolated genomic DNA was performed.

2.1.4 Experimental conditions

In addition to photoautotrophic growth, the glucose-tolerant *Synechocystis* sp. PCC 6803 strain is capable of metabolizing exogenous glucose, e.g. in glucose-supplemented medium. Accordingly, *Synechocystis* is capable of photomixotrophic growth under light conditions (Williams, 1988) and heterotrophic growth in darkness, if provided with a daily pulse of several minutes of white light. This minimal amount of light is necessary to enable growth and survival under dark conditions and is referred to as light-activated heterotrophic growth (LAHG) (Anderson & McIntosh, 1991). Furthermore, *Synechocystis* cells can either live as single planktonic organisms or in sessile communities, called biofilms or biomats.

Photoautotrophic and photomixotrophic growth conditions

For photoautotrophic growth, *Synechocystis* cells were cultivated in liquid BG-11 medium (TES pH 8.0), in a rotary shaker at 140 rpm, 28°C and under continuous illumination with a light intensity of 20 µmol photons $m^{-2}s^{-1}$. For photomixotrophic growth, BG-11 medium was supplemented with glucose (final concentration 10 mM).

Biomatforming growth conditions

For growth conditions, which reflect the lifestyle in sessile communities, photoauto-trophically grown mid-exponential cell cultures were supplemented with glucose (final concentration 10 mM) and incubated without agitation, allowing the cells to sediment and form biomats, which is hereafter referred to as biomatforming

conditions. Under biomatforming conditions, the cells were either incubated under continuous illumination (with a light intensity of 20 µmol photons $m^{-2}s^{-1}$) or under LAHG conditions (in total darkness with 15 min light per 24 h, respectively). In this study, *hik12* mutant lines (*hik12* KO and *hik12* OE) and the corresponding wildtype were incubated under continuous illumination, while *cph2* mutant lines (*cph2* KO and *cph2* OE) and the corresponding wildtype were incubated under LAHG conditions.

2.1.5 Growth experiments

Monitoring growth under varying conditions is a fast way to screen mutant lines. Growth of wildtype and mutant strains in liquid cell cultures was monitored by measuring the increase in absorption at 750 nm (OD_{750}), during a distinct time course. Growth was analysed under photoautotrophic, photomixotrophic and under biomatforming growth conditions, the latter after resuspension of the cells. For monitoring the cell growth on plates, cells were streaked out on BG-11 agar plates with and without glucose (final concentration 10 mM). Depending on the experimental setup, the plates were grown under constant light, under complete dark conditions and/or under LAHG conditions. Cell growth was monitored by taking pictures at different timepoints.

2.1.6 Determination of cell division activity

Proliferation in *Synechocystis* cells occurs via binary fission, an asexual form of reproduction, which comprises the division process of one cell into two daughter cells. Microscopic analyses allow to distinguish between spherical single cells and dumbbell-shaped cells, which undergo separation. Photoautotrophically grown, mid-exponential cells (OD_{750} = 0.3-0.6) were distributed to sterile 1.5 ml-reaction tubes, supplied with glucose at a final concentration of 10 mM and incubated under biomat-forming conditions (without agitation, 28°C, continuous illumination with white light with an intensity of 20 µmol photons $m^{-2}s^{-1}$). The ratio of single cells and dumbbell-shaped cells, which undergo cell division was analysed microscopically before (0 d) and after 14 days of incubation under biomatforming conditions. The ratio was determined by counting 3x50 cells per strain in randomly picked areas, in 15 µl-droplets on a glass slide, thereby distinguishing between single cells and dumbbell-shaped cells. Statistic evaluation was performed using a two-tailed, unpaired Student's *t*-test.

2.1.7 G6PDH enzyme activity measurements

Enzyme activity measurements were performed to determine the specific activity of glucose-6-phosphate dehydrogenase (G6PDH).

Crude protein isolation

For crude protein isolation, cell cultures were harvested by centrifugation (10 min, 4°C, 3500 rpm, Rotor A-4-62, Eppendorf 5810). The pellet was frozen in liquid nitrogen and stored at -80°C till further processing.

Breakage buffer:	HEPES KOH pH 7.5	50 mM
	Glycerol	15% (v/v)
	EDTA pH 8.0	1 mM
	$MgCl_2$	3 mM
	DTT (Dithiothreitol)	1 mM
	PMSF (phenylmethyl-sulfonyl fluoride)	1 mM

For isolation of soluble proteins, the method of Knowles and Plaxton (2003) was used with some modifications. Cell pellets were supplied with 0.8 ml breakage buffer and allowed to thaw on ice. The samples were transferred to 2-ml-reaction tubes, containing 0.3 g glass beads ($\varnothing$ 0.25-0.50 mm; Roth, Karlsruhe, Germany) and frozen in liquid nitrogen. The samples were allowed to thaw in an ultrasonic bath (Bandelin Sonorex RK 100, Berlin, Germany) for 1.5 min. The samples were briefly vortexed and frozen again in liquid nitrogen. After repeating the freeze and thaw cycle three times, debris was removed by centrifugation (10 min, 4°C, 12 000 *g*) and the supernatant was transferred to a new reaction tube and kept on ice.

Determination of the protein content

The protein content of the samples was determined using the Bradford-Assay (Bradford, 1976). BSA (bovine serum albumine, Sigma-Aldrich, Hannover, Germany) was used to create a calibration curve. Bradford solution (BioRad Laboratories, Munich, Germany) diluted at the ratio of 1:4 with H_2O_{dest}, was mixed with increasing BSA concentrations (5, 10, 20 and 30 µg BSA) in total volume of 1 ml for measurements in a spectrophotometer (Uvikon 931, Kontron Instruments, Rossdorf, Germany) or with BSA concentrations of 1, 2, 4 and 6 µg BSA in a total volume of 200 µl for measurements in a microplate reader (Tecan Infinite, Crailsheim, Stuttgart,

Germany) to create the calibration curve. The absorption was measured at a wavelength of 595 nm. Bradford solution without BSA was used as blank reference. The protein content of the samples was calculated using the BSA calibration curve.

G6PDH enzyme activity measurements

In this direct spectrophotometric assay, the specific activity of G6PDH was determined. As key metabolic enzyme of the oxidative pentose phosphate pathway, G6PDH converts glucose-6-phosphate into 6-phosphogluconolactone by reducing $NADP^+$ to NADPH. As the coenzyme strongly absorbs UV light at 340 nm only in its reduced form, the course of the reaction can be measured by following the change in absorbance at 340 nm.

The reaction mix contained 50 mM HEPES KOH (pH 8.0), 10 mM $MgCl_2$*6 H_2O, 0.4 mM NADP, 5 mM G6P and 100 µg of crude protein in a final volume of 1 ml for measurements in a spectrophotometer (Uvikon 931, Kontron Instruments, Rossdorf, Germany) or 20 µg of total protein in a final volume of 200 µl per well (96-well microplates, Greiner Bio-one, Frickenhausen, Germany) for measurements in a microplate reader (Tecan Infinite, Crailsheim, Germany). The reaction was started by addition of glucose-6-phosphate (G6P). H_2O_{bidest} replaced G6P as substrate control. The samples were measured by reading the absorbance at 340 nm for 10 min in 20 sec intervals. The specific enzyme activity A_{spec} was calculated with the following equation after Lambert-Beer-Law:

$$A_{spec} \text{ unit mg}^{-1} = \frac{\Delta_{slope} \text{ min}^{-1} * V_{cuvette} \text{ l}^{-1}}{\varepsilon \text{ mM}^{-1}\text{cm}^{-1} * \text{d cm}^{-1} * \text{protein mg}^{-1}}$$

$\varepsilon = 6.22 \text{ mM}^{-1}\text{cm}^{-1}$, molar extinction coefficient

$\Delta_{slope} = $ initial linear increase of A_{340}

Statistic evaluation was performed using a two-tailed, unpaired Student's *t*-test.

2.1.8 Glycogen determination

The glycogen content in *Synechocystis* cells was quantified using anthrone reagent according to Schneegurt and co-workers (1994) with modifications. 2 ml cell culture were harvested by centrifugation (10 min, RT, 15 000 *g*), washed twice with H_2O_{bidest} and resuspended in 0.2 ml H_2O_{bidest}. After addition of 0.4 ml of 40% KOH, the samples were boiled in a thermo-block (Biometra, Göttingen, Germany) at 90°C for 1 h. After cooling down, the samples were supplemented with 1.2 ml of EtOH (98%) and stored over night at -20°C. After centrifugation (30 min, RT, 15 000 *g*) and

removing the supernatant, pellets were dissolved in 0.1 ml of H_2SO_4 (conc.) and incubated for 10 min at RT. After filling up to 1 ml with H_2O_{bidest}, 0.5 ml of each sample was mixed with 1 ml anthrone reagent (0.2% anthrone [9,10-dihydro-9-oxoanthracene] Sigma-Aldrich, Hannover, Germany, in sulfuric acid) and incubated for 10 min at 90°C. Muscle glycogen (Sigma-Aldrich, Hannover, Germany) was used as reference. For this purpose, muscle glycogen (5, 10, 30 and 60 µg glycogen, dissolved in H_2O_{bidest}) was supplemented with 0.1 ml H_2SO_4 (conc.), filled up with H_2O_{bidest} to 0.5 ml and treated similar to the samples. After samples have been cooled down to RT, the absorbance at 625 nm was measured in a spectro-photometer (Amersham Pharmacia ULTRO-SPEC III spectral-photometer, Hertford-shire, GB) in a quartz cuvette against H_2O_{dest}. Specific glycogen contents were given as µg glycogen per OD_{750}. Statistic evaluation was performed using a two-tailed, unpaired Student's *t*-test.

2.1.9 Measurement of P700 reduction kinetics

Chlorophyll a fluorescence measurements were conducted using Pulse-Amplitude-Modulation (PAM) fluorometry. In order to analyse electron flows at PS I, reduction kinetics of P700, were recorded in presence and absence of specific electron transport inhibitors. Photoautotrophically grown, mid-exponential cell cultures were set to an OD_{750} of 0.6 and adapted to biomatforming conditions for 24 h, either under continuous illumination (*hik12* KO, *hik12* OE and corresponding WT) or in total dark-ness (*cph2* KO, *cph2* OE and corresponding WT). Measurements were taken before the addition of glucose and the transition to biomatforming conditions and after 24 h of incubation under biomatforming conditions (24 h), in presence of glucose at a final concentration of 10 mM, without agitation and under continuous illumination with a light intensity of 20 µmol photons m^{-2} s^{-1}or in complete darkness). By applying specific inhibitors (Table 4) different components of the electron transport chain can be blocked. 3-(3,4-dichlorophenyl)-1,1-dimethylurea (DCMU) inhibits PS II by blocking the plastoquinone-binding site, thereby inhibiting the linear electron flow. 2,5-dibromo-3-methyl-6-isopropyl-*p*-benzoquinone (DBMIB) inhibits the electron transport chain by preventing the re-oxidation of plastoquinone by the cytochrome b_6f complex. Inhibitors used were provided by Sigma-Aldrich (Hannover, Germany).

Table 4: Inhibitors used in PAM measurements for P700$^+$ reduction kinetics.

Inhibitor	Final concentration	Dissolved in
DCMU	10 µM	EtOH (98%)
DBMIB	60 µM	EtOH (98%)

Reduction kinetics of oxidized P700 (P700$^+$) in adapted wildtype and mutant cells were recorded *in vivo* with a dual PAM-100 measuring system (Heinz Walz GmbH, Effeltrich, Germany) equipped with a standard emitter-detector unit DUAL-E and detector unit Dual-DB and the data acquisition software DualPAM. Blue actinic illumination at 460 nm was provided by a LED lamp with max. 700 µmol m^{-2} s^{-1} PAR. *Synechocystis* cell cultures (set to an OD$_{750}$ of 0.6 at timepoint 0 h) were placed in an emitter-detector cuvette assembly unit (ED-101US/MD) at the growth temperature of 28°C. An automated script file for sequential measurements was programmed. A schematic illustration of a measurement sequence is displayed in Figure 4.
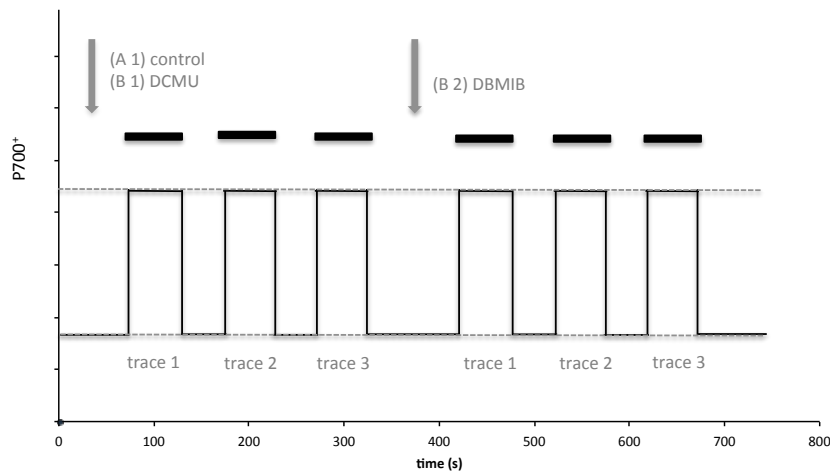
Figure 4: Schematic illustration of a P700$^+$ reduction kinetic measurement sequence.
Black rectangles indicate the 60-s light pulses of blue actinic illumination. Dashed lines indicate completely oxidized (upper line) and reduced (lower line) P700. Grey arrows indicate the addition of inhibitors before and during the measurement.

Complete P700$^+$ oxidation was achieved by 60 s blue light pulses with an intensity of 700 µmol photons m^{-2}s^{-1}. The light pulses of actinic illumination (indicated by black bars) were followed by the reduction of P700$^+$ in the dark. Dashed lines indicate completely oxidized (upper line) and reduced (lower line) P700. The measurement implies 2x3 individual single traces. In the first half of the measurement, the P700$^+$ reduction kinetics were recorded either in absence of an inhibitor (A1 control) or in presence of DCMU (B1 DCMU). After a 120 s break, in the second half of the measurement, the reduction kinetics were recorded after addition of a second inhibitor (B2 DBMIB). Resulting data were analysed as described by Tsunoyama *et al.,* (2009) and Bernát *et al.,* (2009). Rate constants (*k*) in presence and absence of specific inhibitors, respectively, were determined by fitting the decays with single exponential functions according to the following equation:

$$y = A1e^{-kt} + y0 \; \text{ with } \text{k} = \frac{1}{t1}$$

The half-life ($t_{1/2}$) of the re-reduction of P700$^+$ gives an indication of the rate of electron donation to PS I (Howitt *et al.,* 2001). Given the rate constant *k* and *ln* (2), $t_{1/2}$ for each decay was determined:

$$t_{1/2} = \frac{ln(2)}{k}$$

For statistical analysis an ANOVA test was performed, combined with a post-hoc Tukey's highly significant difference (HSD) test at *P* = 0.05. The evaluation was performed using the program IBM SPSS Statistics 19.

2.1.10 ROS detection by luminol-based assay

Luminol-based assays were used to detect ROS generation in cyanobacterial cell cultures in presence and absence of 10 mM glucose. Luminol (5-amino-2,3-dihydro-1,4-phthalazinedione; Sigma-Aldrich, Hannover, Germany) is stepwise oxidized to aminophtalate. When the excited aminophtalate returns into its ground state, blue light of 428 nm is emitted. This chemoluminescence reaction can be detected by a highly sensitive microtiter plate luminometer (Dynatech Laboratories, Houston, Texas, USA). 100 µl of cyanobacterial cell culture were added to the wells of a 96-well multi-titer plate (Greiner Bio-one, Frickenhausen, Germany) containing 150 µl of the reaction mixture (0.02 mM luminol, horseradish peroxidase at 0.02 U/ml and 5 mM sodium phosphate buffer at pH 8). Chemoluminescence was followed for 60 min at 150 s intervals. Recordings of relative luminescence kinetics were plotted over time.

2.1.11 Genexpression analysis

Isolation RNA from *Synechocystis*

Total RNA of *Synechocystis* was isolated according to McGinn and co-workers (2003) with modifications. 10-25 ml of photoautotrophically grown, mid-exponential cell culture was mixed with the same volume of a pre-cooled stop solution (5% [v/v] acidic phenol, 95% [v/v] ethanol). After centrifugation (15 min, 4°C, 3500 rpm, Rotor A-4-62, Eppendorf 5810), the supernatant was discarded and the pellet was washed twice with 0.5 ml STE buffer (50 mM Tris/HCl, pH 8.0, 5 mM EDTA, 0.5% SDS) and stored at -70°C. For RNA isolation the pellets were allowed to thaw on ice and resuspended in pre-cooled STE buffer. After addition of 0.5 ml phenol (prewarmed at 65°C), the samples were mixed by vortexing and incubated at 65°C for 15 min. Phase separation was carried out by centrifugation (15 min, 4°C, 13 000 rpm). The supernatant was transferred to a new reaction tube and mixed with 0.4 ml phenol by

vortexing, followed by centrifugation. The phenol treatment was repeated twice. After transferring the aqueous phase to a new reaction tube, 0.4 ml phenol/chloroform (1:1, [v/v]) was added. After centrifugation, 0.3 ml chloroform was added to the supernatant, followed by mixing and centrifugation. The RNA containing supernatant was transferred to a new reaction tube and mixed with 20 µl sodium acetate (3 M, pH 4.0) and 0.4 ml EtOH (98%, -20°C) and left over night at -20°C for precipitation. After centrifugation and washing the pellet twice with EtOH (80%), the pellets were dried at RT and subsequently resuspended in 30 µl DEPC-treated H_2O. At this stage, the isolated RNA was stored at -70°C. The quantity and purity of the RNA was determined photometrically by absorption at 260 and 280 nm using NanoDrop® (Peqlab Biotechnology, Erlangen, Germany) and by denaturing gel electrophoresis.

Denaturing agarose gel electrophoresis

Denaturing gel electrophoresis was used to analyse the quality and quantity of the isolated RNA. 1.2% agarose (w/v) was heated in 1x MOPS buffer until the agarose was completely melted. Before polymerization, 5% formaldehyde (w/v) (Roth GmbH, Karlsruhe, Germany) was added. 1 µg of RNA, supplemented with RNA loading buffer (Fermentas, St. Leon-Rot, Germany) was denatured at 95°C for 5 min and loaded on the gel. Voltage application was set to 90 V for 35 min. For documentation DeVision G camera and software (Decon, Hohengandern, Germany) was used.

MOPS buffer (10x)	3-(N-morpholino)propan sulfonic acid	200 mM
	Sodium acetate	50 mM
	EDTA	10 mM
	ad H_2O_{DEPC}	1 l

DEPC-treated water (H_2O_{DEPC}): autoclaved H_2O_{bidest} was supplied with 0.1% (w/v) DEPC (diethylenepyrocarbonate) and incubated at RT for 2 h under agitation. The solution was incubated at 37°C over night and autoclaved thereafter.

cDNA synthesis and semi-quantitative RT-PCR

To analyse gene expression semi-quantitative two-step reverse-transcription polymerase chain reactions (RT-PCR) was performed. cDNA was generated using the QuantiTect® Reverse Transcription Kit (QIAGEN, Hilden, Germany) according the manufacturer's instructions. 1 µg of the isolated RNA was reversely transcribed to first strand cDNA. 500 ng of the first strand cDNA was subsequently used as template for PCR amplification with gene-specific primers. As control for constitutive gene expression, a house-keeping gene *RnpB* (*slr0249*), encoding for the RNase P

subunit B was used. Optimal PCR cycle numbers varied between 31 to 32 cycles (31 cycles for *PsaA,* 32 cycles for *RnpB*, *Zwf*, *CtaDI*, *PsbA3*, 33 cycles for *Cph2* and 36 cyles for *Hik12*).

Table 5: Target genes, functions, forward (fw) and reverse (rv) primer sequences, product sizes and optimal annealing temperatures.

Gene	Function	Primer name	Primer sequence	T (°C)	size (bp)
slr0249 (*RnpB*)	RNaseP subunit B	RnpB-1fw RnpB-2rv	TGTCACAGGGAATCTGAGGA AAGGGCGGTATTTTTCTGTG	54.5	88
slr1843 (*Zwf*)	G6PDH	G6PDH-1fw G6PDH-2rv	GCAAAATCTGATGGTGTTCC AATAACCGGCTCGTTCTTCT	54.5	105
slr1137 (*CtaDI*)	Cyt c-ox subunit I	ctaDI-1fw ctaDI-2rv	CTGGGGGCGATTAATTTTGT GATGCTAACACTGGGGTGGA	54.5	117
slr1834 (*PsaA*)	P700 subunit Ia	PsaA-1fw PsaA-2rv	GCACCTGCCAAGTATCTGGT GTACCC CAAACATCGGATTG	54.0	98
sll1867 (*PsbA3*)	PSII/D1	PsbA3-1fw PsbA3-2rv	CTGAGCTTGAGGCCAAATCCTT CTGTTCCCACAATGAAGCGCT	54.0	102
sll0821 (*Cph2*)	Cph2	Cph2-1fw Cph2-2rv	TGCGGCTGTATCGAGAAGGT CATTCATGGGCAATGAGCAA	55.5	166
sll1672 (*Hik12*)	Hik12	Hik12-1fw Hik12-2rv	AAACTCCTCGCTCCCTTTGG GCATTGCCTTTGACCTGACC	56.0	170

Table 6: Reaction mix and PCR program used for semi-quantitative RT-PCR.

Components	Volume		Temperature	Time
Buffer (10x)	2.5 µl	Initial denaturation	95°C	5 min
dNTPs (2 mM)	2.5 µl	Denaturation	95°C	30 sec
Primer 1 (10 pmol)	1.5 µl	Annealing	54.0-54.5°C [1]	30 sec
Primer 2 (10 pmol)	1.5 µl	Elongation	72°C	1 min
template cDNA (500 ng/µl)	1.0 µl	Final Elongation	72°C	5 min
Taq-DNA-Polymerase	0.15 µl			
$H_2O_{bidest.}$	ad 25 µl			

[1] All annealing temperatures used for semi-quantitative RT-PCRs performed here, varied between 54.0 and 54.5°C, depending on the melting temperatures of the specific primers.

2.2 Plants and pathogens

2.2.1 Plant material

Hordeum vulgare

The barley (*Hordeum vulgare* L.) cultivar Pallas, provided by Lisa Munk (Royal Veterinary and Agricultural University, Copenhagen, Denmark) was used for gene function analysis in transient transformation assays. Barley plants were grown for 7 days in a growth chamber (Conviron, Winnipeg, Canada or Sanyo, Munich, Germany) at 18°C, with relative humidity of 65% and a photoperiod of 16 h light irradiance at 90 µmol photons $m^{-2}s^{-1}$. For cultivation of barley plants soil Typ ED 73, (Einheitserde- und Humuswerke, Gebr. Patzer GmbH & Co. KG, Sinntal-Jossa, Germany) was used.

Arabidopsis thaliana

An *Arabidopsis* T-DNA insertion line, deficient in the cytokinin receptor AHK3 (locus *At1g27320*) was analysed in pathogen assays. The AHK3-deficient (loss-of-function) T-DNA-insertion line was acquired from the Nottingham *Arabidopsis* Stock Centre (NASC, Loughborough, UK; accession no. NASC N 6562). The *ahk3-1* allele contains a T-DNA insertion in the 4th intron, which is adjacent to exons encoding the third transmembrane segment. *Arabidopsis Wasilewska* (*Ws*), provided by Erwin Grill (Chair of Botany, Technische Universität München, Munich, Germany) was used as wildtype in all experiments performed. *Arabidopsis* seeds were incubated for 24 h in H_2O_{dest} at 4°C for stratification prior sewing into soil. For cultivation, soil (Fruhstofer Erde, Typ P, Vechta, Germany) was mixed with sand (Quarzsand, granulation: 0.1-0.5 mm Sakret$^{®}$ Trockenbaustoffe Europa GmbH & Co. KG, Wiesbaden, Germany) in a ratio of 2:1. *Arabidopsis* plants were cultivated in a growth chamber (Conviron, Winnipeg, Canada) at 22°C with a relative humidity of 64% and a photoperiod of 10 h light irradiance at 120 µmol photons $m^{-2}s^{-1}$.

2.2.2 Pathogens and inoculation procedures

Blumeria graminis f. sp. hordei (Bgh)

The powdery mildew fungus *Blumeria graminis* forma specialis *hordei* (*Bgh*) race A6, provided by Jörn Pons-Kühnemann (Justus-Liebig Universität, Giessen, Germany) was used to inoculate transiently transformed barley leaves. *Bgh* was maintained on *Hordeum vulgare* cultivar Golden Promise in climate chambers (Conviron, Winnipeg, Canada or Sanyo, München, Germany) at 18°C, with relative humidity of 65% and a

photoperiod of 16 h light irradiance at 90 µmol photons $m^{-2}s^{-1}$. Transiently trans-
formed barley leaf segments were fixed with the abaxial side up on 0.5% (w/v) water
agar. The inoculation was accomplished under a tent-like frame by evenly spreading
the fungal spores, giving a density of 150 conidia/mm^{-2}.

Pseudomonas syringae pv. *tomato* (*Pst*) DC3000

Pseudomonas syringae pv. *tomato* (*Pst*) strain DC3000 was provided by Jörg Durner
(Helmholtz Zentrum, Munich, Germany). For cultivation and maintainance, bacteria
cells were grown on solid King's B medium, containing 50 µg/ml rifampicine and 25
µg/ml tetracycline, and incubated at 28°C for 3 days. Afterwards, the plates were
stored at 4°C and streaked out at 4-week intervals. For cultivation in liquid cultures
cells were grown in King's B medium, supplemented with the appropriate antibiotics,
at 150 rpm, at 28°C for 2 days.

King' s B medium	Difco protease peptone	10 g
	K_2HPO_4	1.5 g
	Glycerol	1.5 g
	Agar (for plates only)	15 g
	ad H_2O_{dest}	1 l
	use HCl to adjust to pH 7.0	

After autoclaving (121°C, 20 min), the medium was supplemented with filter-
sterilized $MgSO_4*7\ H_2O$ (final concentration 5 mM) and the antibiotics rifampicine
(dissolved in DMSO; final concentration 50 µg/ml,) and tetracycline (dissolved in
EtOH [70%], final concentration 25 µg/ml).

For pathogen assays, the optical density of the *Pst* cell culture was determined
photometrically (Amersham Pharmacia ULTROSPEC III spectralphotometer,
Hertfordshire, GB) at a wavelength of 600 nm. An OD_{600} of 0.2 is equivalent to 10^8
cfu ml^{-1}. The bacterial suspension was diluted to 10^4 cfu ml^{-1} in 10 mM $MgCl_2$ and
used for inoculation. Mature leaves of 6-week old *Arabidopsis* plants were infiltrated
at the abaxial sites with 20 µl of the bacterial suspension using a needleless syringe.
Control leaves were mock infiltrated with 10 mM $MgCl_2$. The infiltrated plants were
incubated at 20°C, covered with a transparent plastic dome to maintain high
humidity. To determine bacterial proliferation, one infiltrated leaf per plant was
harvested at 0, 2, 4 and 8 dai (days after infiltration). The marked infiltrated areas
were excised and scaled. After washing with EtOH (70%), the infiltrated area of each

leaf was ground with a small pistil in 200 µl 10 mM $MgCl_2$. Dilution rows (1:10, 1:100, 1:1000 and 1:10 000) were prepared for each sample and dropped in 7x10 µl droplets on King's B medium agar plates. The dilution of 1:10 000 was used for the evaluation. After 2 days of incubation at 28°C, bacterial colonies were counted and the quantity of bacteria per gram of leaf material was evaluated. Statistic evaluation was performed using a two-tailed, unpaired Student's *t*-test. Infiltration assays as described above were also performed on detached *Arabidopsis* leaves. The infiltrated leaves were placed on water agar (0.5% [w/v]) and kept under light (10 h light irradiance at 120 µmol photons $m^{-2}s^{-1}$) or dark conditions. The development of the disease symptoms was monitored and pictures were taken at different timepoints.

2.2.3 Transient transformation of barley epidermal cells

Construction of pGY1-AtCKX1 and pGY1-AtCKX2

The cDNAs of AtCKX1 (*At2g41510*) and AtCKX2 (*At2g19500*), coding for two cytokinin oxidases in *Arabidopsis*, cloned into the pCR-BluntII-TOPO vector (Invitrogen, Darmstadt, Germany), were obtained from Thomas Schmülling (FU Berlin, Berlin, Germany) (Schmülling *et al.,* 2003). The coding sequences of AtCKX1 and AtCKX2 were released with Sal*I* (AtCKX1) and Eco*RI* (AtCKX2) from the pCR-BluntII-TOPO vector and subcloned via *Sal*I (AtCKX1) and blunt-end via *Sma*I (AtCKKX2) into the plant expression vector pGY1. pGY1 was provided by Patrick Schweizer (Leibniz-Institut für Pflanzengenetik und Kulturpflanzenforschung, Gatersleben, Germany). Prior to ballistic delivery into barley epidermal cells, pGY1-AtCKX1 and pGY1-AtCKX2 were sequenced to verify the correct insertion of the coding sequences into the vector. Sequencing was performed by the Agowa sequencing service (Berlin, Germany). Primer sequences are listed in Table 2.

Preparation of tungsten particles

Tungsten particles were used as microcarriers in transient transformation assays. 50 mg tungsten particles were mixed with 1 ml H_2O $_{bidest}$ and incubated for 20 sec in an ultrasonic bath. After centrifugation (1 min, RT, 11 000 *g*), the supernatant was removed and this process was repeated once with water and then twice with EtOH (98%). Particles were allowed to dry for 10 min by incubation at 80°C in a thermoblock. To set a final concentration of 25 mg/ml, particles were resuspended in 2 ml of 50% (v/v) glycerol and 0.1% (v/v) DEPC. After 1 h of incubation on a shaker at 37°C, the particles were incubated for 30 min at 100°C in a thermo-block to inactivate DEPC. Before coating the tungsten particles with plasmid DNA, the particles were

incubated for 10 min in an ultrasonic bath for separation. The plasmids containing the reporter gene (GFP under control of CaMV 35S promotor), together with pGY1-AtCKX1, pGY1-AtCKX2 or empty pGY1 vector control, were added to 12.5 µl of tungsten particles (25 mg/ml). To attach the plasmids to the particles, 12.5 µl calcium chloride (20 mM $CaCl_2$, pH 10) was added drop by drop during continuous vortexing. After 10 min of incubation at RT, the coated particles were spun down and the supernatant was removed. 6 µl of coated tungsten particles per shot remained in the reaction tube.

Table 7: Components per volume/shot.

Component	Volume/shot
Tungsten particles (25 mg/ml)	12.5 µl
Plasmid with reporter gene	0.5 µg
Plasmid with gene of interest/empty vector control	1 µg
20 mM $CaCl_2$ (pH 10)	12.5 µl

Ballistic transformation

For transient transformation of barley epidermal cells, leaf segments of 7-day-old barley plants were placed on petri dishes containing 0.5% (w/v) water agar. The segments were fixed with the abaxial site up. Petri dishes with the fixed leaf segments were placed in the Particle Inflow Gun (Finer *et al.*, 1992), where the bombardment took place under the negative pressure of -0.9 bar vacuum and 8.5 bar helium gas pressure. Right after particle bombardment, the leaf segments were incubated in a growth chamber at 18°C, with relative humidity of 65% and a photoperiod of 16 h light irradiance at 90 µmol photons $m^{-2}s^{-1}$. To allow progression of overexpression, the inoculation with *Bgh* spores was conducted 4 h after bombardment as described in Section 2.2.2.

Microscopic analysis and evaluation of penetration efficiency

48 h after inoculation the penetration efficiency of *Bgh* spores on transformed epidermal cells, was analysed using fluorescence and brightfield microscopy using a Leica DM 1000 microscope (Leica microsystems, Wetzlar, Germany). Transformed cells, expressing the green fluorescent protein (GFP) were evaluated for penetration efficiency, distinguishing between attacked and successfully penetrated cells (haustorium-containing cells) and attacked and non-penetrated cells (papilla forming cells). For each individual variant, a minimum of 80 interactions was evaluated. The

quotient of all penetrated cells and all attacked (penetrated and non-penetrated) cells multiplied by 100 describes the penetration efficiency. Statistic evaluation was performed using a two-tailed, paired Student's *t*-test.

2.2.4 ROS detection by luminol-based assay

Luminol-based assays were used to detect ROS production in plants. *Arabidopsis* leaves of 6 week old plants were harvested and cut in small square pieces of 4 mm^2 in size and incubated floating on water over night in a climate chamber at 22°C with a relative humidity of 64% and a photoperiod of 10 h light irradiance at 120 µmol photons m^{-2}s^{-1}. Prior to the measurement, 2 leaf pieces each were transferred to the wells of a 96-well multi-titer plate (Greiner Bio-one, Frickenhausen, Germany) containing 200 µl of the luminol reaction mixture (0.02 mM luminol, horseradish peroxidase at 0.02 U/ml and 5 mM sodium phosphate buffer at pH 8). Measurements were taken in presence and absence of 10 mM glucose. Chemoluminescence was followed for 60 min at 150 s intervals. Recordings of relative luminescence kinetics were plotted over time.

3 Results

3.1 Functional characterisation of CPH2, a phytochrome photoreceptor in *Synechocystis* sp. PCC 6803

In order to characterise the physiological function of the *Synechocystis* phytochrome photoreceptor CPH2 (*sll0821*), a knockout mutant and the corresponding complementation line were analysed under different growth conditions. *Synechocystis* sp. PCC 6803 cells (hereafter referred to as *Synechocystis*) are able to live as single, planktonic organisms or in sessile communities, the so-called biofilms or biomats. This study was aimed at elucidating the function of CPH2 with a special focus on its effect on the central carbon metabolism during the transition from fast exponential growth to slowed down growth and high cellular density within a biomat.

3.1.1 Generation of *cph2* complementation lines

Two independent *cph2* knockout lines (*cph2-1* and *cph2-2*) and the corresponding glucose-tolerant, parental wildtype strain were provided by Dr. Young Mok Park (Korea Basic Science Institute, Daejeon, South Korea). The knockout lines were generated by inserting a spectinomycine resistance cassette into the coding region of *Cph2* gene, thereby disrupting the functionality of the gene (Moon *et al.,* 2011). In this study, the *cph2*-overexpression line was generated in the *cph2-2* background for functional complementation of the knockout line with a full-length wildtype *cph2* coding sequence under control of the constitutive petJ promotor (Figure 5 A). The *cph2* full length coding sequence was amplified by PCR using Cph2 OX-L (P1)/Cph2 OX-R (P2) primers, thereby introducing *Nde*I (5' end) and *Bgl*II (3' end) restriction sites for subsequent cloning into the vector psk9 (Figure 5 A). Stable transformation of *Synechocystis* via chromosomal integration was performed essentially according to Grigorieva and Shestakov (1982), as described in detail in Section 2.1.3. For complementation, the *cph2* knockout line 2 (*cph2-2*) was used as parental strain. Transformation resulted in five chloramphenicole-resistant colonies. After restreaking on selective media for segregation, the analysis of the transformants by PCR, using the primers psk9-fw-seq (P3) and Cph2-OX-L1 (P4) (Figure 5 A), led to the identification of four mutants, *cph2* OE1, 2, 7 and 8, carrying the OE construct (Figure 5 B). Primer sequences are given in Table 2. Gene expression analysis using semi-quantitive reverse transcription polymerase chain reaction (RT-PCR) confirmed the overexpression of *cph2* (Figure 5 C). The parental strain, *cph2-1* and

cph2-2 knockouts and the *cph2* complementation/overexpression mutants are in the following referred to as WT, *cph2* KO 1, *cph2* KO 2 and *cph2* OE, respectively.
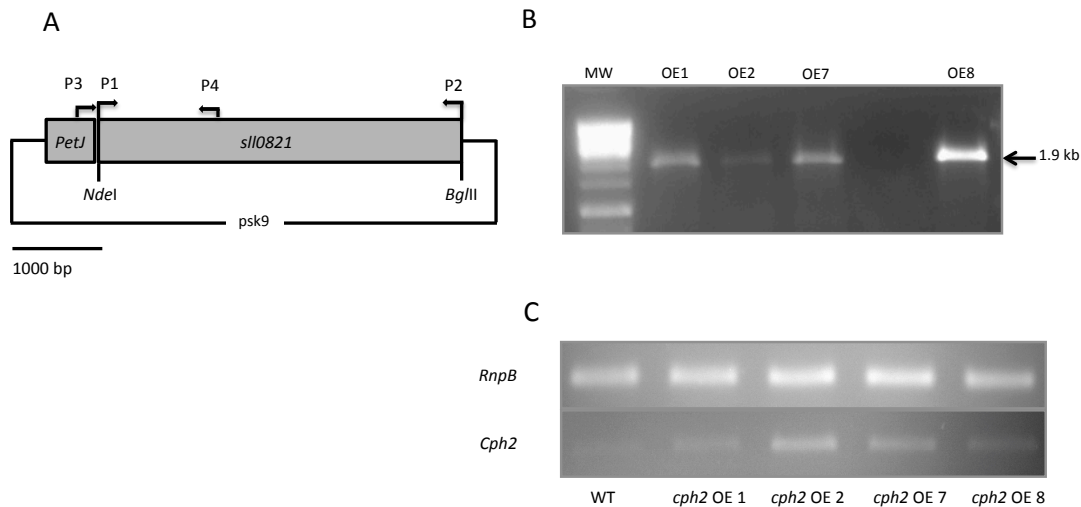

Figure 5: Generation of *cph2* overexpression construct (A), verification of successful genomic integration (B) and transcript overexpression of *cph2* (C).

(A) *Cph2* overexpression construct used for *Synechocystis* transformation. Primer P1/P2 used for amplification of full length *cph2* (4015 bp) and Primer P3/P4 used for verification of the correct insertion in the transformants are indicated. Restriction sites used for cloning: *Nde*I and *Bgl*II.

(B) Verification of positive genomic integration of the construct in four transformants (designated as *cph2* OE1, OE2, OE7 and OE8) by PCR on genomic DNA (estimated fragment size: 1986 bp, black arrow). For complementation, the *cph2* knockout line 2 (*cph2-2*) was used as parental strain. MW, molecular mass standard.

(C) Verification of *cph2* overexperession by semi-quantitative RT-PCR. Total RNA of WT and *cph2* OE clone 1, 2, 7 and 8 was isolated. After reverse transcription, 500 ng of first strand cDNA was used as template for PCR (33 cycles for *RnpB* and *Cph2*). PCR products were analysed on a 1.5% agarose gel and stained with ethidium bromide. The constitutively expressed RNase P gene (*RnpB*) was included as control.

3.1.2 Growth characteristics: *cph2* KO is impaired in growth under biomatforming conditions

Besides photoautotrophic growth, certain strains of *Synechocystis* are capable of mixotrophic growth in presence of metabolizable sugars, e.g. glucose (Williams, 1988). These glucose-tolerant *Synechocystis* strains are capable to grow photomixo-trophically under light conditions, as well as heterotrophically in darkness, if supplied with glucose and a daily pulse of white light of about 5 min at least. The latter type of growth is referred to as light-activated heterotrophic growth (LAHG) (Anderson & McIntosh, 1991). To provide insights into growth characteristics and to screen for physiological effects of the non-functionality of *Cph2*, growth of WT and *cph2* KO and OE strains was analysed under different growth conditions (photoautotrophic, photomixotrophic and LAHG/biomatforming conditions).

To analyse growth under photoautotrophic or photomixotrophic growth conditions, photoautotrophically grown precultures of WT, *cph2* KO and OE strains were diluted to an initial OD_{750} of 0.3 and incubated at 140 rpm, 28°C, under continuous illumination with a light intensity of 20 µmol photons m^{-2} s^{-1} and in presence (photo-mixotrophic) or absence (photoautotrophic) of 10 mM glucose. In photoautotrophic cultures, growth was monitored by daily measurements of OD_{750} in a time course from 0 to 4 days. Due to the acceleration of growth after addition of glucose in mixotrophic cultures, OD_{750} was recorded in a time course from 0 to 9 hours in measuring intervals of 3 hours. For growth under biomatforming conditions, cultures of WT, *cph2* KO and *cph2* OE were grown photoautotrophically to an OD_{750} of 0.6-0.8. After addition of glucose (final concentration 10 mM), the cell cultures were incubated without agitation, allowing the cells to sediment and form biomats for 96 h (hereafter referred to as biomatforming conditions). Under biomatforming conditions, WT, *cph2* KO and OE strains were incubated in darkness with 15 min light per 24 h, respectively, which is considered as LAHG conditions (Anderson & McIntosh, 1991; Tabei *et al.,* 2009). To determine the growth of the biomats, the cells were resuspended at 0, 48 and 96 h and the OD_{750} was determined.

The growth kinetics of WT, *cph2* KO and OE strains are presented in Figure 6. Under photoautotrophic growth conditions (A), WT, *cph2* KO and *cph2* OE grew at similar rates. The accelerated growth under photomixotrophic growth conditions (B) compared to photoautotrophic conditions, indicated that WT, *cph2* KO and *cph2* OE are capable to utilise exogenous glucose and therefore are capable of photo-mixotrophic growth. However, no significant differences in growth of WT, *cph2* KO and *cph2* OE were detectable under both conditions. In contrast, incubation without agitation under LAHG conditions (C) resulted in growth cessation of *cph2* KO, which becomes further obvious in the comparison of the slopes (m) between 0-48 h ($m_{WT, 0-48 h}$ = 0.010 ± 0.001, $m_{cph2 KO, 0-48 h}$ = 0.007 ± 0.0004, $m_{cph2 OE, 0-48 h}$ = 0.012 ± 0.001) and between 48-96 h ($m_{WT, 48-96 h}$ = 0.004 ± 0.001, $m_{cph2 KO, 48-96 h}$ = 0.001 ± 0.0004, $m_{cph2 OE, 48-96 h}$ = 0.004 ± 0.002). The complementation of *cph2* KO 2 with the *cph2* overexpression construct (*cph2* OE clone 8) resulted in growth kinetics similar to those observed for the WT under LAHG/biomatforming conditions, thereby indicating that the growth phenotype of *cph2* KO was due to the deletion of *Cph2*.
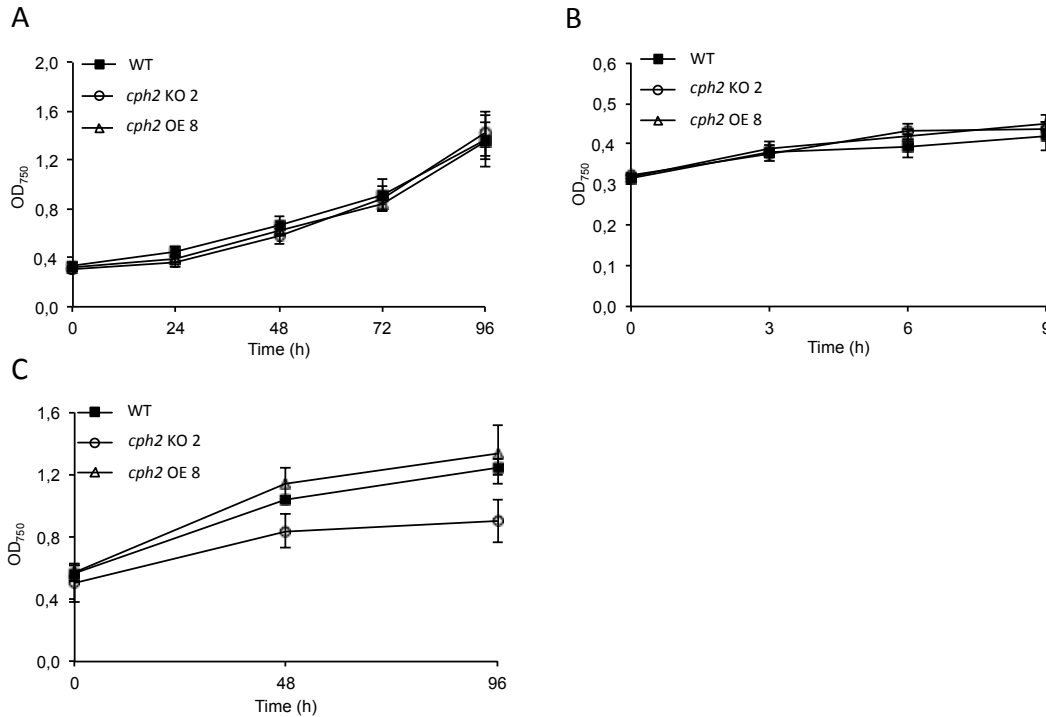
Figure 6: Growth kinetics of *Synechocystis* WT, *cph2* KO and *cph2* OE under distinct growth conditions.

Exponentially growing cultures of WT, *cph2* KO and *cph2* OE were diluted to an OD_{750} of 0.3 (for photoautotrophic and photomixotrophic growth) or 0.6 (for growth under LAHG/biomat-forming conditions) and incubated under photoautotrophic (A), photomixotrophic (in presence of 10 mM glucose) (B) and LAHG/biomatforming conditions (C). WT (filled rectangle), *cph2* KO 2 (open circle) and *cph2* OE clone 8 (open triangle). OD_{750} was determined at indicated timepoints. Error bars represent standard error, based on mean values of 6 (A, B) and 3 (C) independent experiments.

3.1.3 Incubation under LAHG/biomatforming conditions results in a reduced G6PDH activity in *cph2* KO

In their natural environment, *Synechocystis* cells are subjected to a diurnal light-dark cycle, during which the organism has to adapt its metabolism by switching between a photoautotrophic and a dark heterotrophic metabolic mode (Sundaram *et al.,* 1998). When light is available, *Synechocystis* grows photoautotrophically by assimilating inorganic carbon via the Calvin cycle, using energy provided by photosynthetic light reactions. The resulting sugar products are subsequently converted into the storage carbohydrate glycogen, which serves as metabolic energy source under non-photosynthetic conditions (Osanai *et al.,* 2007). The degradation of glycogen provides G6P, which is catabolized via the OPPP, the lower energy-conserving phase of glycolysis and the incomplete TCA cycle (Stal & Moezelaar, 1997). In *Synechocystis*, the OPPP is the major pathway of glucose catabolism under heterotrophic growth conditions (Pelroy *et al.,* 1976; Schaeffer & Stanier, 1978; Yang *et al.*, 2002; Singh *et al.,* 2004). The enzyme glucose-6-phosphate dehydrogenase (G6PDH) catalyzes the

rate-determining step of the OPPP, the conversion of glucose-6-phosphate to 6-phosphogluconolactone, thereby controlling the carbon flow into the pathway (Singh *et al.,* 2004). Due to its key function in glucose catabolism, enzyme activities of G6PDH were analysed in *cph2* KO, *cph2* OE and WT cells, grown under photoautotrophic, photomixotrophic and LAHG/biomatforming conditions.

Photoautotrophically grown, mid-exponential cultures of WT, *cph2* KO and OE strains were incubated in presence (photomixotrophic conditions) and absence (photoautotrophic conditions) of 10 mM glucose for 24 h (140 rpm, 28°C, continuous illumination with a light intensity of 20 µmol photons m^{-2} s^{-1}). Specific G6PDH enzyme activities of WT, *cph2* KO and *cph2* OE strains were determined and are presented in Figure 7 A. Data are normalized relative to the WT under photoautotrophic growth conditions. Under photoautotrophic and photomixotrophic conditions no significant differences in G6PDH activity of WT, *cph2* KO and *cph2* OE were observable. Under photomixotrophic conditions there is a tendency of increased G6PDH activity in all lines, which indicates that WT, *cph2* KO and OE mutants are capable to utilise exogenous glucose and therefore are capable of mixotrophic glucose metabolism. In order to analyse specific G6PDH activities under LAHG/biomatforming conditions, photoautotrophically grown, mid-exponential cultures of WT, *cph2* KO and OE strains were supplied with glucose and transferred to LAHG conditions without agitation. After 96 h of incubation under LAHG/biomatforming conditions, the specific G6PDH enzyme activities of WT, *cph2* KO and OE strains were determined and are presented in Figure 7 B. Data are normalized relative to the WT. Enzyme activity measurements after 96 h of incubation under LAHG/biomatforming conditions revealed that G6PDH activity in extracts of both independent *cph2* knockout clones was significantly reduced compared to the WT (P < 0.01, Student's *t* test). Overexpression of CPH2 resulted in complementation of G6PDH activity in *cph2* OE clone 8, while *cph2* OE clone 2 and 7 partially complement G6PDH activity, indicating that the decreased enzyme activity in *cph2* KO under LAHG/biomatforming conditions results from the deletion of *cph2*. The G6PDH activity in *cph2* overexpression clones 7 and 8 was proved significantly different to *cph2* KO1 and KO2 (P < 0.05, Student's *t* test) and in *cph2* OE clone 2 significantly different to *cph2* KO1 (P < 0.05, Student's *t* test).
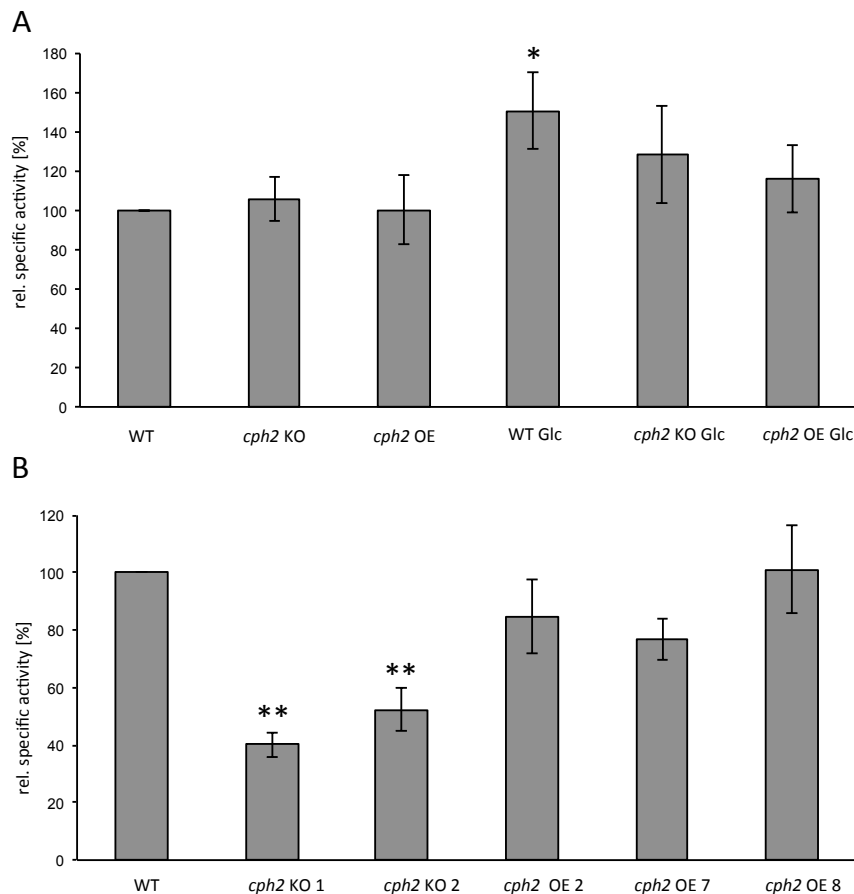
Figure 7: Specific G6PDH enzyme activity of WT, *cph2* KO and *cph2* OE strains under photoautotrophic and photomixotrophic (A) and under LAHG/biomatforming (B) growth conditions.

(A) Photoautotrophically grown, mid-exponential (OD_{750} = 0.6-0.8) cell cultures of *Synechocystis* WT and *cph2* mutant strains (*cph2* KO clone 2 and *cph2* OE clone 8) were assayed for the activity of G6PDH in presence and absence of glucose. Where indicated, the cells were supplied with glucose at a final concentration of 10 mM (Glc) for 24 h, prior to the extraction of proteins. 100 µg of crude protein were used in a total volume of 1 ml assay solution to determine G6PDH activity. Data are normalized to the WT under photoautotrophic growth conditions (0.073 ± 0.010 U/µg protein, set as 100% for each individual experiment). Columns represent average values of minimum 7 independent experiments. Bars represent standard errors. Asterisks indicate significant difference at $P < 0.05$, according to Student's *t* test.

(B) Photoautotrophically grown, mid-exponential cell cultures (OD_{750} = 0.6-0.8) of WT and *cph2* mutant strains (*cph2* KO clone 1 and 2, *cph2* OE clone 2, 7 and 8) were supplied with glucose at a final concentration of 10 mM and incubated without agitation under LAHG conditions (darkness with 15 min light per 24 h) for 96 h. 100 µg of crude protein were used in a total volume of 1 ml assay solution to determine G6PDH activity. Data are normalized to the WT (0.036 ± 0.013 U/µg protein, set as 100% for each individual experiment). Columns represent average values of minimum 3 independent experiments. Bars represent standard errors. Asterisks indicate significant difference at $P < 0.01$, according to Student's *t* test.

3.1.4 Incubation under LAHG/biomatforming conditions induces downregulation of *CtaDI* expression in *cph2* KO

To analyse the expression of key metabolic and photosynthetic genes in WT, *cph2* KO and OE under different growth conditions (photoautotrophic, photomixotrophic and LAHG/biomatforming conditions), semi-quantitative reverse-transcription polymerase chain reactions (RT-PCR) were conducted. Total RNA of mid-exponential WT, *cph2* KO and *cph2* OE cell cultures was isolated after 24 h under photoautotrophic/photomixotrophic conditions and after 96 h under LAHG/biomatforming conditions and subjected to semi-quantitative two-step RT-PCR.
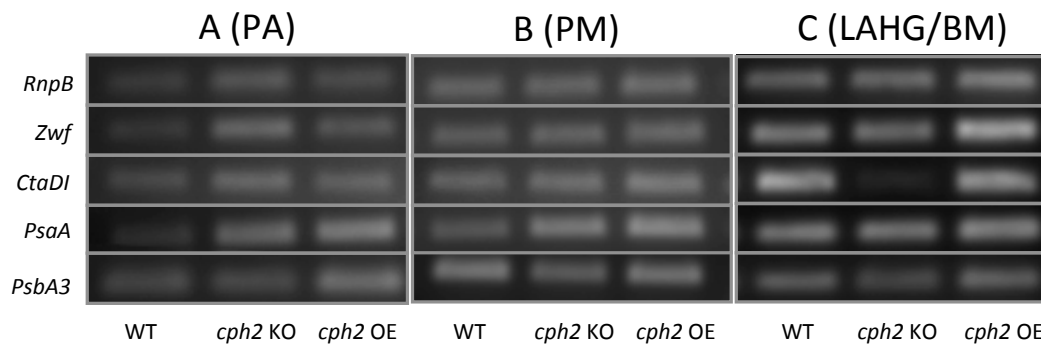

Figure 8: Gene expression analysis of key metabolic and photosynthetic genes in WT, *cph2* KO and *cph2* OE by semi-quantitative RT-PCR.

Effects of different growth conditions on the expression of key metabolic and photosynthetic genes were examined by semi-quantitative RT-PCR. Total RNA of WT and *cph2* mutants (*cph2* KO clone 2 and *cph2* OE clone 8; OD_{750} = 0.6-0.8) was isolated after 24 h under photoautotrophic (A) and photomixotrophic (in presence of 10 mM glucoese) (B) conditions and after 96 h under LAHG/biomatforming conditions (C). After reverse transcription, 500 ng of first strand cDNA was used as template for semi-quantitative RT-PCR (32 cycles, except for *PsaA* [31 cycles]). PCR products were analysed on a 1.5% agarose gel and stained with ethidium bromide. Data presented are representative for three independent experiments. Ribosomal RNA was tested before first strand cDNA synthesis to ensure non-degradation of total RNA (data not shown).
Analysed genes: *RnpB* (*slr0249*), housekeeping*; Zwf* (*slr1843*), G6PDH*; CtaDI* (*slr1137*), cytochrome *c* oxidase; *PsaA* (*slr1834*), photosystem I*; PsbA3* (*sll1867*), photosystem II.

Besides the housekeeping gene *RnpB* (*slr0249*), encoding for subunit B of ribonuclease P (Vioque, 1992), the transcript levels of four genes involved in glucose metabolism and photosynthesis were analysed in WT, *cph2* KO and *cph2* OE under different growth conditions (Figure 8). *Zwf* (*slr1843)* and *CtaDI* (*slr1137*) were among the analysed genes involved in glucose metabolism, encoding for G6PDH and for subunit I of the cytochrome *c* oxidase complex, the terminal component of the respiratory chain, respectively. Among the photosynthesis-related genes, the transcript levels of *PsaA* (*slr1834*) and *PsbA3 (sll1867)* were analysed, encoding for subunit Ia of the P700 apoprotein and for PS II D1 protein, respectively. Gene expression analysis after 24 h of incubation under photoautotrophic (Figure 8 A) and

photomixotrophic (Figure 8 B) growth conditions revealed similar expression patterns for *Zwf* and *CtaDI* in WT, *cph2* KO and *cph2* OE with exception of *PsaA* and *PsbA3*, which display a slightly induced transcript accumulations in *cph2* OE under both conditions. In contrast, incubation under LAHG/biomatforming conditions for 96 h led to distinct changes in the gene expression pattern (Figure 8 C). The transcript level of *CtaDI* in *cph2* KO was significantly downregulated in comparison to WT and *cph2* OE, whereas WT and *cph2* OE showed induced transcript accumulation of *CtaDI* under LAHG/biomatforming conditions compared to photoautotrophic and photo-mixotrophic conditions. Complementation of *cph2* KO resulted in a *CtaDI* expression pattern similar to the WT, thereby suggesting that the downregulation of *CtaDI* in *cph2* KO under LAHG/biomatforming conditions resulted from the deletion of *Cph2*.

3.1.5 Analysis of electron transport activities

Electron transport in the cyanobacterial thylakoid membrane is a complex process due to the existence of converging metabolic pathways. Three intersecting electron flows have been found dominant in *Synechocystis* thylakoid membranes: linear photosynthetic electron transport from water to NADP$^+$ via PS II and PS I, respiratory electron transport from NADPH and succinate to cytochrome *c* oxidase and cyclic electron transport around PS I. Electron input converges at the PQ-pool, from where the electrons are subsequently passed on to PS I via cytochrome b_6f complex and/or finally transferred to molecular oxygen by the respiratory oxidases.
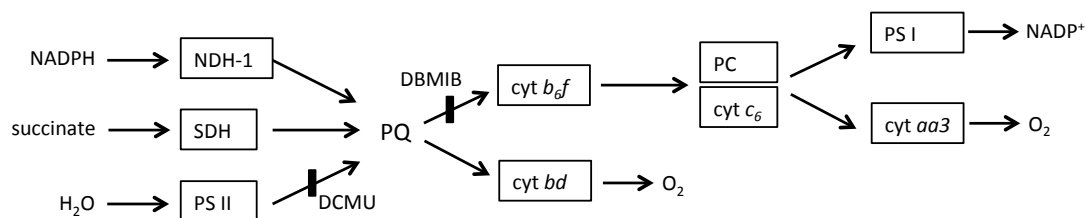
Figure 9: Overview of the electron transport pathways in the thylakoid membrane of *Synechocystis* and sites of action of inhibitors used (modified after Berry *et al.,* 2002).

Abbreviations: NDH-1, NADPH dehydrogenase 1; SDH, succinate dehydrogenase; PS I and II; photosystem I and II; PQ, plastoquinone pool; cyt b_6f, cytochrome b_6f complex; PC, plastocyanin; cyt c_6, cytochrome c_6; cyd *bd*, cytochrome *bd*-type quinol oxidase; cyt *aa3*, cytochrome *aa3*-type cytochrome *c* oxidase; NADP(H), nicotinamide-adenine dinucleotide phosphate (reduced form); Inhibitors (indicated as thick black bars): DCMU, 3-(3,4-dichlorophenyl)-1,1-dimethylurea; DBMIB, 2,5-dibromo-3-methyl-6-isopropyl-*p*-benzoquinone;

Chlorophyll a fluorescence measurements represent a non-invasive method, providing real-time information of key aspects of photosynthetic light capture and electron transport. Using Pulse-Amplitude-Modulation (PAM) measurements, reduction kinetics of oxidized P700 (P700$^+$) were recorded in WT, *cph2* KO and *cph2* OE, in presence and absence of specific electron transport inhibitors to analyse

electron transport activities in the thylakoid membrane. Figure 9 gives a schematic overview of the described electron flows and the sites of action of the inhibitors used. $P700^+$ reduction kinetics were recorded in photoautotrophically grown, mid-exponential WT, *cph2* KO and *cph2* OE before the addition of glucose and the transition to biomatforming conditions (0 h), which refers to photoautotrophic growth conditions and after incubation under biomatforming/dark conditions for 24 h. Following, the half-life ($t_{1/2}$) of the re-reduction of $P700^+$ was determined, giving an indication of the rate of electron donation to PS I (Howitt *et al.,* 2001). In order to illustrate the principles of this quantification, $P700^+$ reduction kinetic decays of untreated and DCMU-treated WT, *cph2* KO and *cph2* OE after 24 h of incubation under biomatforming/dark conditions are displayed in Figure 10 A and B. Cells were irradiated with blue light to keep P700 in its oxidized form (indicated by black bars). When the blue light is switched off, $P700^+$ returns into its reduced state. Corresponding rate constants (k) for the calculation of $t_{1/2}$ were obtained by fitting the decays with single exponential functions, as described in Section 2.1.9. $T_{1/2}$ of $P700^+$ reduction in untreated, DCMU- and DCMU/DBMIB-treated samples of WT, *cph2* KO and *cph2* OE are summarized Figure 10 C and D, before and after 24 h of incubation under biomatforming conditions, respectively. In untreated (control) samples, $t_{1/2}$ of $P700^+$ reduction of WT, *cph2* KO and *cph2* OE displayed no significant differences before and after 24 h of incubation under biomatforming/dark conditions (Figure 10 C, D). DCMU is a PS II inhibitor, which inhibits the linear electron transport by blocking the plastoquinone-binding site. Treatment with DCMU resulted in increased $t_{1/2}$ of $P700^+$ reduction in samples of WT, *cph2* KO and *cph2* OE adapted to photoautotrophic conditions (Figure 10 C), indicating a reduced electron flow to $P700^+$. Since the linear electron transport is blocked, electron input into the PQ pool originates from electron flows via SDH and NDH-1, from NADPH generated by the heterotrophic metabolism or PS I under blue light illumination. Due to the missing electron input from PS II, the PQ pool is more oxidized in DCMU-treated samples compared to untreated samples. This results in increased $t_{1/2}$ of $P700^+$ reduction in DCMU-treated cells, as it takes longer to re-reduce $P700^+$ after switching off blue light illumination. In samples adapted to biomatforming/complete dark conditions, treatment with DCMU resulted in a significantly increased $t_{1/2}$ of $P700^+$ reduction in *cph2* KO compared to the WT (ANOVA, followed by Tukey's test $P = 0.05$) (Figure 10 D), which is also reflected in the $P700^+$ reduction kinetic decays displayed in Figure 10 B. The higher increase in $t_{1/2}$ of $P700^+$ reduction indicates that *cph2* KO adapted to biomatforming/dark conditions, has less electron input into the PQ-pool compared to the WT.
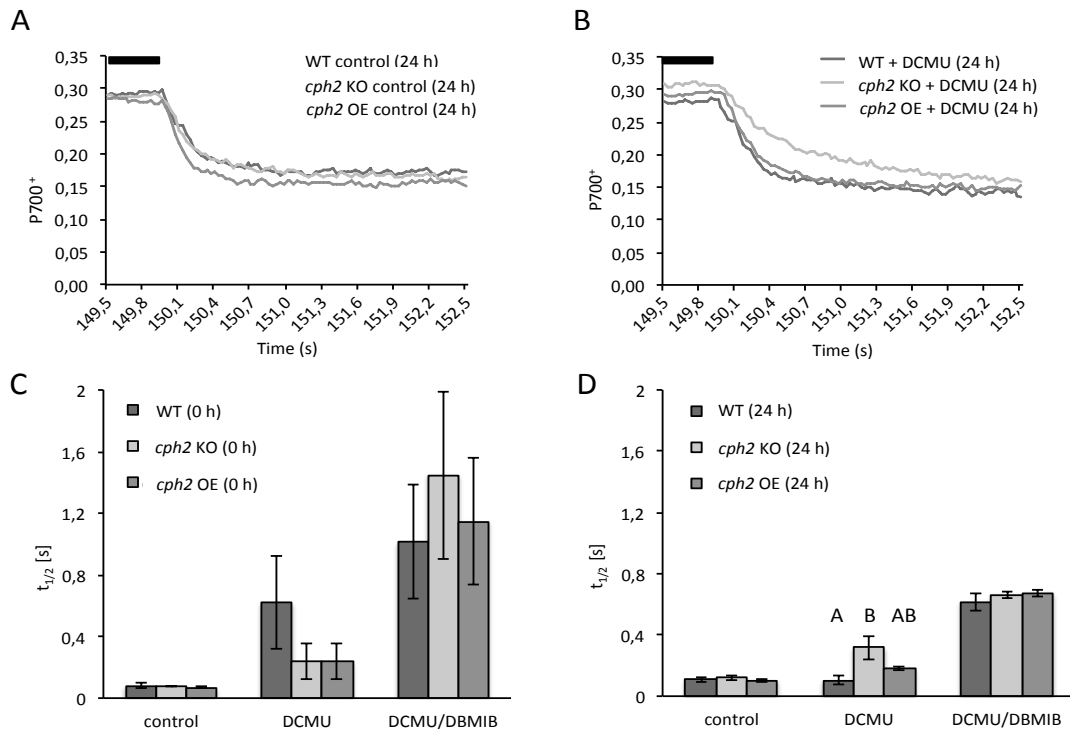
Figure 10: P700$^+$ reduction kinetics and corresponding half-life in WT, *cph2* KO and *cph2* OE before and after 24 h of incubation under biomatforming, dark conditions in presence and absence of specific electron transport inhibitors.

Cell cultures of WT, *cph2* KO and *cph2* OE were photoautotrophically grown to an OD$_{750}$ of 0.6. P700$^+$ reduction kinetics were recorded before the addition of glucose and the transition to biomatforming conditions (0 h) and after 24 h of incubation under biomatforming conditions (24 h), in presence of glucose at a final concentration of 10 mM, without agitation and in darkness. Measurements were conducted in untreated (control), DCMU and DCMU/DBMIB-treated cells (final concentrations, 10 µM [DCMU], 60 µM [DBMIB]). P700$^+$ reduction kinetic decays of untreated (A) and DCMU-treated (B) WT, *cph2* KO and OE cells after 24 h of incubation under biomatforming/dark conditions. Curves correspond to three averaged traces of the same sample. Black bars symbolize time intervals (60 s) when blue light is on to keep P700 in its oxidized form. When the blue light is switched off, P700$^+$ is reduced. Corresponding t$_{1/2}$ of the P700$^+$ reduction was determined in untreated (control) cells and DCMU- and DCMU/DBMIB-treated cells, before (C) and after 24 h (D) of incubation under the described conditions. Data represent the average value of three independent experiments ± standard error. For statistical analysis an ANOVA test was performed, combined with a post-hoc Tukey's test for each group (control, DCMU, DCMU/DBMIB). Letters A, B and AB show the grouping of data sets according to Tukey's highly significant difference (HSD) test; columns without a common letter are significantly different at *P* = 0.05.

DBMIB is a Q$_0$ site inhibitor of cytochrome *b$_f$*, which prevents the reoxidation of plastoquinone, thereby inhibiting the electron input from the PQ pool into the cytochrome *b$_6$f* complex. However, the inhibition with DBMIB does not result in a complete electron blockage. Therefore, it takes longer to re-reduce P700$^+$ after switching off the blue light, which is reflected in increased t$_{1/2}$ of P700$^+$ reduction. Since most of the electron input into the PQ pool originates from PSII in the presence of light, the additional blockage of linear electron transport by DCMU upon simultaneous DBMIB/DCMU-treatment should result in a more effective inhibition by DBMIB. In samples adapted to photoautotrophic conditions, simultaneous treatment

with DCMU and DBMIB resulted in increased $t_{1/2}$ of P700$^+$ reduction in WT, *cph2* KO and *cph2* OE (Figure 10 C), indicating a strongly restricted electron flow to P700$^+$. In samples adapted to biomatforming/dark conditions, this effect is no longer detectable as WT, *cph2* KO and *cph2* OE showed similarly increased $t_{1/2}$ of P700$^+$ reduction (Figure 10 D). Compared to samples adapted to photoautotrophic conditions, the increase in $t_{1/2}$ of P700$^+$ reduction upon DCMU/DBMIB-treatment was lower under biomatforming/dark conditions, which might indicate a generally reduced electron flux under biomatforming conditions. Together, the increase in $t_{1/2}$ of P700$^+$ reduction upon DCMU-treatment in *cph2* KO adapted to biomatforming/dark conditions and the similar $t_{1/2}$ of P700$^+$ reduction upon DCMU/DBMIB-treatment in WT, *cph2* KO and *cph2* OE adapted to biomatforming/dark conditions, indicates that the electron input into the PQ pool might be affected in *cph2* KO. This further supports the assumption of a reduced ability to metabolize glucose in *cph2* KO.

3.2 Functional characterisation of HIK12, a histidine kinase in *Synechocystis* sp. PCC 6803

Synechocystis includes 44 putative genes for histidine kinases (Hiks) on its chromosome (Kaneko *et al*., 1996; Mizuno *et al.,* 1996) and three putative genes for Hiks on its plasmids (Kaneko *et al.,* 2003), all of which are potential sensory histidine kinases. Among them, the histidine kinase 12 (HIK12) shows structural homology to the histidine kinases of the cytokinin receptor family in *Arabidopsis.* A sequence alignment of the ligand-binding domains of the cytokinin receptors in *Arabidopsis* and the structurally homologous domain in *Synechocystis* HIK12 is given in Figure 23 and is discussed in detail in Section 4.2. To provide insights into the function of the *Synechocystis* cytokinin receptor-like protein HIK12 (*sll1672*), a *hik12* knockout mutant and the corresponding complementation were characterised with a special focus on its effects on the central carbon metabolism during the shift from planktonic lifestyle to a sessile lifestyle within a biomat.

3.2.1 Generation of *hik12* complementation lines

The *hik12* (*sll1672*) knockout mutant (hereafter referred to as *hik12* KO) and the corresponding glucose-tolerant wildtype were obtained from Dr. Iwane Suzuki (Graduate School of Life and Environmental Sciences, University of Tsukuba, Tsukuba, Japan). The knockout line was generated by inserting a spectinomycine resistance cassette into the coding region of *hik12* gene, thereby disrupting the functionality of the gene (Suzuki *et al.,* 2000). In this study, a *hik12* overexpression line was generated in the background of *hik12* KO for functional complementation of

the knockout line with a full-length *hik12* coding sequence under the control of the constitutive active petJ promotor (Figure 11 A). The *hik12* full length coding sequence was amplified by PCR, using Hik12 OX-LB_neu (P1)/Hik12 OX-term (P2) primers, thereby introducing *Cla*I restriction sites at the 5' and 3' end for subsequent cloning into the vector psk9 (Figure 11 A). Besides the *Cla*I restriction sites, an *oop* terminator was introduced at the 3' end by the primer P2 (Figure 11 A).
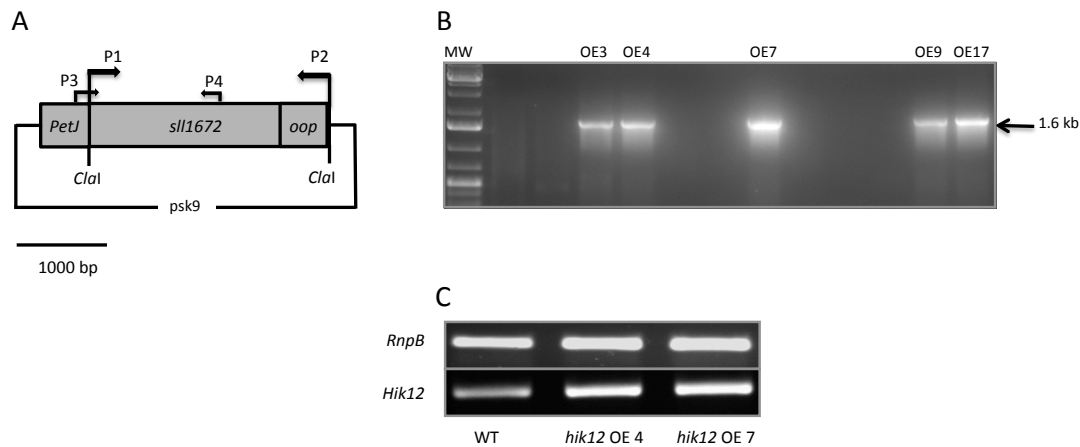

Figure 11: Generation of *hik12* overexpression construct (A), verification of successful genomic integration (B) and transcript overexpression of *hik12* (C).

(A) *Hik12* overexpression construct used for *Synechocystis* transformation. Primer P1/P2, used for amplification of full-length *hik12* (2561 bp) and primer P3/P4, used for verification of the correct insertion in the transformants, are indicated. The *oop* terminator was introduced at the 3' end by primer P2. Restriction sites used for cloning: *Cla*I.
(B) Verification of positive genomic integration of the construct in five transformants (designated as *hik12* OE3, OE4, OE7, OE9 and OE17) by PCR on genomic DNA (estimated fragment size: 1654 bp, black arrow). MW, molecular mass standard.
(C) Verification of *hik12* overexpression by semi-quantitative RT-PCR. Total RNA of WT and *hik12* OE clone 4 and 7 was isolated. After reverse transcription, 500 ng of first strand cDNA was used as template for PCR (32 cycles for *RnpB* and 36 cycles for *Hik12*). PCR products were analysed on a 1.5% agarose gel and stained with ethidium bromide. The constitutively expressed RNase P gene (*RnpB*) was included as control.

Stable transformation of *Synechocystis* via chromosomal integration was performed essentially according to Grigorieva and Shestakov (1982), as described in Section 2.1.3. For complementation, the *hik12* knockout strain was used as parental strain. Transformation resulted in 30 chloramphenicole-resistant colonies. After restreaking on selective media for segregation, the analysis of 12 transformants by PCR on genomic DNA, using psk9-fw-seq (P3) and Hik12 SDM2 (P4) primers (Figure 11 A), led to the identification of five mutants (*hik12* OE clone 3, 4, 7, 9 and 17) carrying the OE construct (Figure 11 B). Gene expression analysis using semi-quantitative RT-PCR confirmed the overexpression of *hik12* (Figure 11 C). The parental strain, *hik12* knockout and *hik12* overexpression mutants are in the following referred to as WT, *hik12* KO and *hik12* OE, respectively.

3.2.2 Growth characteristics: incubation under biomatforming conditions leads to growth cessation in *hik12* KO

To screen for physiological effects of the loss of *Hik12*, growth of WT, *hik12* KO and *hik12* OE strains was analysed under different (photoautotrophic, photomixotrophic and photomixotrophic/biomatforming) growth conditions. To analyse growth under photoautotrophic or photomixotrophic conditions, photoautotrophically grown pre-cultures of WT, *hik12* KO and *hik12* OE strains were diluted to an initial OD_{750} of 0.3 and incubated at 140 rpm, 28°C, under continuous illumination with a light intensity of 20 µmol photons m^{-2} s^{-1}, in presence (photomixotrophic) or absence (photoauto-trophic) of 10 mM glucose. In photoautotrophic cultures, growth was monitored by measurements of the OD_{750} in a time course from 0 to 4 days. Due to the accelerated growth in presence of glucose, the OD_{750} in photomixotrophic cultures was recorded in a time course from 0 to 9 hours, in measuring intervals of 3 hours.

For growth under biomatforming conditions, cell cultures of WT, *hik12* KO, *hik12* OE clones 4 and 7 were grown photoautotrophically to an OD_{750} of 0.6-0.8. After addition of glucose (final concentration 10 mM), the cell cultures were incubated without agitation, allowing the cells to sediment and form biomats, under continuous illumination with a light intensity of 20 µmol photons m^{-2} s^{-1} for 96 h (hereafter referred to as biomatforming conditions). To determine the growth of the biomats, the cells were resuspended at 0, 48 and 96 h and the OD_{750} was determined.

The growth kinetics of WT, *hik12* KO, *hik12* OE clones 4 and 7 are presented in Figure 12. No differences in growth were observed for WT, *hik12* KO and both *hik12* OEs, neither under photoautotrophic growth conditions (A), nor under photomixo-trophic growth conditions (B). The accelerated growth under photomixotrophic growth conditions (B) indicated that WT, *hik12* KO and both *hik12* OEs are capable of mixotrophic growth. The analysis of the growth kinetics under biomatforming conditions (C) revealed a growth cessation in *hik12* KO, while WT, *hik12* OE 4 and 7 continued to grow, *hik12* KO ceased in growth after 48 h, which is further reflected in the slope (m) between 48 and 96 h ($m_{WT, 48-96 h}$ = 0.009 ± 0.0033, $m_{hik12 KO, 48-96 h}$ = 0.002 ± 0.0018, $m_{hik12 OE 4, 48-96 h}$ = 0.008 ± 0.0041, $m_{hik12 OE 7, 48-96 h}$ = 0.011 ± 0.0008). The complementation of *hik12* KO with the *hik12* overexpression construct resulted in growth kinetics similar to those observed for the WT.
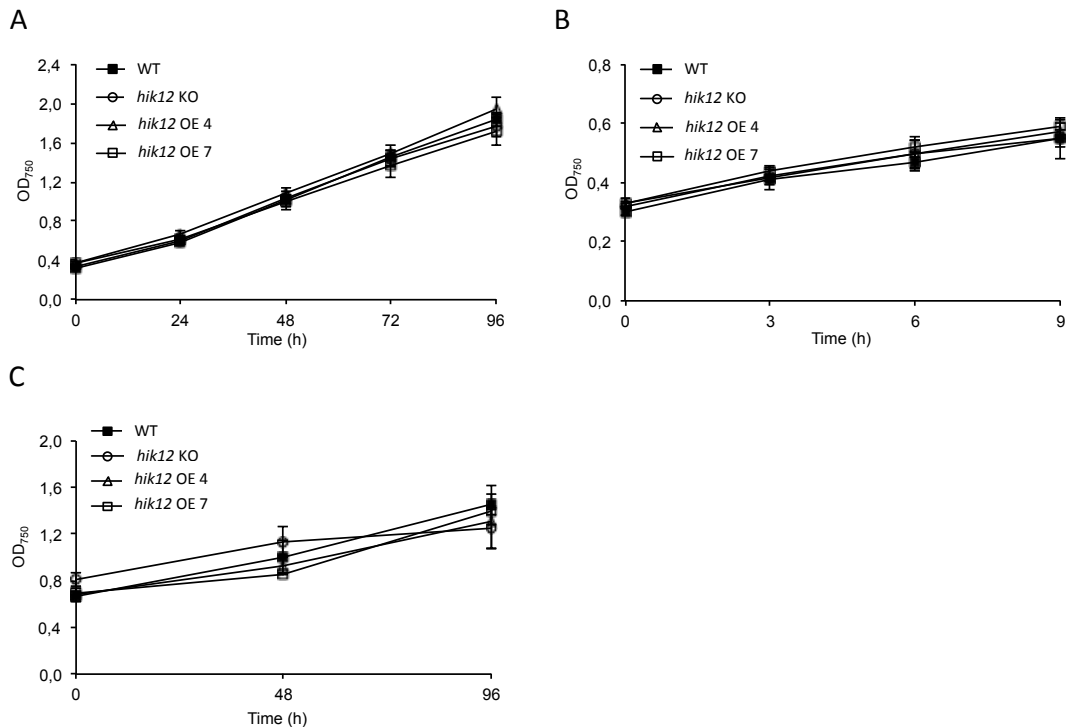
Figure 12: Growth kinetics of *Synechocystis* WT, *hik12* KO, *hik12* OE 4 and *hik12* OE 7 under distinct growth conditions.

Exponentially growing cultures of WT, *hik12* KO and *hik12* OE clone 4 and 7 were diluted to an OD_{750} of 0.3 (for photoautotrophic and photomixotrophic growth) or 0.6 (for growth under biomatforming conditions) and incubated under photoautotrophic (A), photomixotrophic (in presence of 10 mM glucose) (B) and biomatforming conditions (C). WT (filled rectangle), *hik12* KO 2 (open circle), *hik12* OE clone 4 (open triangle) and *hik12* OE clone 7 (open rectangle). OD_{750} was determined at indicated timepoints. Error bars represent standard error, based on mean values of 4 (A), 3 (B) and minimum 3 (C) independent experiments.

3.2.3 Incubation under biomatforming conditions results in decreased cell division activity in *hik12* KO

Growth in *Synechocystis* implies proliferation via binary fission, an asexual form of reproduction, which includes the cell division process of one cell into two daughter cells. Microscopic analyses enable to distinguish between these cells, either being spherical, single cells or dumbbell-shaped cells, which undergo separation. Besides the growth kinetics in liquid cultures, microscopic analyses of the cell division activity were conducted. For this purpose, photoautotrophically grown, mid-exponential cells (OD_{750} = 0.3-0.6) were distributed to sterile 1.5 ml-reaction tubes, supplied with glucose at a final concentration of 10 mM and incubated under biomatforming conditions (without agitation, 28°C, continuous illumination with an intensity of 20 µmol photons $m^{-2}s^{-1}$). Cell division activity in WT and *hik12* KO was analysed before the addition of glucose and the transition to biomatforming conditions (0 d) and after incubation under biomatforming conditions for 14 days by determining the relative amount of dumbbell-shaped cells (Figure 13). The analysis revealed that in photo-

autotrophically grown WT and *hik12* KO no significant differences in the relative amount of dumbbell-shaped cells and thus in cell division activity were observable before incubation under biomatforming conditions (0 d). In contrast, continuous incubation under biomatforming conditions for 14 days led to a significant decrease in the cell division activity in *hik12* KO ($P < 0.001$, Student's *t* test), thereby confirming the results of the growth kinetics under biomatforming conditions (Figure 12 C).
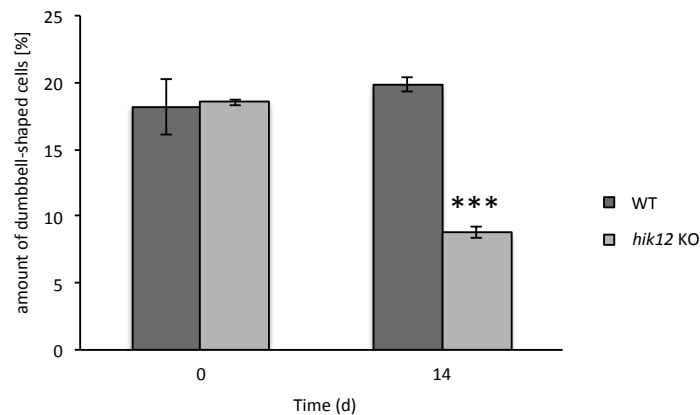

Figure 13: Cell division activity in WT and *hik12* KO before (0 d) and after 14 d of incubation under biomatforming conditions.

Cell division activity in WT and *hik12* KO was analysed microscopically by determining the ratio between single, spherical cells and dumbbell-shaped cells undergoing separation, before incubation under biomatforming conditions and the addition of glucose (0 d) and after incubation under biomatforming conditions for 14 d. Data are presented as the relative amount of dumbbell-shaped cells. Columns represent average values of three independant experiments. Bars represent standard errors. Asterisks indicate significant difference at $P < 0.001$ according to Student's *t* test.

3.2.4 Incubation under biomatforming conditions results in increased glycogen content in *hik12* KO

In cyanobacteria, photosynthetic carbon assimilation results in the accumulation of polysaccharides, mostly glycogen (Nakamura *et al.,* 2005). Glycogen serves as reserve carbohydrate to meet the metabolic needs under non-photosynthetic conditions (Stal & Moezelaar, 1997; Knowles & Plaxton, 2003; Singh & Sherman, 2005; Takahashi *et al.,* 2008) or for adapatational processes in response to environmental stress stimuli (Preiss, 1984; Suzuki *et al.,* 2010). To analyse the glycogen content within the cells, the glycogen content was determined in *hik12* KO and WT after incubation under biomatforming conditions. For this purpose, photo-autotrophically grown, mid-exponential cultures were set to an OD_{750} of 0.4, supplied with glucose at a final concentration of 10 mM and incubated for 14 d under biomatforming conditions (without agitation, 28°C, continuous illumination with a light intensity of 20 µmol photons m^{-2} s^{-1}).

The glycogen content in *hik12* KO and WT cells was determined after 14 days of incubation under biomatforming conditions. The resulting glycogen contents are presented as µg glycogen/OD_{750} and are displayed in Figure 14. The analysis revealed a significant increase in the glycogen content in *hik12* KO cells ($P < 0.01$, Student's *t* test), which amounts to more than twice as much as in WT cells.
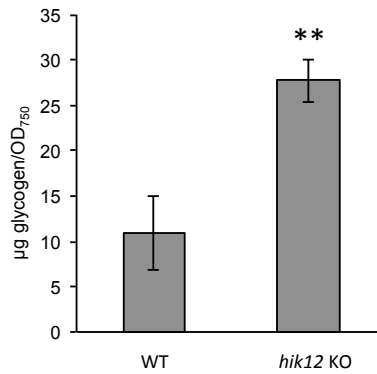

Figure 14: Glycogen content in WT and *hik12* KO after 14 days of incubation under biomatforming conditions.

Specific glycogen contents are given as µg glycogen per OD_{750}. Columns represent average values of 3 (WT) and 5 (*hik12* KO) independent experiments. Bars represent standard errors. Asterisks indicate significant difference at $P < 0.01$ according to Student's *t* test.

3.2.5 Incubation under biomatforming conditions results in a reduced G6PDH activity in *hik12* KO

Due to its key function in the OPPP, the central glucose degrading pathway in cyanobacteria (Schaeffer & Stanier, 1978; Yang *et al.*, 2002; Singh *et al.,* 2004), the enzyme activity of G6PDH was analysed in WT, *hik12* KO and *hik12* OE, grown under photoautotrophic, photomixotrophic and biomatforming growth conditions. Photoautotrophically grown, mid-exponential cultures of WT, *hik12* KO and *hik12* OE were incubated in presence (photomixotrophic conditions) and absence (photoauto-trophic conditions) of 10 mM glucose for 24 h (140 rpm, 28°C, continuous illumination with a light intensity of 20 µmol photons m^{-2} s^{-1}). Specific G6PDH enzyme activities were determined and are presented in Figure 15 A. Data are normalized to WT under photoautotrophic growth conditions. Under photoautotrophic conditions, *hik12* KO and *hik12* OE 4 displayed slightly, but not significantly reduced G6PDH activities compared to the WT. The exposure to glucose for 24 h under photomixotrophic conditions resulted in slight, but not significantly reduced G6PDH activity in WT, *hik12* KO and *hik12* OE. The decrease of G6PDH enzyme activity in WT, *hik12* KO and OE might be explained by a less developed glucose tolerance of this particular WT strain and its deriving KO and OE. For the analysis of specific G6PDH activities under biomatforming conditions, photoautotrophically grown, mid-

exponential cultures of WT, *hik12* KO and *hik12* OE were supplied with glucose and incubated without agitation, at 28°C, under continuous illumination with a light intensity of 20 µmol photons m^{-2} s^{-1}. After 96 h of incubation under biomatforming conditions, the cells were assayed for the activities of G6PDH. Data are presented in Figure 15 B and are normalized to the WT.
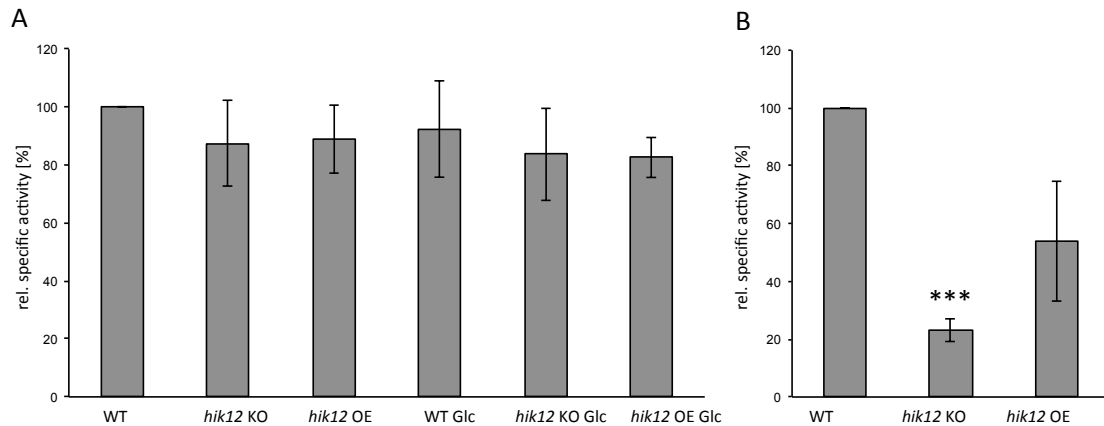

Figure 15: Specific G6PDH enzyme activity of WT, *hik12* KO and *hik12* OE under photoautotrophic and photomixotrophic (A) and under photomixotrophic/bio-matforming (B) growth conditions.

(A) Photoautotrophically grown, mid-exponential (OD_{750} = 0.6-0.8) cell cultures of WT and *hik12* mutant strains (*hik12* KO and *hik12* OE clone 4) were assayed for the activities of G6PDH in presence and absence of glucose. Where indicated, the cells were supplied with glucose at a final concentration of 10 mM (Glc) for 24 h, before the extraction of proteins. 100 µg of crude protein were used in a total volume of 1 ml assay solution to determine G6PDH activity. Data are normalized to the WT under photoautotrophic growth conditions (0.116 ± 0.007 U/µg, set as 100% for each individual experiment). Columns represent average values of 4 independent experiments. Bars represent standard errors.
(B) Photoautotrophically grown, mid-exponential cell cultures (OD_{750} = 0.6-0.8) were supplied with glucose at a final concentration of 10 mM and incubated without agitation for 96 h. 100 µg of crude protein were used in a total volume of 1 ml assay solution to determine G6PDH activity. Data are normalized to the WT (0.064 ± 0.013 U/µg, set as 100% for each individual experiment). Columns represent average values of minimum 3 independent experiments. Bars represent standard errors. Asterisks indicate significant difference at $P < 0.001$ according to Student's t test.

Incubation under biomatforming conditions for 96 h resulted in a significantly decreased G6PDH activity in *hik12* KO compared to the WT ($P < 0.001$, Student's t test), which indicates a deficiency in the ability of *hik12* KO to utilise exogenous glucose as carbon source. Overexpression of HIK12 resulted in a partial complementation of G6PDH activity, reaching more than double the value than in *hik12* KO. A reduced G6PDH activity under biomatforming conditions was verified in the background of another WT strain (provided by K. Marin, University of Cologne, Cologne, Germany). This KO line was generated by full replacement of the coding sequence of *Hik12* with a kanamycine resistance cassette as detailed in Section

2.1.3 and in Supplementary figure 1. As shown in Supplementary figure 2, the KO of *Hik12* results in reduced G6PDH activities compared to the WT.

3.2.6 *hik12* KO is impaired in the upregulation of *CtaDI* gene expression under biomatforming conditions

The expression patterns of genes involved in glucose metabolism were analysed in WT, *hik12* KO and *hik12* OE under different growth conditions (photoautotrophic, photomixotrophic and biomatforming conditions). Total RNA of mid-exponential (OD_{750} = 0.6-0.8) WT, *hik12* KO and *hik12* OE cell cultures was isolated after 24 h under photoautotrophic/photomixotrophic conditions and after 96 h under biomatforming conditions and subjected to semi-quantitative two-step RT-PCR.
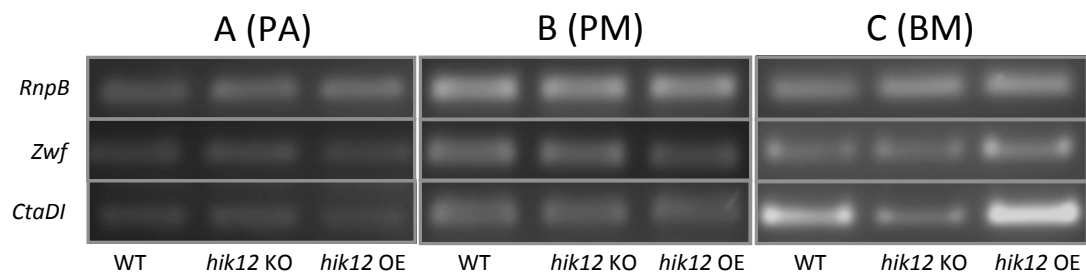
Figure 16: Gene expression analysis of key metabolic genes in WT, *hik12* KO and *hik12* OE by semi-quantitative RT-PCR.

Effects of different growth conditions on the expression of key metabolic genes were examined by semi-quantitative RT-PCR. Total RNA of WT and *hik12* mutants (*hik12* KO and *hik12* OE clone 4) was isolated after 24 h under photoautotrophic (A) and photomixotrophic (in presence of 10 mM glucoese) (B) conditions and after 96 h under biomatforming conditions (C). After reverse transcription, 500 ng of first strand cDNA was used as template for semi-quantitative RT-PCR (32 cycles). PCR products were analysed on a 1.5% agarose gel and stained with ethidium bromide. Data presented are representative for three independent experiments. Ribosomal RNA was tested before first strand cDNA synthesis to ensure non-degradation of total RNA (data not shown). The constitutively expressed RNase P gene (*RnpB*) was included as control.
Analysed genes: *RnpB* (*slr0249*), housekeeping; *Zwf* (*slr1843*), G6PDH; *CtaDI* (*slr1137*), cytochrome *c* oxidase.

The expression patterns of two genes, encoding for key enzymes in glucose metabolism (*Zwf* and *CtaDI*) and one housekeeping gene (*RnpB*) were analysed in WT, *hik12* KO and *hik12* OE under different growth conditions (Figure 16). The analysis of the transcript levels after 24 h of incubation under photoautotrophic conditions (Figure 16 A) and photomixotrophic conditions (Figure 16 B) revealed relatively low, but similar expression levels of *Zwf* and *CtaDI* in WT, *hik12* KO and *hik12* OE. After incubation under biomatforming conditions for 96 h, distinct changes in the gene expression pattern were observable. The transcript levels of *CtaDI* in WT and *hik12* OE were significantly upregulated compared to photoautotrophic and photomixotrophic conditions, whereas *hik12* KO showed no induced transcript

accumulation of *CtaDI* under biomatforming conditions (Figure 16 C). The complementation of *hik12* KO with *hik12* OE construct resulted in a *CtaDI* expression pattern similar to the WT, indicating that the deficiency in the KO mutant to up-regulate *CtaDI* under biomatforming conditions resulted from the deletion of *Hik12*.

3.2.7 Analysis of electron transport activities

To analyse electron transport activities in the thylakoid membrane, reduction kinetics of oxidized P700 (P700$^+$) were recorded in samples of WT, *hik12* KO and *hik12* OE in presence and absence of specific electron transport inhibitors. P700$^+$ reduction kinetics were recorded in photoautotrophically grown, mid-exponential WT, *hik12* KO and *hik12* OE before the addition of glucose and the transition to biomatforming conditions (0 h), which refers to photoautotrophic growth conditions and after incubation under biomatforming conditions (in presence of glucose, without agitation, under continuous illumination) for 24 h. In terms of evaluation, the half-life ($t_{1/2}$) of the re-reduction of P700$^+$ was determined as described in Section 2.1.9. Detailed information about electron flows and the sites of action of the inhibitors used are given in Figure 9. $T_{1/2}$ of P700$^+$ reduction in untreated, DCMU- and DCMU/DBMIB-treated samples of WT, *hik12* KO and *hik12* OE are presented in Figure 17 A and B, before and after 24 h of incubation under biomatforming conditions, respectively.
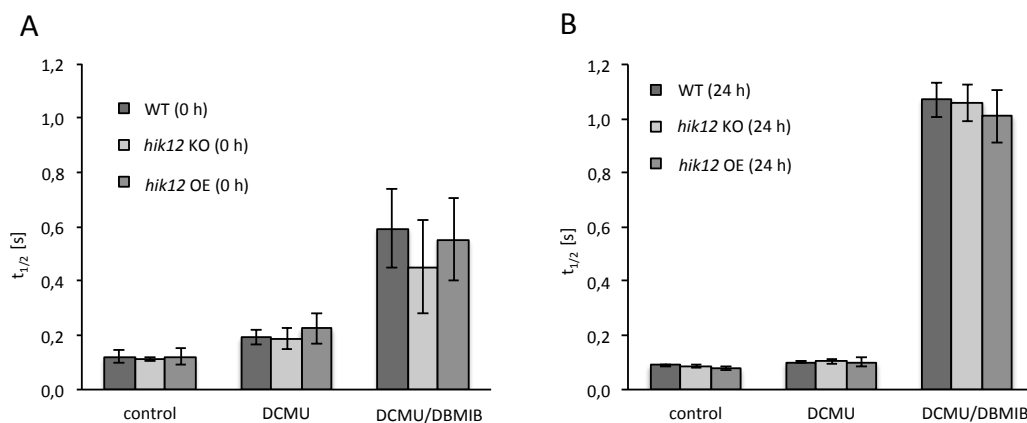
Figure 17: Half-life ($t_{1/2}$) of P700$^+$ reduction in WT, *hik12* KO and *hik12* OE before (0 h) and after 24 h of incubation under biomatforming conditions in presence and absence of specific electron transport inhibitors.

Cell cultures of WT, *hik12* KO and *hik12* OE were photoautotrophically grown to an OD$_{750}$ of 0.6. P700$^+$ reduction kinetics were recorded before the addition of glucose and the transition to biomatforming conditions (0 h) and after 24 h of incubation under biomatforming conditions (24 h), in presence of glucose at a final concentration of 10 mM, without agitation and under continuous illumination with a light intensity of 20 µmol photons m^{-2} s^{-1}. Measurements were conducted in untreated (control), DCMU and DCMU/DBMIB-treated cells (final concentrations, 10 µM [DCMU], 60 µM [DBMIB]). Data represent the average value of 3 independent experiments. For statistical analysis an ANOVA test was performed with a post-hoc Tukey's highly significant difference (HSD) test at *P* = 0.05 for each group (control, DCMU, DCMU/DBMIB).

$T_{1/2}$ of P700$^+$ reduction of WT, *hik12* KO and *hik12* OE displayed no significant differences before and after 24 h of incubation under biomatforming conditions, in presence and absence of both inhibitors tested. In samples of WT, *hik12* KO and *hik12* OE adapted to photoautotrophic conditions, treatment with DCMU resulted in increased $t_{1/2}$ of P700$^+$ reduction, indicating a reduced electron flow to P700$^+$. Since the linear electron transport is blocked by DCMU, the reduced electron flow to P700$^+$ indicates a reduced electron input into the PQ pool via SDH and/or via NDH-1 (originating from NADPH, which was generated by glucose degradation or PS I during blue light illumination) in samples adapted to photoautotrophic conditions. Simultaneous treatment with DCMU and DBMIB, the latter inhibits the electron input from the PQ pool into the cytochrome b_6f complex, resulted in highly increased $t_{1/2}$ of P700$^+$ reduction in WT, *hik12* KO and *hik12* OE compared to DCMU-treated samples. The inhibition with DBMIB does not result in a complete electron blockage, causing a strongly reduced electron flow to P700$^+$, which is reflected in the observed increase in $t_{1/2}$ of P700$^+$ reduction in WT, *hik12* KO and *hik12* OE before and after incubation under biomatforming conditions. In comparison to samples adapted to photoautotrophic conditions, treatment with DCMU after incubation under biomat-forming conditions resulted in only slightly increased $t_{1/2}$ of P700$^+$ reduction in WT, *hik12* KO and *hik12* OE, indicating an increased electron input under biomatforming conditions. As a result, $t_{1/2}$ of P700$^+$ reduction in DCMU-treated samples after biomat induction amounts to approximately half the value compared to samples adapted to photoautotrophic conditions. This could be explained by a higher electron input into the electron transport chain from heterotrophic sources after biomat induction in presence of glucose. In conclusion, electron transport activities do not differ between WT, *hik12* KO and *hik12* OE after 24 h of biomat induction in the light.

3.2.8 *hik12* KO shows constitutive ROS production

Reactive oxygen species (ROS) are highly reactive compounds, which are produced as toxic byproducts of respiratory and photosynthetic electron transport and during stress situations (Tichy & Vermaas, 1999; Apel & Hirt, 2004; Pérez-Pérez *et al.,* 2009; Bernroitner *et al.,* 2009). The most important ROS include the superoxide anion radical ($O_2^{\bullet-}$), hydrogen peroxide (H_2O_2) and the hydroxyl radical ($OH^\bullet$) and are produced during the stepwise reduction of molecular oxygen (O_2) to water (H_2O). In plants, ROS are known to play an important role in defense reactions against pathogen attacks (Lamb & Dixon, 1997). As the phytohormone cytokinin recently emerged to play a major role in plant-pathogen interactions (Walters *et al.,* 2008; Pertry *et al.,* 2009; Choi *et al.,* 2011) and due to sequence homology of HIK12 to the

Arabidopsis cytokinin receptor family, the ROS production in the cyanobacterial cell cultures was determined, using a luminol-based assay. ROS-mediated oxidation of luminol was recorded as relative chemoluminescence units for 60 min in photoauto-trophically grown, mid-exponential WT and *hik12* KO cells, in presence and absence of glucose. Luminol assay solution/buffer without cells was included as control. Measurements were carried out in 96-well plates in a microtiter plate luminometer. The total volume of 250 µl per well consisted of 100 µl of cell culture and 150 µl of luminol assay solution. As shown in Figure 18, no distinct chemoluminescence reactions and thus no ROS production was detectable in WT cells, except from background emissions. A striking increase in chemoluminescence emissions, indicative of ROS production, was detectable in *hik12* KO cells during the initial 20 min of the measurement. Thereafter, a phase of relatively constant chemo-luminescence emission signals was reached, which slowly declined in the last 20 min of the measurement. Furthermore, the addition of glucose, prior to the measurement, did not affect chemoluminescence emissions, neither in WT nor in *hik12* KO cells.
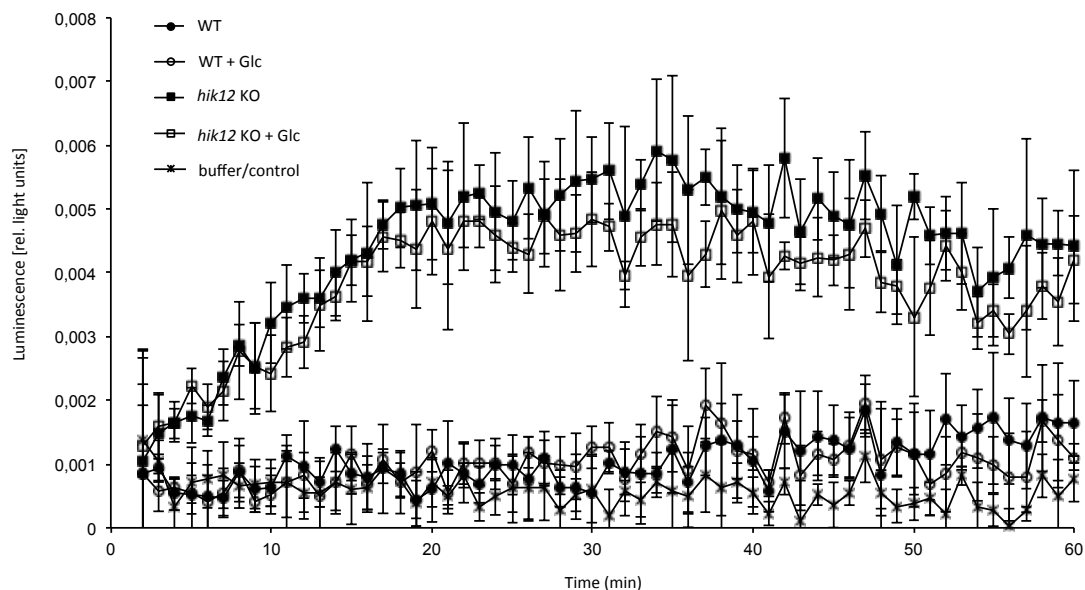
Figure 18: ROS production in WT and *hik12* KO cells in presence and absence of exogenous glucose.

ROS-mediated oxidation of luminol was recorded as relative chemoluminescence units for 60 min in photoautotrophically grown, mid-exponential WT (circles) and *hik12* KO (rectangles) cells, in presence (open symbols) and absence (filled symbols) of 10 mM glucose. Luminol assay solution/buffer without cells was included as control (filled triangle). Error bars represent standard deviation, based on mean values of five samples per strain and condition (+/- glucose). Data presented are representative for three independent experiments.

3.3 Analysis of cytokinin function in plant-pathogen interactions

Cytokinins are a class of aminopurine-based phytohormones that regulate various physiological and developmental processes in higher plants, which include cell division and differentiation, chloroplast development, seed germination, delay of leaf senescence, nutrient mobilization and stress responses (Kakimoto, 2003; Balibrea Lara *et al.,* 2004; Sakakibara, 2006; Müller & Sheen, 2007, Bari & Jones, 2009; Hwang *et al.,* 2012). Recently, evidence has been found that cytokinins are involved in processes related to defense mechanisms during plant-pathogen interactions (Argueso *et al.,* 2009; Choi *et al.,* 2010). To provide further insight into cytokinin function in plants and their involvement in defense mechanisms, different approaches, implying transient overexpression of cytokinin-degrading enzymes in the biotrophic host-pathogen system barley-*Bgh* (*Blumeria gr*aminis f.sp. *hordei*) and the analysis of an *Arabidopsis* cytokinin receptor-deficient mutant in interaction with *Pseudomonas syringae* pv. *tomato* DC3000 (*Pst*) were conducted.

3.3.1 Simultaneous overexpression of two cytokinin oxidases in barley cells increased resistance to powdery mildew

To examine the function of cytokinin in defense mechanisms, the effect of altered cytokinin levels was analysed during plant-pathogen interaction. Therefore, two cytokinin degrading enzymes of *Arabidopsis*, the cytokinin oxidases AtCKX1 and AtCKX2, were transiently overexpressed in barley cv. Pallas leaves and analysed in interaction with the barley-powdery mildew fungus *Blumeria graminis* f.sp. *hordei* (*Bgh*). In this compatible interaction, the fungus penetrates the plant cell and develops its characteristic digitate-shaped feeding organ, the haustorium. Ballistic transformation of single cells is a reliable method for assessing gene functions in plant-pathogen interactions, in particular in interactions of members of the tribe *Triticeae* and powdery mildew fungi (Panstruga, 2004). Barley epidermal cells were transiently transformed via particle bombardment, inoculated with *Bgh* spores and analysed microscopically. Tungsten particles served as microcarriers to deliver the expression vectors into single epidermal cells. The particles were coated with plasmid DNA of the expression construct of AtCKX1, AtCKX2, AtCKX1 and AtCK2 together or the empty vector as control, together with plasmid DNA of the green fluorescent protein (GFP) as reporter gene. All genes were subcloned into the plant expression vector pGY1 to be controlled by the constitutive cauliflower mosaic virus (CaMV) 35S promotor (Hückelhoven *et al.,* 2003; Schweizer *et al.,* 1999). Due to the

CaMV 35S promotor, pGY1 can be used for overexpression of genes in plant cells. Four hours after transformation, the barley leaves were inoculated with spores of *Bgh* giving a density of 150 conidia mm^{-2}. 48 hours after inoculation (hai), transformed cells were identified by fluorescence microscopy for the presence of GFP fluorescence. Using fluorescence microscopy, the outcome of interactions was evaluated as penetration efficiencies (PE), thereby distinguishing between attacked and successfully penetrated cells (haustorium-containing cells) and attacked and non-penetrated cells (papilla forming cells). Microscopic analysis revealed, that single overexpression of AtCKX1 (Figure 19 A) and AtCKX2 (Figure 19 B)*,* resulted in no significant differences in PE of *Bgh* in transformed barley epidermal cells. To analyse potential synergistic effects, both cytokinin oxidases were simultaneously overexpressed. As shown in Figure 19 C, simultaneous overexpression of AtCKX1 and AtCKX2 resulted in a significantly reduced PE of *Bgh* ($P < 0.05$, Student's *t* test).
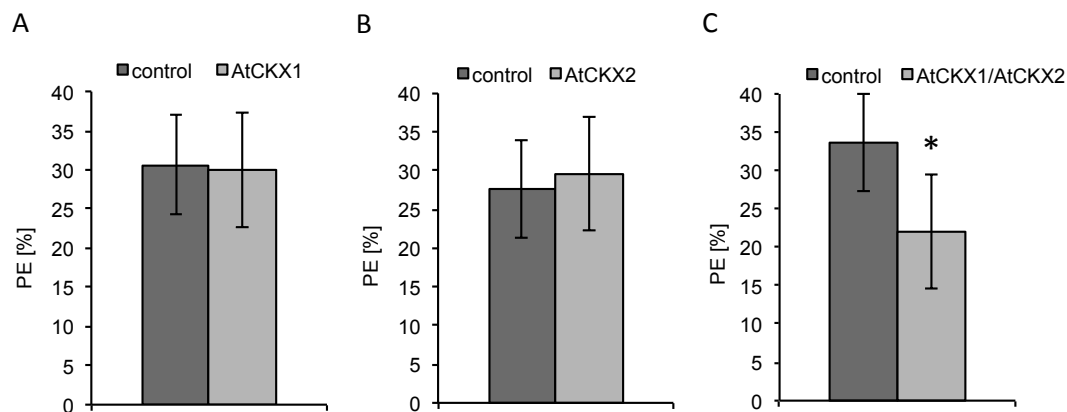
Figure 19: Penetration efficiencies of *Bgh* spores on transiently transformed barley epidermal cells, overexpressing *Arabidopsis* cytokinin oxidases AtCKX1 (A), AtCKX2 (B) and AtCKX1/AtCKX2 simultaneously (C).

Penetration efficiencies (PE) of *Blumeria graminis* f. sp. *hordei* (*Bgh*) spores on barley epidermal cells (cv. Pallas), transiently overexpressing *Arabidopsis* cytokinin oxidases AtCKX1 (A), AtCKX2 (B) and AtCKX1/AtCKX2 simultaneously (C). As control, cells were transformed with the empty vector pGY1. Co-transformed GFP served as reporter gene, allowing the detection of transformed cells by means of fluorescence microscopy. Columns in A, B and C represent average values of three independent experiments (in each experiment a minimum of 80 interactions was analysed). Bars represent standard errors. The asterisk indicates significant difference at $P < 0.05$ according to Student's *t* test.

3.3.2 The *Arabidopsis* AHK3 cytokinin receptor mutant is impaired in the defense response to *P. syringae*

Besides the involvement in various developmental processes, cytokinins are known to have a profound effect on leaf senescence (Mok, 1994; Kim *et al.,* 2006). A direct link between cytokinin effects and plant responses to biotrophic pathogens has been suggested (Walters *et al.*, 2008), as defense responses are associated with altered senescence phenotypes, well known as the phenomenon of "green island" formation

(Walters & McRoberts, 2006). In *Arabidopsis,* the cytokinin signal is perceived by three sensor histidine kinases AHK2, AHK3 and AHK4 (Inoue *et al.*, 2001; Suzuki *et al.,* 2001; Ueguchi *et al*., 2001; Yamada *et al.,* 2001). Among them, AHK3 has been identified as the cytokinin receptor controlling senescence in leaves (Kim *et al*., 2006). To investigate the function of cytokinins in plant-pathogen interactions, the AHK3 loss-of-function T-DNA insertion line (NASC Nr. N6562; Higuchi *et al.,* 2004; Nishimura *et al.,* 2004) was analysed in pathogen assays during the interaction with the hemibiotrophic pathogen *Pseudomonas syringae* pv. *tomato* DC3000 (*Pst*). The insertion of T-DNA in AHK3-T-DNA insertion plants used was confirmed by PCR on genomic DNA (Supplementary figure 3). To monitor the development of disease symptoms, detached leaves of 6-week old *Arabidopsis* WT and AHK3 cytokinin receptor-deficient (*ahk3* KO) plants were infiltrated with *Pst* at a density of 10^4 cfu ml^{-1} in 10 mM $MgCl_2$ and incubated on water agar in darkness. Pictures of infiltrated leaves were taken at 5 and 8 days after inoculation (dai) and are representative for three independent experiments (Figure 20 A).
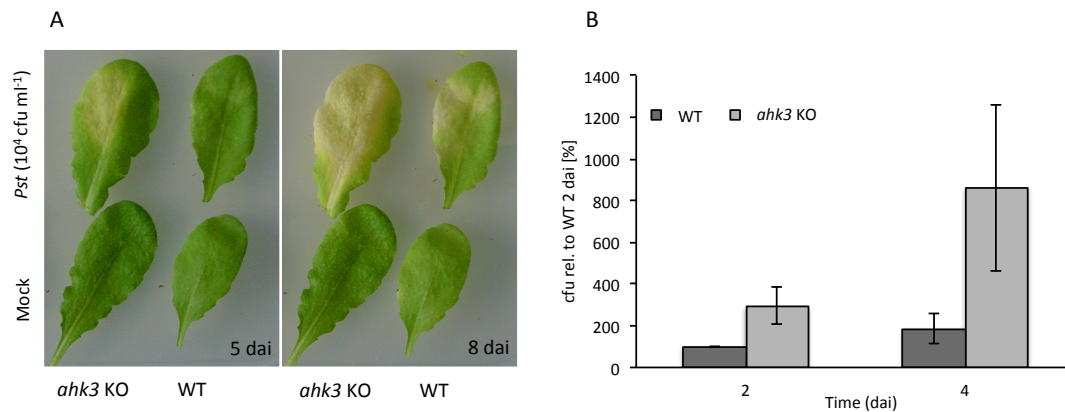
Figure 20: Responses of *Arabidopsis* AHK3 receptor-deficient mutant and WT plants to *Pseudomonas syringae* pv. *tomato* DC3000 (*Pst*).

(A) Disease symptom development in detached leaves of 6-week old *Arabidopsis* WT (Wasilewska) and AHK3 receptor-deficient (*ahk3* KO) plants, infiltrated with a bacterial suspension of virulent *Pseudomonas syringae* pv. *tomato* DC3000 at a density of 10^4 cfu ml^{-1} in 10 ml $MgCl_2$. Mock inoculation with 10 mM $MgCl_2$ was used as control. The infiltrated leaves were incubated on water agar (0.5% w/v) in darkness. Pictures of infiltrated leaves were taken at 5 and 8 dai and are representative for 3 independent experiments.
(B) Bacterial proliferation in WT and *ahk3* KO. Infiltrated, non-detached leaves were sampled at 2 and 4 dai. The infiltrated areas were cut out, scaled, ground in 10 mM $MgCl_2$ and dropped in 7x10 µl droplets in dilution rows on King's B medium agar plates. After 2 days of incubation, bacterial colonies were counted and quantified by evaluating the amount of bacteria per gram leaf material. Data are expressed in colony forming units (cfu) and are normalized to the WT at 2 dai ($1.48*10^7$ cfu/g fresh weight). Columns represent average values of 3 independent experiments. Bars represent standard errors.

Pst is infectious for *Arabidopsis* and becomes visible as chlorotic leaf spots turning into necrosis. As shown in Figure 20 A, *ahk3* KO leaves displayed a clear phenotype in disease symptom development, comprising of necrotic areas at the site of *Pst*

infiltration, while mock infiltration with 10 mM $MgCl_2$ did not lead to the development of necrotic lesions. The disease symptoms in *ahk3* KO leaves developed markedly faster compared to the WT. The necrotic lesions in WT leaves were not formed until 8 dai, while the leaves of *ahk3* KO were rendered almost entirely chlorotic at 8 dai.

To determine bacterial proliferation in WT and *ahk3* KO, non-detached leaves were infiltrated as described above. Samples were harvested at 2 and 4 dai. The infiltrated areas were cut out, scaled, ground in 10 mM $MgCl_2$ and dropped in dilution rows on King's B medium agar plates. After 2 days of incubation, bacterial colonies were counted and quantified by evaluating the amount of bacteria per gram leaf material. Data are expressed in colony forming units (cfu) and are normalized to the WT at 2 dai. The analysis of bacterial growth sampled from infiltrated WT and *ahk3* KO revealed that *Pst* proliferates faster in *ahk3* KO compared to the WT (Figure 20 B). The amount of bacteria sampled from *ahk3* KO leaves at 2 dai was more than three times as high as in WT leaves. From 2 dai to 4 dai, the amount of *Pst* sampled from WT leaves almost doubled, while *Pst* from *ahk3* KO leaves increased almost three-fold. These results further support the observed phenotype in disease symptom development, thereby indicating a function of AHK3 in the defense response of *Arabidopsis* to *Pseudomonas syringae* pv. *tomato*.

3.3.3 *Arabidopsis ahk3* KO displays constitutive ROS production

To analyse the ROS production in *Arabidopsis* WT and cytokinin receptor-deficient mutant (*ahk3* KO) leaves, luminol-based assays were conducted. ROS-mediated oxidation of luminol was recorded as relative chemoluminescence units for 60 min in samples of *Arabidopsis* WT and *ahk3* KO leaves, in presence and absence of glucose. Luminol assay solution/buffer without leaf samples was included as control. Prior to the measurement, the excised leaf samples were incubated floating on a water surface. Measurements were carried out in 96-well plates in a microtiter plate luminometer. Two leaf pieces per well were added to 200 µl assay solution/buffer, immediately before the measurement. As shown in Figure 21, no distinct chemo-luminescence reactions and thus no ROS production was detectable in the WT, except from background emissions. In contrast, increasing chemoluminescence emission signals, indicative of ROS production, were detectable in *ahk3* KO, until a phase of relatively constant chemoluminescence emission signals was reached after 30 min. The addition of glucose prior to the measurement, did not affect chemo-luminescence emission in WT and *ahk3* KO.
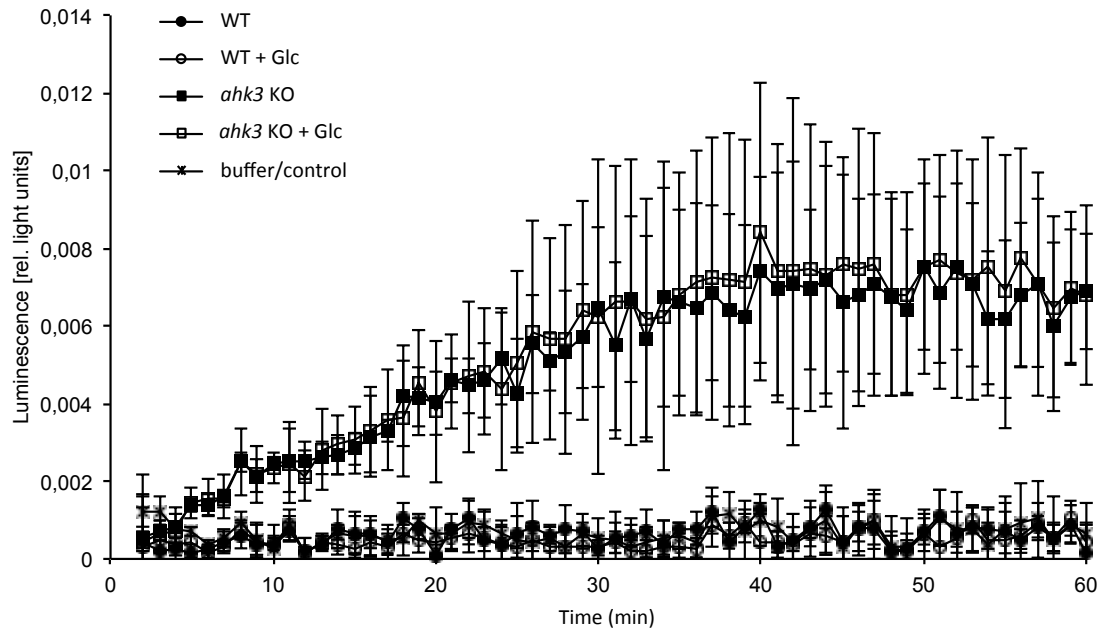
Figure 21: ROS production in *Arabidopsis* WT and *ahk3* KO leaf explants in presence and absence of glucose.

ROS-mediated oxidation of luminol was recorded as relative chemoluminescence units for 60 min in leaf samples (cut in square pieces of 4 mm^2) of 6-week old *Arabidopsis* WT (circles) and *ahk3* KO (rectangles) samples. Measurements were carried out in presence (open symbols) and absence (filled symbols) of 10 mM glucose. Luminol assay solution/buffer without leaf samples was included as control (filled triangle). Prior to the measurement, excised leaf samples were incubated floating on a water surface over night in a climate chamber at 22°C with a relative humidity of 64% and a photoperiod of 10 h light irradiance at 120 µmol photons m^{-2}s^{-1}. Data presented are representative for three independent experiments. Error bars represent standard deviation, based on mean values of five samples per strain and condition (+/- glucose).

4 Discussion

Analysing the metabolic and physiological responses to individual gene deletions can provide deeper insights into an organism's control and regulation of the metabolism. During the endosymbiontic event, many cyanobacterial genes have been transferred to the plant nucleus. In particular, genes coding for proteins involved in signal transduction are highly conserved among cyanobacteria and plants, which renders cyanobacteria into suitable model organisms for the analysis of signal transduction mechanisms.

This thesis contributes to the understanding of signalling processes and their effects on the metabolism by analysing the functions of the signalling components CPH2 and HIK12 in the cyanobacterium *Synechocystis* sp. PCC 6803. For CPH2, an involvement of this cyanobacterial phytochrome photoreceptor in various light-dependent processes has been demonstrated (Park *et al.,* 2000; Wilde *et al.,* 2002; Fiedler *et al.,* 2004; Moon *et al.,* 2011; Savakis *et al.,* 2012), while HIK12 is one of more than 40 histidine kinases in *Synechocystis* of yet indefinite function, but with similarity to plant cytokinin receptors.

In the present study, knockout and overexpression mutants were physiologically analyzed under distinct growth conditions, with particular interest in the central carbon metabolism and the transition from fast exponential to slowed down growth in biomats. The obtained results show a clear regulatory function of both proteins on the central carbon metabolism, which is substantiated in a strongly retarded growth phenotype in the knockout mutants, correlating with a reduced G6PDH activity and altered transcript levels of cytochrome *c* oxidase encoding *CtaDI* gene, which manifests after the transition to biomatforming conditions, in *cph2* KO under heterotrophic, in *hik12* KO under photomixotrophic conditions.

Besides the well-known involvement in essential developmental and physiological processes throughout the plant life, the phytohormone cytokinin has recently emerged as main factor in plant-pathogen interactions. The last part of this thesis focuses on the function of cytokinin in regulating susceptibility or basal resistance in the interaction of pathogens with barley and *Arabidopsis.* The results obtained further support an essential function of cytokinins in plant-pathogen interactions by confirming that cytokinins affect plant immunity.

4.1 Physiological characterisation of the cyanobacterial phytochrome CPH2 and its regulatory function on the central carbon metabolism

Light is a basic need for all photosynthetic organisms. With the diurnal changes in light quality and quantity, photosynthetic organisms are in the constant need to adapt to changing light conditions, which requires appropriate adjustments of the metabolism in order to maintain energy homeostasis. In cyanobacteria, the response to changes in light intensity and spectral qualities is accomplished by various different photoreceptors coupled to signal transduction networks (Montgomery, 2007). Among them, the best-studied photoreceptors in cyanobacteria are the bilin-containing photoreceptors of the phytochrome family (Rockwell & Lagarias, 2010). These photoreceptors photointerconvert between red (Pr) and far-red (Pfr) absorbing forms by utilising a tetrapyrrole chromophore that is covalently bound to a cysteine residue. Like in plants, the cyanobacterial phytochrome CPH1 (*slr0473*) contains an N-terminal photosensory module, which confers Pr/Pfr-like photochromicity (Yeh *et al*., 1997; Hughes *et al.*, 1997). The related phytochrome-like photoreceptor CPH2 (*sll0821*) differs in its domain organisation. CPH2 is a hybrid photoreceptor, comprising of an N-terminal Pr/Pfr photosensory module (Park *et al.,* 2000; Wu & Lagarias, 2000) and a C-terminal cyanobacteriochrome module that photointer-converts between blue and green light absorbing forms (Savakis *et al.,* 2012). Furthermore, CPH2 possesses GGDEF and EAL domains, whose diguanylate cyclase (DGC) and phosphodiesterase (PDE) activities are known to be involved in the synthesis and breakdown of the second messenger c-di-GMP, respectively (Ryan *et al.,* 2006; Cotter & Stibitz, 2007; Pesavento & Hengge, 2009; Yan & Chen, 2010). Most GGDEF and EAL domains found in bacteria are coupled to a signal input or sensory domain, which include blue light sensing (Barends *et al.,* 2009), red/far red light sensing (GAF-PHY domain), domains involved in oxygen sensing (PAS domains) and phytochrome binding (GAF-PHY domains) (Hengge, 2009; Galperin, 2006; Schirmer & Jenal, 2009). Upon perception of environmental changes, e.g. changes in light abundance or oxygen, the primary signals are trans-mitted to DGC or PDE that activate the biosynthesis or degradation of c-di-GMP, which functions as allosteric regulator of downstream target proteins (Yan & Chen, 2010). Although much about the downstream regulation cascades remains unknown, c-di-GMP has been shown to play an important role in adhesion, cell-to-cell communication, exopolysaccharide formation and motility (Tischler & Camilli, 2004) and in particular, in many bacterial species in regulating the transition between

motile and sessile lifestyles (Römling *et al*., 2005; Jenal & Malone, 2006; Cotter & Stibitz, 2007; Pesavento & Hengge, 2009; Yan & Chen, 2010).

Based on the structural organisation of CPH2, including the ability to perceive red/far-red and blue light and the existence of GGDEF and EAL domains, it is conceivable that light perceived by CPH2 modulates the activity of GGDEF and EAL domains. This was recently confirmed by Savakis and co-workers (2012), who demonstrated that c-di-GMP is a functional second messenger in *Synechocystis* sp. PCC 6803 and that CPH2 functions as its primary, light-regulated modulator. Aside from its involvement in adaptional processes during light-dark transitions (Park *et al.,* 2000) and the regulation of growth under changing light conditions (Fiedler *et al.,* 2004), CPH2 was reported to be involved in phototactic motility, in particular in the inhibition of phototaxis towards blue light (Wilde *et al.,* 2002) and UV-A light (Moon *et al.,* 2011). Savakis and co-workers (2012) provided the first evidence that c-di-GMP is directly involved in the light-dependent regulation of cyanobacterial phototaxis.

In this study, the physiological effects of the loss of CPH2 in *Synechocystis* sp. PCC 6803 were analysed with a special focus on the central carbon metabolism. For this purpose, growth kinetics, specific enzyme activities and gene expression patterns for WT, *cph2* knockout (loss-of-function) and *cph2* overexpression (complementation) mutants were analysed under different growth conditions.

4.1.1 Deletion of CPH2 negatively affects growth under LAHG/biomatforming conditions

To screen for physiological effects, growth kinetics were analysed under different growth conditions in WT, *cph2* KO and *cph2* OE. The analysis of the growth kinetics revealed no differences in growth between WT, *cph2* KO and *cph2* OE under photoautotrophic and photomixotrophic growth conditions (Figure 6 A, B). The accelerated growth upon addition of glucose under photomixotrophic conditions (Figure 6 B) compared to photoautotrophic conditions, indicates that WT, *cph2* KO and *cph2* OE are capable of utilising exogenous glucose and therefore are capable of photomixotrophic growth (Williams, 1988; Anderson & McIntosh, 1991). This is in accordance with findings of Knowles and co-workers (2003) and Anderson and McIntosh (1991), who reported similar growth profiles for *Synechocystis* sp. PCC 6803 under photoautotrophic and photomixotrophic growth conditions.

For CPH2, Fiedler and co-workers (2004) demonstrated an involvement in photo-autotrophic growth under different light qualities and quantities, which was reflected in decreased growth rates of *cph2* knockout mutants under red light (660 nm)

illumination. The present study focuses on the function of CPH2 under LAHG/ biomatforming conditions. To this end, growth of WT, *cph2* KO and *cph2* OE was analysed after the transition from light to darkness with a daily amount of 15 min white light, in presence of glucose as exogenous carbon source. These conditions are referred to as light-activated heterotrophic growth (LAHG) (Anderson & McIntosh, 1991; Tabei *et al.,* 2009). For *Synechocystis* to grow heterotrophically on glucose, a minimal amount of light, e.g. for 5 min every 24 h, is necessary to keep the cells metabolically active (Tabei *et al.,* 2009). LAHG was chosen as it allows to exclude almost entirely the effect of photosynthesis on the metabolism of the cells. Furthermore, due to the existence of GGDEF and EAL domains in CPH2, we speculated about a function of CPH2 in the switch between motile and sessile lifestyles. The analysis of growth kinetics revealed that incubation under LAHG/bio-matforming conditions led to a considerably lower growth rate compared to that obtained under photoautotrophic or photomixotrophic conditions. Most of all, the *cph2* KO mutant was characterized by growth cessation under LAHG conditions (Figure 6 C). Under non-photosynthetic conditions, the cells have to meet their energy demands for maintenance and growth by switching their metabolic mode to light-activated heterotrophic energy generation (Stal & Moezelaar, 1997; Knowles & Plaxton, 2003). The primary energy source for heterotrophic metabolism is glucose, deriving from glycogen catabolism or exogenous glucose. Hence, the growth cessation of *cph2* KO might reflect a deficiency in utilising either exogenous glucose or glucose residues derived from carbon stores, thereby indicating a regulatory function of CPH2 on growth under LAHG/biomatforming conditions. To elucidate the cause of the observed growth phenotype of *cph2* KO further research of the sugar catabolism and its corresponding pathways was performed. For this purpose, the specific activity of G6PDH, an enzyme indispensable for glucose catabolism and the transcript levels of key metabolic genes were analysed.

4.1.2 Deletion of *cph2* affects G6PDH enzyme activity and the transcript level of *CtaDI*, encoding cytochrome *c* oxidase, under LAHG/biomatforming conditions

In cyanobacteria, the OPPP is widely accepted to be the main route of glucose catabolism, for both the breakdown of glycogen and exogenously supplied glucose (Hagen & Meeks, 2001; Yang *et al*., 2002). The initial step of glucose degradation is the conversion of glucose-6-phosphate to 6-phosphogluconolactone, which is catalyzed by the enzyme glucose-6-phosphate dehydrogenase (G6PDH). G6PDH represents the rate-determining step of glucose degradation by controlling the

carbon flow into the OPPP (Yang *et al*., 2002; Singh *et al.,* 2004; Singh & Sherman, 2005). The analysis of the specific G6PDH enzyme activity provides further information about the assumed deficiency of *cph2* KO in metabolising glucose, which is substantiated by a significantly reduced G6PDH enzyme activity in both independent *cph2* loss-of-function mutants after incubation under LAHG/biomatforming conditions (Figure 7 B). After the transition from photoautotrophic to dark heterotrophic conditions in presence of glucose, CO_2 assimilation via the Calvin cycle is subsequently inactivated and the major metabolic pathway switches from the Calvin cycle to the OPPP (Pelroy *et al.,* 1976). This is in accordance with the analysis of metabolic flux distributions by Yang and co-workers (2002), which revealed that over 90% of glucose is catabolized through the OPPP during heterotrophic growth. Thus, the strongly reduced G6PDH activity in *cph2* KO should result in significantly lower glucose degradation by the OPPP. This in turn could explain the inability of *cph2* KO to grow under LAHG/biomatforming conditions. In addition to the shift from photoautotrophy to dark heterotrophy, the cells were subjected to biomatforming conditions, which includes the transition from a motile, fast growing lifestyle to a sessile, slow-growing lifestyle with high cellular density within a biomat. In this context, the reduced enzyme activity in *cph2* loss-of-function mutant might also indicate that CPH2 has a special function in the induction of G6PDH enzyme activity or in protein expression under biomatforming conditions. Notably, overexpression of CPH2 in the *cph2* KO background resulted in complementation of enzyme activity and growth kinetics, confirming that the observed phenotype is caused by the deletion of *Cph2*. Furthermore, the fact that no significant differences in enzyme activities of WT, *cph2* KO and *cph2* OE were observable under photoautotrophic and photomixotrophic conditions (Figure 7 A) indicates a specific function of CPH2 during the shift from light to dark heterotrophy under biomatforming conditions.

The supply of glucose to photoautotrophically grown cells leads to various changes in growth and carbon metabolism (Yang *et al.*, 2002; Knowles & Plaxton, 2003; Lee *et al.,* 2005; Osanai *et al*., 2005; Singh & Sherman, 2005), as well as in photosynthesis and respiration (Ryu *et al.,* 2004, Lee *et al.,* 2005; Kurian *et al.,* 2006). Despite the numerous responses to glucose, profiles of transcript abundance and protein levels did not show significant differences in photoautotrophic and photomixotrophic cultures (Yang *et al.,* 2002; Knowles & Plaxton, 2003; Tu *et al.*, 2004; Singh & Sherman, 2005; Kahlon *et al.,* 2006), indicating that the response to glucose is mainly accomplished on alterations at the level of post-translational modifications or modulation of enzyme activities (Kahlon *et al.,* 2006). To examine the effects of

cph2 deletion on the transcriptional level, gene expression profiles of two key metabolic and photosynthetic genes, respectively, were analysed using semi-quantitative RT-PCR. In addition to *Zwf* (*slr1843)*, encoding for G6PDH, a second metabolism-related gene, *CtaDI* (*slr1137),* encoding for subunit I of the cytochrome *c* oxidase complex, the terminal component of the respiratory chain, and two photosynthesis-related genes, *PsaA* (*slr1834*) and *PsbA3 (sll1867*), encoding for subunit Ia of the P700 apoprotein and for PS II D1 protein, respectively, were analysed under different growth conditions. Consistent with the results obtained in growth and enzyme activities, the presence or absence of exogenous glucose did not significantly alter the gene expression patterns of both metabolic genes in WT, *cph2* KO and *cph2* OE, which is reflected in similar expression patterns for *Zwf* and *CtaDI* under photoautotrophic and photomixotrophic conditions (Figure 8 A, B). This is in accordance with Yang and co-workers (2002), who demonstrated that levels of mRNA transcripts encoding various key enzymes of the central carbon metabolism were not significantly altered upon the presence or absence of exogenous glucose. Solely, under both photoautotrophic and photomixotrophic growth conditions, the photosynthesis-related genes, *PsaA* and *PsbA3* displayed a slightly induced transcript accumulation in the *cph2* overexpression mutant (Figure 8 A, B). Using DNA microarrays, Singh and co-workers (2009) demonstrated that illumination of *Synechocystis* with light that preferentially excites PS II or PS I, has a significant impact on transcript levels of genes involved in various processes. They found that preferential excitation of *Synechocystis* cells with PS I light (λ_{max} ~ 455 nm) or PS II light (λ_{max} ~ 627 nm) led to the complementary regulation of photosystem genes. Possibly, the observed slightly induced transcript accumulation in *cph2* comple-mentation mutant (Figure 8 A, B) might be due to the spectral composition of light in the incubator and/or a side effect of the expression of *cph2* under the control of the constitutive petJ promotor. Beyond that, changes in the redox poise of the PQ pool, possibly due to the overexpression, might also be considered to cause the observed changes in the expression levels in *cph2* complementation mutant, since the expression levels of certain photosynthetic genes are regulated by the redox status of the PQ pool (Bendall & Manasse, 1995; Alfonso *et al.,* 1999; Li & Singh, 2000; Ma & Mi, 2008).

The transition from photoautotrophic to LAHG and biomatforming conditions revealed an interesting transcriptional pattern for *cph2* KO. In contrast to the strong effect on the enzyme activity level (Figure 7 B), the transcript level of *Zwf,* encoding for G6PDH, was not significantly altered in WT, *cph2* KO and *cph2* OE under

LAHG/biomatforming conditions (Figure 8 C). This inconsistency of the *Zwf* transcript level and the enzymatic activity of G6PDH support the previously assumed regulation of G6PDH at the post-translational level. This corresponds to the findings of Yang and co-workers (2002), who demonstrated, using carbon isotope labelling, that the metabolic flux through G6PDH was enhanced under heterotrophic conditions, even though the transcript levels of *Zwf* remained unaltered. This might further indicate that the regulation of the metabolic flux through G6PDH was accomplished post-translational. This is also in accordance with the finding that the activities of enzymes involved in the glycolytic and OPP pathway, such as G6PDH, Fructose-1,6-bisphosphatase, phosphofructokinase, Fructose-1,6-bisphosphatase-aldolase and pyruvate kinase, are regulated by changes in metabolite concentrations (Stal & Moezelaar, 1997; Sundaram *et al.,* 1998; Yang *et al.,* 2002; Knowles & Plaxton, 2003; Lee *et al.,* 2007). In the case of G6PDH, this includes NADPH, ATP, G6P, glutamine and $Rib1,5P_2$ (Schaeffer & Stanier, 1978; Cossar *et al.,* 1984; Plaxton & Podesta, 2006; Lee *et al*., 2007).

Under heterotrophic conditions, in the absence of light or at very low light intensities, the respiratory electron transport chain has a much higher capacity of electron flow than the photosynthetic electron transport chain (Vermaas, 2001). Under these conditions, catabolic pathways mainly provide electron input into the electron transport chain. Electrons from NADPH, generated through glucose oxidation, mainly by G6PDH, enter the electron transport chain via NDH-1, are transported via the PQ pool/cytochrome b_6f complex and are finally transferred to molecular oxygen. Among the three terminal oxidases identified so far in *Synechocystis* (Hart *et al.,* 2005), cytochrome *c* oxidase has been confirmed to function as main terminal oxidase (Schmetterer, 1994) for electrons generated from NADPH (Howitt & Vermaas, 1998; Ryu *et al.,* 2003). According to its function as terminal component of the respiratory electron transport chain, cytochrome *c* oxidase encoding gene *CtaDI* was analysed as second metabolism-related gene, thereby displaying an interesting transcriptional pattern in *cph2* KO under LAHG/biomatforming conditions. In contrast to the unchanged transcript levels of *Zwf* and both photosynthetic genes, the transcript level of *CtaDI,* is clearly downregulated in *cph2* KO mutant under LAHG/biomat-forming conditions (Figure 8 C). Furthermore, the complementation of *cph2* KO displays a gene expression pattern for *CtaDI* similar to the WT (Figure 8 C). The phenotype in *CtaDI* expression has been observed specifically during acclimation to LAHG/biomatforming conditions. Thus, one could assume that CPH2 has a function in the regulation of cytochrome *c* oxidase expression under LAHG/biomatforming

conditions. The strong underexpression of *CtaDI* in *cph2* KO under LAHG/biomat-forming conditions should result in a significantly reduced cytochrome *c* oxidase activity. Recent data (Rheinhard Pröls, Technische Universität München, Munich, Germany, personal communication) indeed show strongly reduced cytochrome *c* oxidase activity under these conditions for *cph2* KO. This in turn could result in an overreduced electron transport chain, as the electrons cannot be removed. As G6PDH activity is inactivated under reducing conditions (Plaxton & Podesta, 2006; Lee *et al.*, 2007), the underexpression of *CtaDI* might cause the lower G6PDH activity in *cph2* KO. Therefore, cytochrome *c* oxidase might be a target of CPH2 in regulating the heterotrophic metabolism under LAHG/biomatforming conditions. This hypothesis has been supported since recent measurements of fluorescence induction, which allow to monitor the redox state of the PQ pool, evidence the assumed overreduction of the PQ pool in *cph2* KO (Rheinhard Pröls, Technische Universität München, Munich, Germany, personal communication).

4.1.3 P700$^+$ reduction kinetics: Analysis of electron transport activities

To further sustain the regulatory function of CPH2 on the glucose metabolism under heterotrophic/biomatforming conditions, P700$^+$ reduction kinetics were used to analyse electron transport activities in the cyanobacterial thylakoid membrane. In *Synechocystis*, the thylakoid membrane contains both photosynthetic and respiratory electron transport chains, which intersect and share electron carriers (Figure 1) (Schmetterer, 1994; Vermaas, 2001). Among them, the PQ pool represents the central switching point of both respiratory and photosynthetic electron transport, where the electron inputs from photosynthetic linear, cyclic and respiratory electron transport pathways, converge. The PQ pool is oxidized by PS I and by cytochrome *c* oxidase via cytochrome *b$_6$f* complex or directly by cytochrome *bd*-type quinol oxidase (Endo, 1997). In addition to its central role in the electron transport chain, the redox state of the PQ pool regulates the transcription of various genes, among them, genes encoding for photosynthetic proteins (Pfannschmidt *et al.,* 1999; Alfonso *et al.,* 2000; Li & Sherman, 2000; Hihara *et al.,* 2003; Kufryk & Vermaas, 2006). Furthermore, the redox poise of the PQ pool can directly mediate the regulation of metabolic processes (Alfonso *et al.,* 1999, 2000; El Bissati & Kirilovsky, 2001; Vermaas, 2001; Ma & Mi*,* 2008).

In the light, the photosynthetic electron transport chain has a higher capacity of the electron flow than the respiratory chain (Vermaas, 2001). Accordingly, linear electron

transport from water to $NADP^+$ via PS II and PS I, is the prevalent electron transport pathway, which implies that the PQ pool is mainly reduced by electrons deriving from water-splitting activity of PS II and not by electrons deriving from the heterotrophic metabolism. In samples adapted to photoautotrophic conditions, treatment with the PS II inhibitor DCMU resulted in increased $t_{1/2}$ of $P700^+$ reduction in WT, *cph2* KO and *cph2* OE compared to untreated samples (Figure 10 C). Since the linear electron transport is blocked by DCMU, electron input into the PQ pool originates from electron flows via SDH and NDH-1, from NADPH generated mainly by glucose oxidation in the heterotrophic metabolism or by PS I during blue light illumination. Due to the reduced amount of electrons, the PQ pool is more oxidized in DCMU-treated samples compared to untreated samples, resulting in increased $t_{1/2}$ of $P700^+$ reduction, as it takes longer to re-reduce $P700^+$ after switching off blue light illumination.

In darkness or at very low light intensities, the respiratory electron transport chain has a higher capacity of electron input than PS II (Vermaas, 2001). In samples adapted to dark/biomatforming conditions, treatment with DCMU resulted in a significantly increased $t_{1/2}$ of $P700^+$ reduction in *cph2* KO compared to the WT (Figure 10 D). The higher increase in $t_{1/2}$ of $P700^+$ reduction in *cph2* KO indicates a reduced electron input into the PQ pool. This might either be caused by a reduced electron input from NADPH, generated by PS I during blue light illumination or by a reduced electron input from the heterotrophic metabolism, which would further sustain the previously assumed reduced ability of *cph2* KO in metabolising glucose. A possible explanation for the reduced electron input from the heterotrophic metabolism is that G6PDH activity is significantly lower under LAHG/biomatforming conditions (Figure 7 B). An alternative explanation could be an overreduced PQ pool, resulting from the non-functionality of cytochrome *c* oxidase, which could inactivate G6PDH. DBMIB prevents the reoxidation of plastoquinone, thereby inhibiting the electron input from the PQ pool into the cytochrome *b_6f* complex. The inhibition with DBMIB does not result in a complete electron blockage, which explains why $P700^+$ reduction is detectable. In samples adapted to photoautotrophic conditions, simul-taneous treatment with DCMU and DBMIB resulted in increased $t_{1/2}$ of $P700^+$ reduction in WT, *cph2* KO and *cph2* OE (Figure 10 C), indicating a strongly restricted electron flow to $P700^+$. After the transition to dark/biomatforming conditions, this effect is no longer observable, as WT, *cph2* KO and *cph2* OE displayed increased, but not significantly different $t_{1/2}$ of $P700^+$ reduction (Figure 10 D). Notably, the increase in $t_{1/2}$ of $P700^+$ reduction upon DCMU/DBMIB-treatment was higher in

samples adapted to photoautotrophic conditions than to dark/biomatforming conditions. This might indicate a reduced electron flux in samples adapted to dark/biomatforming conditions, resulting from a generally slowed down metabolism under dark/biomatforming conditions.

Together, the increase in $t_{1/2}$ of $P700^+$ reduction upon DCMU-treatment in *cph2* KO adapted to dark/biomatforming conditions and the similar $t_{1/2}$ of $P700^+$ reduction upon DCMU/DBMIB-treatment in WT, *cph2* KO and *cph2* OE adapted to dark/biomatforming conditions, indicate that the electron input into the PQ pool, from heterotrophic sources via SDH or NDH-1 or from NADPH, generated by PS I during blue light illumination, might be affected in *cph2* KO. This corroborates a regulatory function of CPH2 on glucose metabolism during the reorganisation of the metabolism, concomitant with the transition from photoautotrophic to heterotrophic/biomatforming growth conditions.

4.1.4 CPH2 has an essential regulatory function on glucose metabolism under LAHG/biomatforming conditions

This study provides evidence for the cyanobacterial phytochrome CPH2 playing a significant role in the regulation of the central carbon metabolism of *Synechocystis* sp. PCC 6803 under heterotrophic (LAHG)/biomatforming conditions. The transition from photoautotrophic to LAHG/biomatforming conditions and concomitant the reorganisation of the metabolism, revealed a physiological phenotype in the *cph2* loss-of-function mutant, including reduced growth, reduced G6PDH enzyme activity and a strongly downregulated transcript level of cytochrome *c* oxidase encoding *CtaDI* gene. Based on these data, it is most likely that the primary effect of *cph2* deletion on the regulation of the metabolism is the downregulation of cytochrome *c* oxidase. Cytochrome *c* oxidase might further regulate the activity of G6PDH, possibly at the post-translational level via the redox state of the PQ pool or via a so far unknown (feedback) mechanism, leading to a reduced ability in metabolising glucose, which causes the reduced growth phenotype under LAHG/biomatforming conditions. The mechanism by which CPH2 regulates cytochrome *c* oxidase expression remains elusive and is a topic for further studies.

In photosynthetic organisms, glucose metabolism encompasses indispensable metabolic pathways. However, only few of the corresponding regulatory proteins have been identified so far. In *Synechocystis*, for example, some sensors have been identified that affect the glucose metabolism under different trophic conditions. Kahlon and co-workers (2006) demonstrated that the histidine kinase 31 (HIK31) in

Synechocystis is involved in the regulation between photoautotrophic and photo-mixotrophic modes of growth. Furthermore, histidine kinase 8 (HIK8) and the RNA polymerase sigma factor SIGE have been identified as regulatory proteins on glucose catabolism (Singh & Sherman, 2005, 2007). With the results obtained in this study, the cyanobacterial phytochrome CPH2 has been identified as a new regulatory protein of glucose metabolism. This includes the identification of a new function of CPH2, in addition to its already known function in phototaxis and motility (Wilde *et al.,* 2002; Fiedler *et al.,* 2005; Moon *et al.,* 2011; Savakis *et al.,* 2012).

The hypothetical model in Figure 22 connects the physiological functions with the structural organisation of CPH2, suggesting that CPH2 may act as a light-responsive, non-kinase enzyme that possibly regulates various physiological processes via c-di-GMP signalling. C-di-GMP-mediated signalling encompasses enzymes that synthesize and degrade c-di-GMP and downstream c-di-GMP-binding effector proteins. Upon binding of the first messenger (e.g. light in certain wavelength regions, oxygen and phosphorylation) to the sensory domain (e.g. PAS, GAF-PHY and GAF domains) (Galperin, 2006; Hengge, 2009; Schirmer & Jenal, 2009; Yan & Chen, 2010), the cellular concentration of the second messenger c-di-GMP is altered through diguanylate cyclase (DGC) or phosphodiesterase (PDE) activities (Galperin *et al.*, 2001). The GGDEF domain-containing DGC utilises guanosine triphosphate (GTP) as substrate and catalyzes the formation of c-di-GMP, while EAL domain-containing PDE degrades c-di-GMP into guanosine monophosphate (GMP) through the linear intermediate pGpG (Ryan *et al.,* 2006; Jenal & Malone, 2006; Tamayo *et al.,* 2007; Yan & Chen, 2010). C-di-GMP can function as an allosteric regulator of downstream proteins (effectors or receptors). Upon binding of c-di-GMP, these proteins undergo conformational changes, leading to the either positive or negative regulation of important cellular functions or phenotypic transitions, including exopoly-saccharide synthesis, cell-to-cell communication, virulence, motility and biofilm formation (Tischler & Camilli, 2004; Pesavento & Hengge, 2009; Yan & Chen, 2010).
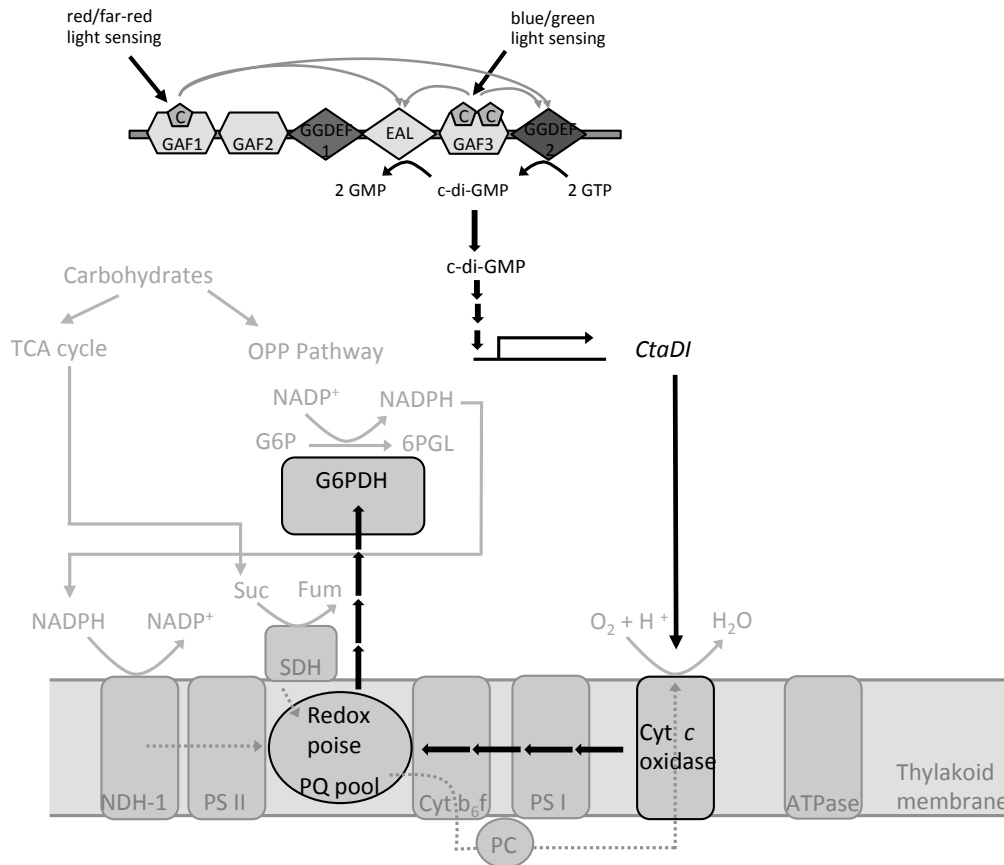
Figure 22: Hypothetical model of the phytochrome photoreceptor CPH2 and its regulatory function on glucose metabolism under heterotrophic (LAHG)/biomat-forming conditions.

According to the working hypothesis, the perception of light leads to conformational changes within CPH2, which affect the activity of GGDEF and EAL domains. This in turn activates the biosynthesis or degradation of c-di-GMP. The altered c-di-GMP level might regulate the transcription of cytochrome *c* oxidase encoding *CtaDI* gene. The activity of cytochrome *c* oxidase could further regulate the activity of G6PDH at the post-translational level, via the redox poise of the PQ pool or another unknown posttranslational regulatory mechanism. The reduced G6PDH activity could cause the reduced ability in metabolising glucose, leading to the observed strongly retarded growth phenotype under LAHG/biomatforming conditions.

Abbreviations: GAF, domain present in vertebrate cGMP-specific phosphodiesterases, in cyanobacterial adenylate cyclases and in the formate lyase transcription activator FhlA; C, cysteine residues in the GAF-domains, which covalently bind the chromophore; GGDEF and EAL, domains with conserved sequence motifs, Gly-Gly-Asp-Glu-Phe and Glu-Ala-Leu, respectively, known to be involved in turnover of c-di-GMP. GTP, guanosine triphosphate; c-di-GMP, bis-(3'-5')-cyclic dimeric guanosine monophosphate; GMP, guanosine monophosphate; *CtaDI,* gene encoding for cytochrome *c* oxidase subunit I; G6P, glucose-6-phosphate; 6PGL, 6-phosphogluconolactone; G6PDH, glucose-6-phosphate dehydrogenase; NDH-1, type I NADPH dehydrogenase; SDH, succinate dehydrogenase; Suc, succinate; Fum, fumarate; PS I and II; photosystem I and II; PQ pool, plastoquinone pool; cyt b_6f, cytochrome b_6f complex; PC, plastocyanin; cyt *c* oxidase, cytochrome *c* oxidase; ATPase, ATP synthase complex; NADP(H), nicotinamide-adenine dinucleotide phosphate (reduced form); OPP Pathway, oxidative pentosephosphate pathway; TCA cycle, tricarboxylic acid cycle.

CPH2 possesses a unique domain organisation, including two N-terminal (GAF1 and GAF2) and a C-terminal GAF domain (GAF3). GAF1 and GAF3 contain bilin-binding sites, conserved cysteine residues, which confer Pr/Pfr-like photochromicity (Wu & Lagarias, 2000) and the ability of blue light perception (Wilde *et al.,* 2002; Fiedler *et al.,* 2005; Ulijasz *et al.,* 2009). Similar to the known mechanism in plant phyto-chromes (reviewed by Nagatani, 2010; Rockwell & Lagarias, 2010), the perception of light (Pr, Pfr or blue light or possibly cross talk of red and blue light) might lead to a conformational change of the bilin-chromophore in CPH2, which triggers a sub-sequent conformational change in the protein. This primary signal might cause changes in the activity of GGDEF and EAL domains in CPH2, which activate the biosynthesis or degradation of c-di-GMP. Recently, Savakis and co-workers (2012) confirmed that the EAL domain and the C-terminal GGDEF2 domain are catalytically active in CPH2. Moreover, they demonstrated that the light-regulated activity of c-di-GMP-synthesizing or degrading enzymes is modulated by CPH2. CPH2 is known to be involved in phototactic motility, in particular in the inhibition of phototaxis towards blue light (Wilde *et al.,* 2002) and UV-A light (Moon *et al.,* 2011). The recent work by Savakis and co-workers (2012) links the involvement of CPH2 in phototaxis and motility to c-di-GMP and its light-dependent regulation.

To conclude, CPH2 may regulate the glucose metabolism primarily via trans-criptional control of cytochrome *c* oxidase encoding *CtaDI* gene. Thereby, light-induced conformational changes in CPH2 might affect the activity of GGDEF and EAL domains and consequently the intracellular concentration of c-di-GMP, a second messenger known for its involvement in phenotypic transitions, phototaxis and motility (Park *et al.,* 2000; Wilde *et al.,* 2002; Fiedler *et al.,* 2004; Moon *et al.,* 2011). Recent data by Savakis and co-workers (2012) made this hypothesis even more intelligible by confirming that GGDEF and EAL domain are functional in CPH2, that c-di-GMP is a functional second messenger in *Synechocystis* and that CPH2 functions as its primary, light-regulated modulator. The next steps would be to confirm that c-di-GMP is responsible for the regulation of the glucose metabolism and the existence of cross talk between red light and blue light signalling. The latter could be analysed by point mutations of the cysteine residues within the chromophor binding domains. Additionally, a detailed understanding of light-mediated glucose metabolism in cyanobacteria would further help to understand the regulation of photosynthesis and heterotrophy in other photosynthetic organisms.

4.2 Physiological characterisation of the cyanobacterial histidine kinase HIK12 and its regulatory function on the central carbon metabolism

Histidine kinases are sensory components of sophisticated signal transduction systems, which confer the ability to monitor environmental and intracellular cues and to respond appropriately by regulating adaptational processes. In *Synechocystis,* over 40 histidine kinases have been identified, all of which hold potential sensor domains. Although considerable progress has been made to identify histidine kinases and their involvement in sensing (stress) stimuli, e.g. high light, cold and oxidative stress, heat, salt stress, hyperosmotic stress and phosphate limitation (Hirani *et al*., 2001; Mikami *et al.,* 2002; Hsiao *et al.,* 2004; Paithoonrangsarid *et al*., 2004; Shoumskaya *et al.,* 2005; Suzuki *et al.,* 2005; Kanesaki *et al.,* 2007), the physiological functions of many histidine kinases remain still elusive. Among them, the histidine kinase 12 (HIK12) is of particular interest due to its structural homology to the sensor histidine kinases AHK2, AHK3 and AHK4 of the cytokinin receptor family in *Arabidopsis* (Inoue *et al.,* 2001; Suzuki *et al*., 2001; Ueguchi *et al.,* 2001; Yamada *et al*., 2001). The structural homology is based on the existence of an approximately 250 amino acid long domain in the N-terminal parts of all three AHK receptors and in HIK12. In *Arabidopsis,* this so-called CHASE (cyclases, histidine kinase associated sensory protein) domain was identified to be responsible for cytokinin binding (Heyl *et al.,* 2007), whereas the structurally homologous domain in *Synechocystis*, the so-called MASE (membrane associated sensor) domain is of unknown function so far.

```
HIK12  (505)    TTEGEVVLTSNFRNAEQ
AHK2   (418)    RASGKGVLTSPFKLLKS
AHK3   (281)    RSSGKGVLTAPFPLIKT
AHK4   (301)    RETGKAVLTSPFRLLET
                 *   ***   *
```

Figure 23: Sequence alignment of the ligand-binding CHASE domain in *Arabidopsis* cytokinin receptors AHK2, AHK3 and AHK4 and the putative ligand-binding MASE domain in HIK12 of *Synechocystis* sp. PCC 6803.

Protein sequences of *Arabidopsis* AHK2 (AT5G35750.1), AHK3 (AT1G27320.1) and AHK4 (AT2G01830.2) were retrieved from the TAIR database (www.arabidopsis.org). The protein sequence of *Synechocystis* sp. PCC 6803 HIK12 (*sll1672*) was retrieved from the cyanobase database (www.genome.kazusa.or.jp/cyanobase/Synechocystis). The alignment was conducted with the Multiple Sequence Alignment (MSA) tool of ClustalW (www.ebi.ac.uk/Tools/msa/). Numbers in brackets indicate the amino acid positions of the conserved threonine residue (indicated by a black frame) of the respective proteins. Grey boxes indicate fully or partly conserved amino acids within the protein sequences. Asterisks indicate conserved amino acids in all protein sequences tested.

Sequence analysis by aligning the (putative) ligand-binding domains revealed that the cyanobacterial HIK12 (*sll1672*) possesses a threonine residue, which is part of a **V**aline/**L**eucine/**T**hreonine motif in its MASE domain, which is conserved in all three *Arabidopsis* cytokinin receptors (Figure 23). In *Arabidopsis*, this conserved threonine at position 301 (T301) within the CHASE domain of AHK4 was identified to be among the amino acids essential for cytokinin binding, including tryptophane at position 244 (W244), lysine at position 297 (K297), phenylalanine at position 304 F304), arginine at position 305 (R305) and threonine at position 317 (T317) (Heyl *et al.,* 2007). Mutagenesis of T301 led to a complete loss of cytokinin binding activity (Yamada *et al.,* 2001) and was originally discovered as *woodenleg* (*wol*) mutation in a screen for altered root morphology (Mähönen *et al.,* 2000). Heyl and co-workers (2007) could further confirm the importance of these amino acids in cytokinin binding by substitution of W244, F304, R305 and T317 to alanine, resulting in dramatic alterations of cytokinin binding, ranging from strong reductions to total loss of cytokinin binding. Although the conservation at the amino acid level of the ligand-binding CHASE domains in AHK2, AHK3 and AHK4 is relatively low with only 65% (Spíchal *et al.,* 2004; Heyl *et al.,* 2007), the secondary structure is highly homologous with a characteristic pattern of α-helices and β-sheets (Heyl & Schmülling, 2003). Moreover, the mutated amino acids, which led to the strongest effect (W244, F304, R305 and T301), are located in close vicinity to two predicted β-sheets within the center part of the CHASE domain. This led to the hypothesis that these β-sheets are part of a binding pocket for cytokinins (Heyl *et al.,* 2007). In addition to the conserved threonine residue at position 301 in AHK4 and position 505 in HIK12, several but not all of the amino acids (Figure 23), which have been identified to be important for cytokinin binding in plants, are also conserved in *Synechocystis*. Considering the evolutionary relationship between plant chloroplasts and their cyanobacterial ancestors, it is conceivable that the cytokinin signalling system in plants is an inheritage from their cyanobacterial ancestors (Anantharaman & Aravind, 2001; Mougel & Zhulin, 2001). Following the endosymbiotic event, corresponding genes could have been transferred to the plant nucleus and developed into cytokinin receptors. Vice-versa, one could suggest a putative function of HIK12 in cytokinin sensing in *Synechocystis*. In this context, Selivankina and co-workers (2006) found first evidence of cyanobacteria responding to cytokinin by demonstrating that the cytokinin *trans*-zeatin affects the transcriptional activity in *Synechocystis.* This led to the conclusion that cyanobacteria hold at least the molecular targets for cytokinin signal recognition. However, not much is known about cytokinin signalling in *Synechocystis*. In this study the function of HIK12, a

cyanobacterial histidine kinase with homology to the cytokinin receptor family in *Arabidopsis* was analysed. For this purpose, *hik12* loss-of-function and over-expression mutants, the latter for functional complementation of the knockout, were physiologically analysed. Results show a regulatory function of HIK12 on glucose metabolism after the transition from a planktonic lifestyle to a sessile lifestyle within a biomat.

4.2.1 Deletion of HIK12 negatively affects growth under biomatforming conditions

The analysis of the growth kinetics revealed no differences in growth between WT, *hik12* knockout (loss-of-function) and both *hik12* overexpression (complementation) mutants under photoautotrophic and photomixotrophic conditions (Figure 12 A, B). The accelerated growth upon addition of glucose under photomixotrophic conditions (Figure 12 B) compared to photoautotrophic conditions indicates that WT, *hik12* KO and both *hik12* OE mutants are capable of photomixotrophic growth (Williams, 1988; Anderson & McIntosh, 1991). Similar growth patterns under photoautotrophic and photomixotrophic conditions were reported by Kahlon and co-workers (2003) and Anderson and McIntosh (1991). In contrast, after 48 h of incubation under biomat-forming conditions led to growth cessation in *hik12* KO, while the overexpression of HIK12 in the *hik12* KO background complemented this phenotype (Figure 12 C). This indicates that HIK12 has a critical role in the regulation of growth under biomat-forming conditions. *Synechocystis* cells proliferate via binary fission, an asexual form of reproduction, which comprises the cell division process of one cell into two daughter cells. Microscopic analysis enables to distinguish between single spherical cells and dumbbell-shaped cells, undergoing cell division. Accordingly, in an actively growing culture, which implies high cell division activity, more dumbbell-shaped cells than single cells are expected. The finding that HIK12 is involved in the regulation of growth under biomatforming conditions is further corroborated by the results obtained in microscopic analyses. In *hik12* KO, the relative amount of dumbbell-shaped cells was significantly decreased after 14 days of incubation under biomat-forming conditions in presence of glucose, while that in the WT remained almost unchanged (Figure 13). The reduced cell division activity in *hik12* KO might suggest either a direct regulatory function of HIK12 on cell division processes or an indirect function, e.g. via regulation of the metabolism.

4.2.2 Deletion of HIK12 results in reduced G6PDH enzyme activity and a lower transcript level of *CtaDI,* encoding cytochrome *c* oxidase, under biomatforming conditions

Synechocystis performs oxygenic photosynthesis to convert light energy to chemical energy. Using NADPH and ATP, generated through photosynthesis, inorganic carbon is assimilated via the Calvin cycle. The fixed carbon enters either the glycolytic pathway or is stored as reserve carbohydrate in the form of glycogen. Glycogen can be degraded to provide glucose residues to meet the metabolic needs under non-photosynthetic conditions (Stal & Moezelaar, 1997; Knowles & Plaxton, 2003; Singh & Sherman, 2005; Takahashi *et al.,* 2008) or for adaptational processes in response to environmental stress stimuli (Preiss, 1984; Suzuki *et al.,* 2010). In order to determine the cause for the observed growth phenotype in *hik12* KO both directions of glucose processing, the degradation via the OPPP and the accumulation of glycogen were analysed. The analysis of the specific G6PDH enzyme activity, the rate-limiting enzyme in the OPPP (Yang *et al.,* 2002; Singh *et al.,* 2004; Singh & Sherman, 2005) revealed a reduced ability of *hik12* KO in degrading glucose. This is substantiated by a significant decrease in G6PDH activity after incubation under biomatforming conditions (Figure 15 B). Overexpression of HIK12 in the *hik12* KO background complemented this phenotype. Under photo-autotrophic and photomixotrophic conditions, however, no significant differences in G6PDH activity between WT, *hik12* KO and *hik12* OE were observed (Figure 15 A). In *Synechocystis*, excess carbon is stored in the form of glycogen, the main carbon storage compound in cyanobacteria (Nakamura *et al.,* 2005). Under biomatforming conditions, *hik12* KO had a higher amount of glycogen compared to the WT (Figure 14). Thus, the reduced rate of G6PDH activity together with the increased accumulation of glycogen within *hik12* KO, indicate a regulatory function of HIK12 on the glucose metabolism. The increased glycogen content in *hik12* KO could result from the redirection of G6P into glycogen, caused by the reduced G6PDH activity. This would also be an explanation for the observed growth retardation of *hik12* KO under biomatforming conditions.

To further analyse the effects of *hik12* deletion, gene expression profiles of two key metabolic genes, *Zwf* (*slr1843)*, encoding for G6PDH and *CtaDI* (*slr1137),* encoding for subunit I of the cytochrome *c* oxidase complex, the terminal component of the respiratory chain, were examined under different growth conditions using semi-quantitative RT-PCR. The analysis of the gene expression patterns revealed no significant differences in the transcript levels of *Zwf* and *CtaDI* in WT, *hik12* KO and

hik12 OE under photoautotrophic or photomixotrophic conditions (Figure 16 A, B). This is in accordance with previous reports, demonstrating that transcript levels of various genes encoding key enzymes of the central carbon metabolism are not significantly affected upon the presence or absence of exogenous glucose (Yang *et al.,* 2002; Tu *et al.,* 2004; Singh & Sherman, 2005; Kahlon *et al.*, 2006). Although the expression patterns for *Zwf* and *CtaDI* are not significantly altered under photoauto-trophic and photomixotrophic conditions, incubation under biomatforming conditions resulted in an interesting transcriptional pattern. Under biomatforming conditions, the transcript level of cytochrome *c* oxidase encoding *CtaDI*, was significantly upregulated in WT and *hik12* OE, while the *hik12* KO displayed no induced transcript accumulation (Figure 16 C). The incapability of *hik12* KO to upregulate *CtaDI* expression under biomatforming conditions was reversed in the complementation mutant, indicating that the observed transcriptional pattern is caused by the deletion of *hik12*. Notably, the lower *CtaDI* expression in *hik12* KO was only observed after the transition to biomatforming conditions. Other than the strong effect on the enzyme activity level (Figure 15 B), the transcript level of *Zwf*, encoding for G6PDH, was not significantly altered in WT, *hik12* KO and *hik12* OE under biomatforming conditions (Figure 16 C). The fact that the *Zwf* transcript level is similar in WT, *hik12* KO and *hik12* OE, although the G6PDH activity differs, further substantiates the previously mentioned regulation of G6PDH at the post-translational level. This is in accordance with reports, demonstrating that the activity of enzymes involved in glycolytic and OPP pathways is regulated at the post-translational level by changes in metabolite concentrations (Stal & Moezelaar, 1997; Sundaram *et al.,* 1998; Yang *et al.,* 2002; Knowles & Plaxton, 2003; Lee *et al.,* 2007).

Together, the results obtained in this study clearly indicate a regulatory function of HIK12 on the glucose metabolism under biomatforming conditions. The incapability of *hik12* KO to upregulate *CtaDI* expression under biomatforming conditions should result in a reduced cytochrome *c* oxidase activity and accordingly in a limited respiration. As previously discussed for *cph2* KO, the reduced cytochrome *c* oxidase activity could result in an overreduced electron transport chain, as the electrons cannot be removed. As G6PDH is inactivated under reducing conditions (Plaxton & Podesta, 2006; Lee *et al*., 2007), the incapability to upregulate *CtaDI* expression might be the cause for the reduced G6PDH activity in *hik12* KO. Thus, cytochrome *c* oxidase might be the direct target of HIK12 in regulating the glucose metabolism under biomatforming conditions. For future work it is important to determine the activity of cytochrome *c* oxidase in *hik12* KO and the redox state of the PQ pool.

4.2.3 P700$^+$ reduction kinetics: Analysis of electron transport activities

The analysis of P700$^+$ reduction kinetics revealed no significant differences in determined $t_{1/2}$ of P700$^+$ reduction between WT, *hik12* KO and *hik12* OE, neither before nor after incubation under biomatforming conditions (Figure 17). However, there is an induction in glucose metabolism observable after biomat induction. The less increased $t_{1/2}$ of P700$^+$ reduction in DCMU-treated samples after biomat induction compared to that under photoautotrophic conditions indicates a higher electron input from heterotrophic sources, indicating that the cells have adapted to the presence of exogenous glucose. A possible explanation for the absence of any significant differences in $t_{1/2}$ of P700$^+$ reduction between WT, *hik12* KO and *hik12* OE could be that the biomat induction takes place under light conditions, which implies that the general energy metabolism is still highly active in the cells, other than under dark conditions as seen in Section 3.1.5. Furthermore, as HIK12 is not a light sensor, other than the phytochrome photoreceptor CPH2 (Section 4.1.3), which showed a clear effect on P700$^+$ reduction kinetics after the switch from light to dark conditions, it could take longer to see an effect of *hik12* KO on electron transport activities after biomat formation. Considering that HIK12 might be involved in sensing signals associated with the cell cycle activity, the time span of 24 h might be too short to see HIK12-mediated effects on the metabolism. As the strong effects of *hik12* deletion on G6PDH enzyme activity (Figure 15 B) and on the transcript level of cytochrome *c* oxidase encoding *CtaDI* (Figure 16 C) were observed after 96 h of incubation under biomatforming conditions, it will be inevitable for future work to repeat the measurements after 96 h of incubation under biomatforming conditions.

4.2.4 Deletion of *hik12* leads to constitutive ROS production

Inherently, oxygenic photosynthesis and aerobic respiration give rise to the generation of reactive oxygen species (ROS), which are continuously formed as byproducts of these aerobic processes (Tichy & Vermaas, 1999; Apel & Hirt, 2004; Pérez-Pérez *et al.,* 2009). The different ROS types, including hydrogen peroxide (H_2O_2), superoxide anion radical ($O_2{}^{\bullet-}$) and the hydroxyl radical ($OH^{\bullet}$) cause oxidative damage to nucleic acids, proteins and lipids (Apel & Hirt, 2004; Latifi *et al.,* 2009). ROS are inevitably generated during photosynthetic electron transport, at PS II, where singlet oxygen is produced by energy input to oxygen from photosensitized chlorophyll and at PS I, where superoxide anion radicals are generated by the Mehler reaction (reviewed by Latifi *et al.,* 2009). H_2O_2 and $OH^{\bullet}$ are produced during

the stepwise reduction of molecular oxygen (O_2) to water (H_2O). To cope with the cytotoxic properties of ROS, the cells possess detoxification systems, ROS-scavenging enzymes, such as superoxide dismutases, catalase-peroxidases and peroxiredoxins (Jeanjean *et al.,* 2007; Pérez-Pérez *et al.,* 2009, Bernroitner *et al.,* 2009). Accordingly, the cells are in the constant need to strictly control ROS production and detoxification, in order to maintain their cellular redox balance. However, the equilibrium between ROS production and scavenging can be perturbed by environmental stress factors, such as high light intensities, leading to redox imbalances and subsequently to increased ROS production (Apel & Hirt, 2004; Scheibe *et al.,* 2005). The luminol-based assay, conducted to analyse the ROS production within *hik12* KO and WT cells, revealed a constitutive ROS production in *hik12* KO (Figure 18). Environmental stress factors, such as high light, which might cause the ROS production precedent redox imbalances, can be excluded, as the measurement took place in darkness. Moreover, the WT displayed no further chemoluminescence emissions, indicative for ROS production, than the background emissions. Glucose was added prior to the measurement to check for electron imbalances in the respiratory chain. The presence or absence of exogenous glucose did not influence the observed ROS production, neither in *hik12* KO nor in the WT (Figure 18), indicating that the redox status of the PQ pool or imbalances in the electron transport chain are rather unlikely to cause the constitutive ROS production in *hik12* KO. Furthermore, the measurements were conducted in exponentially growing, photoautotrophic cultures. Therefore, no differences in cytochrome *c* oxidase activity and consequently no overreduction of the electron transport chain are expected. Thus, these results indicate rather defects in ROS-scavenging or reduced activities of the scavenging enzymes to cause the constitutive ROS production in *hik12* KO. However, further research is inevitable to elucidate the cause of the constitutive ROS production and to clarify the correlation between the deletion of *hik12* and the striking ROS production.

4.2.5 HIK12 has a regulatory function on glucose metabolism under biomatforming conditions

Histidine kinases are the essential sensory components of sophisticated signal trans-duction systems that confer the ability to perceive a wide range of signals and to respond appropriately by regulating various adaptational processes. Although considerable progress has been made in the past years, the physiological functions of many Hiks in *Synechocystis* have not yet been characterized. In *Synechocystis*, the histidine kinases HIK8 and HIK31 are involved in the regulation of glucose

catabolism (Singh & Sherman, 2005) and in the regulation between different trophic modes of growth (Kahlon *et al.,* 2006), respectively. The results obtained in this study provide evidence that with HIK12 another histidine kinase with a regulatory function on the central carbon metabolism of *Synechocystis* sp. PCC 6803 has been identified. After the transition from photoautotrophic to photomixotrophic/biomat-forming conditions, *hik12* KO shows a clear phenotype, comprising of growth cessation, reduced G6PDH enzyme activity, an increased amount of the carbon storage compound glycogen and the incapability to upregulate the transcript level of cytochrome *c* oxidase encoding *CtaDI* gene. The results obtained in this study confirm a function of HIK12 in the regulation of glucose metabolism. Based on these results, two hypotheses have been developed, which are summarized in a hypothetical model presented in Figure 24.

With regard to the observed growth phenotype and the significantly reduced cell division activity in *hik12* KO, it is assumable that HIK12 has a regulatory function on cell division processes under biomatforming conditions. In this context, the reduced cell division activity and concomitantly the reduced growth might be the consequence of the restricted availability of biosynthetic intermediates required for growth, resulting from the reduced glucose degradation by G6PDH, the rate-limiting enzyme of glucose catabolism. This would also explain the increased amount of glycogen, probably resulting from the redirection of G6P to glycogen, caused by the reduced G6PDH activity. According to the endosymbiont theory (Margulis, 1970), cyanobacteria are the evolutionary ancestors of plant chloroplasts (Anantharaman & Aravind, 2001; Mougel & Zhulin, 2001). In the course of the endosymbiotic event, many cyanobacterial genes were transferrred into the plant nucleus. Especially, genes coding for proteins involved in photosynthesis and signal transduction are highly conserved among cyanobacteria and plants. Considering the homology of HIK12 to the cytokinin receptor family in *Arabidopsis*, in particular the conserved threonine residue in the cytokinin binding domain of *Arabidopsis* and in the putative ligand-binding domain of HIK12, the cytokinin signalling system in plants might be an inheritage of their cyanobacterial ancestors during the evolution of the chloroplast. A putative function for HIK12 in cytokinin signalling in *Synechocystis* is assumable. HIK12 could either be a cytokinin receptor or could recognize similar molecules. Furthermore, the assumed regulatory function of HIK12 on cell division activity under biomatforming conditions corresponds to the growth-stimulating effect of cytokinins in plants (Mok & Mok, 2001; Dello Ioio *et al.,* 2008; Perilli *et al.,* 2010).
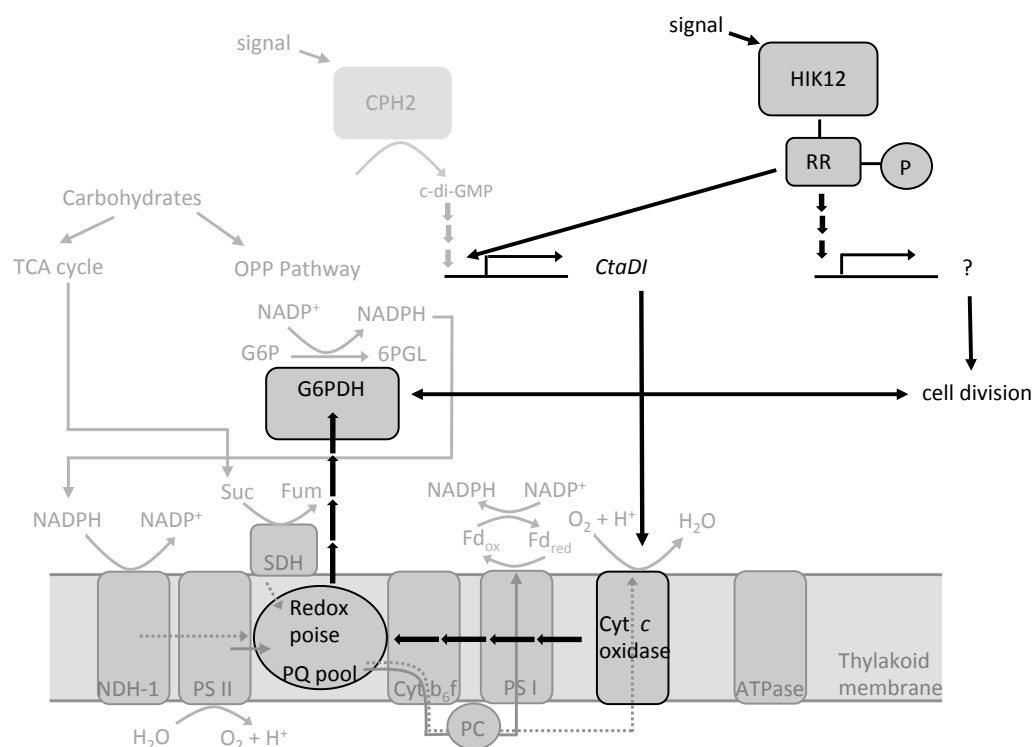
Figure 24: Hypothetical model of the histidine kinase 12 and its regulatory function on glucose metabolism under photomixotrophic/biomatforming conditions.

According to the working hypothesis, signal perception by HIK12 leads to the phosphorylation (P) of its response regulator (RR). This in turn could modulate the transcription of cytochrome *c* oxidase encoding *CtaDI* gene or another so far unknown target gene, which could be involved in the regulation of cell division processes. The activity of cytochrome *c* oxidase might further regulate the activity of G6PDH at the posttranslational level, via the redox poise of the PQ pool or another unknown posttranslational regulatory mechanism. The reduced G6PDH activity might cause the reduced ability in metabolising glucose, leading to the observed strongly retarded growth phenotype under biomatforming conditions. The downregulation of G6PDH could also be a consequence of a feedback inhibition, caused by the reduced cell division events and concomitantly the reduced cellular demand for biosynthetic intermediates. Alternatively, the reduced cell division events could affect the glucose metabolism.

Abbreviations: CPH2, cyanobacterial phytochrome 2; c-di-GMP, bis-(3'-5')-cyclic dimeric guanosine monophosphate; *CtaDI,* gene encoding for cytochrome *c* oxidase subunit I; G6P, glucose-6-phosphate; 6PGL, 6-phosphogluconolactone; G6PDH, glucose-6-phosphate dehydrogenase; NDH-1, type I NADPH dehydrogenase; SDH, succinate dehydrogenase; Suc, succinate; Fum, fumarate; PS I and II; photosystem I and II; PQ pool, plastoquinone pool; cyt b_6f, cytochrome b_6f complex; PC, plastocyanin; cyt *c* oxidase, cytochrome *aa3*-type cytochrome *c* oxidase; Fd_{ox}/Fd_{red}, ferredoxin in oxidized and reduced forms, respectively; ATPase, ATP synthase complex; NADP(H), nicotinamide-adenine dinucleotide phosphate (reduced form); OPP Pathway, oxidative pentosephosphate pathway; TCA cycle, tricarboxylic acid cycle.

Based on the results obtained by Selivankina and co-workers (2006), *Synechocystis* possesses the molecular targets for cytokinin signal recognition. Nevertheless, it is inevitable for future work to provide evidence that the putative ligand-binding domain in HIK12 binds cytokinin. In *Arabidopsis*, definitive evidence for AHK2, AHK3 and AHK4 functioning as cytokinin receptors was provided by complementation ex-

periments in heterologous bacterial and yeast systems (Inoue *et al.,* 2001; Suzuki *et al.,* 2001; Ueguchi *et al.,* 2001; Yamada *et al.,* 2001). When expressed in *E. coli* cells, AHKs confer the ability to complement the Δ*rcsC* histidine kinase mutant, which is impaired in the regulation of extracellular polysaccharide synthesis, in a cytokinin-dependent manner (Suzuki *et al.,* 2001; Ueguchi *et al.,* 2001; Yamada *et al.,* 2001). Similarly, the budding yeast histidine kinase Δ*sln1* mutant, which is lethally defective in osmosensing, was complemented by expressing AHKs in a cytokinin-dependent manner (Inoue *et al.,* 2001; Ueguchi *et al.,* 2001). Accordingly, due to the homology of HIK12 to AHKs, expression of HIK12 in these heterologous bacterial or yeast systems could be used to give evidence for HIK12 functioning as cytokinin receptor. Interestingly, Reiser and co-workers (2003) demonstrated that the yeast osmosensor SLN1, which is one of the two sensory components of the high osmolarity glycerol (HOG) pathway (Wurgler-Murphy *et al.,* 1997), monitors changes in turgor pressures caused by hyperosmotic stress. They showed that the plant cytokinin receptor AHK4 can substitute the SLN1 osmosensing function and that its kinase activity is similarly regulated by turgor pressure, leading to the suggestion that AHK4 could have dual sensor functions as cytokinin receptor and osmosensor in plants (Reiser *et al.,* 2003). Due to the homology of AHKs and HIK12, it is further conceivable that HIK12 is involved in osmosensing in *Synechocystis*.

The reduced G6PDH activity/*CtaDI* expression could also be the consequence of a feedback inhibition, caused by the reduced cell division events and concomitantly the reduced cellular demand for biosynthetic intermediates. The strong effect of *hik12* deletion on the expression of cytochrome *c* oxidase encoding *CtaDI* indicates that cytochrome *c* oxidase is the primary target of HIK12, with HIK12 possibly acting as positive regulator of cytochrome *c* oxidase transcription under biomatforming conditions. In this context, cytochrome *c* oxidase might further regulate the activity of G6PDH, possibly at the post-translational level via the redox state of the PQ pool or via a so far unknown (feedback) mechanism. The reduced G6PDH activity could result in the redirection of G6P to glycogen, which would be an explanation for the increased amount of glycogen in *hik12* KO cells. To further clarify the regulatory function of HIK12, it is inevitable for future work to determine the activity of cytochrome *c* oxidase. Another important aspect is to provide evidence for a correlation between the observed effects of *hik12* deletion and the hormone cytokinin. A possible approach would be to analyse the enzyme activities of cytochrome *c* oxidase and G6PDH and the transcript levels of the corresponding genes in presence and absence of cytokinin.

4.3 Cytokinin function in plant-pathogen interactions

Cytokinins are a class of phytohormones that regulate various physiological and developmental processes throughout the plant life (Kakimoto, 2003; Balibrea Lara *et al.,* 2004; Sakakibara, 2006; Müller & Sheen, 2007; Bari & Jones, 2009; Hwang *et al.,* 2012). Besides processes associated with active growth, metabolism and plant development, cytokinins have further been suggested to be involved in plant-pathogen interactions (Walters & McRoberts, 2006; Robert-Seilaniantz *et al.,* 2007; Walters *et al.,* 2008). This suggestion was based on the striking similarity of several well-established cytokinin functions and changes in host physiology during plant-pathogen interactions (Walters & McRoberts, 2006; Walters *et al.,* 2008). The role of cytokinins in plant-pathogen interactions, the underlying mechanisms and eventual cross talk with other defense-related plant hormones remain elusive. The results obtained in this study further support an essential function of cytokinin in plant-pathogen interactions. Altered cytokinin levels within transiently transformed barley epidermal cells influenced the susceptibility against powdery mildew spores in this biotrophic host-pathogen system. Furthermore, an *Arabidopsis* cytokinin receptor-deficient mutant was impaired in the defense response against the hemibiotrophic pathogen *Pseudomonas syringae* pv. *tomato* (*Pst*), which is in accordance with the recent finding by Choi and co-workers (2010), who demonstrated that modulated cytokinin levels or signalling activity correlates with altered resistance. Interestingly, the *Arabidopsis* AHK3 cytokinin receptor-deficient mutant displayed a constitutive ROS production. Modulation of ROS production is often associated with plant defense responses to pathogen challenge (Hückelhoven, 2007).

4.3.1 Overexpression of cytokinin oxidases positively affects resistance in the barley-powdery mildew interaction

The powdery mildew fungus *Blumeria graminis* f. sp. *hordei* (*Bgh*) is an obligate biotrophic phytopathogen. In a compatible interaction, the fungus successfully colonizes its host and develops its feeding organ, the haustorium, within the host cell. The fungus continues its growth by developing secondary hyphae and haustoria and finally accomplishes its infection cycle by spreading new spores from arising conidiophores. During the interaction with biotrophic fungal pathogens, the host undergoes characteristic alterations in physiology and metabolism, which include reduced photosynthetic rates, the accumulation of nutrients at infection sites and in later stages of the infection, the formation of the so-called green islands (Walters & McRoberts, 2006). Green islands describe the phenomenon of infection sites, which

remain green while the rest of the leaf senesces (Walters *et al.,* 2008). Notably, the changes in host physiology strikingly resemble well-established functions of the phytohormone cytokinin during leaf senescence (Balibrea Lara *et al.,* 2004), thereby linking cytokinin effects and plant responses to biotrophic pathogens. Beyond that, there has been some debate about the origin of cytokinin in infected leaves. It is not clear yet, if it is the pathogen producing cytokinin or the host or even both (Werner & Schmülling, 2009). Biotrophic fungal pathogens, including *Bgh,* might produce cytokinins to modulate the hormonal balance of their host, leading to the suppression of defense responses (Walters & McRoberts 2006; Robert-Seilaniantz *et al.,* 2007). In any case, green islands, which are formed by biotrophic pathogens, function as a nutritional source for pathogen growth and propagation (Walters & McRoberts, 2006). Furthermore, in green islands that are associated with pustule formation by fungal pathogens, increased levels of cytokinin have been detected (Lopez-Carbonell *et al.,* 1998). A possible role of cytokinins in plant-pathogen interactions has been proposed by Walters and McRoberts (2006), who suggested that in the early stage of plant-pathogen interaction, the accumulation of cytokinins, probably released by the fungus, leads to increased cell-wall invertase activity. This in turn causes nutrient mobilisation towards the infection site, reductions in photosynthetic metabolism and the development of green islands.

To investigate the impact of an altered cytokinin level during the early stage of host-pathogen interaction, cytokinin-degrading enzymes were transiently overexpressed in barley epidermal cells. Transformed cells were analysed during the early stage of interaction with the biotrophic powdery mildew fungus *Bgh*, in terms of resistance to penetration attempts of the fungus. The analysis revealed that simultaneous overexpression of the *Arabidopsis* cytokinin oxidases 1 and 2 (AtCKX1 and 2) mediated a significant decrease in the penetration success of *Bgh*, while single overexpression of AtCKX1 or AtCKX2 had no significant influence on the penetration efficiency of *Bgh* (Figure 19). In *Arabidopsis*, cytokinin synthesizing and degrading enzymes are located in different subcellular compartments (Werner *et al.,* 2003; Sakakibara, 2006). In particular, cytokinin degradation is compartmentalized to the endoplasmatic reticulum (ER), the vacuole, the extracellular space and the cytoplasm (Motyka *et al.,* 1996; Werner *et al.,* 2003; Köllmer, 2009), suggesting that cytokinin homeostasis needs to be controlled at different locations of the cell (Wulfetange *et al.,* 2011a). In this context, the different subcellular localization of both cytokinin oxidases, with AtCKX1 being targeted to the vacuole and AtCKX2 being located in the ER lumen (Werner *et al.,* 2003; Galuszka *et al.,* 2004;

Gajdosová *et al.,* 2010) points to distinct functions for both isoenzymes. Supposedly, the simultaneous overexpression of AtCKX1 and 2 is necessary to alter the endogenous cytokinin level at different cellular compartments to a certain extent, which affects host-pathogen interactions.

A possible explanation for the decreased penetration efficiency of *Bgh* in AtCKX1/2 overexpressing barley cells might be attributed to the function of cytokinin in suppressing programmed cell death (Gan & Amasino, 1995; Walters & McRoberts, 2006). Cytokinins, secreted by the pathogen in the early host-pathogen interaction, might suppress host cell death, thereby enabling the pathogen to feed on living host tissue (Murphy *et al.,* 1997; Ashby, 2000). Accordingly, a decreased cytokinin level, resulting from the overexpression of AtCKX1/AtCKX2 could result in a regression of cell death suppression. This in turn leads to a decreased susceptibility of the host, as *Bgh* as a biotrophic fungus is dependent on nutrient acquisition from living host tissue. This leads to another possible explanation, based on the function of cytokinins in nutrient mobilisation and in source-sink regulation (Roitsch *et al.,* 2003; Balibrea Lara *et al.,* 2004; Walters & McRoberts, 2006). During plant-pathogen interaction, biotrophic fungi establish strong metabolic sinks for nutrients and carbohydrates (Walters & McRoberts, 2006; Walters *et al.,* 2008). A central modulator of sink activity is the extracellular invertase, which is a key sucrose-cleaving enzyme, having an essential function in source-sink regulation and in supplying carbohydrates to sink tissues (Tang *et al.,* 1999; Goetz *et al.,* 2001; Roitsch *et al.,* 2003). Extracellular invertases are upregulated by several stimuli affecting carbohydrate requirements, which include growth-stimulating phyto-hormones such as cytokinins (Roitsch, 1999; Roitsch *et al.,* 2003). Walters and McRoberts (2006) suggested that accumulated cytokinins, probably released by the fungus, lead to an increase in invertase activity and concomitantly to the establishment of a strong nutrient sink. The reduced penetration efficiency of *Bgh* in cells overexpressing AtCKX1/AtCKX2 could be explained by a reduced cytokinin level, which in turn leads to the downregulation of invertase expression and hence in a less efficient sink induction. Accordingly, the nutrient acquisition of the pathogen is less efficient, which negatively affects the fungal growth and development.

4.3.2 Loss-of-function of AHK3 results in enhanced susceptibility of *Arabidopsis* to *Pseudomonas syringae* pv. *tomato*

Interaction between signalling pathways is an important mechanism for regulating plant defense responses against various pathogens. In addition to salicylic, ethylene and jasmonates, which are considered as the main hormones mediating defense signalling (Bari & Jones, 2009), only recently the involvement of other hormones, such as cytokinins, abscisic acid, auxin, gibberellic acid and brassinosteroids in defense signalling pathways has been recognized. In this context, the very recent finding that *Arabidopsis* cytokinin receptors are located in the endoplasmatic reticulum (ER; Wulfetange *et al.,* 2011a; Caesar *et al.,* 2011) and not as previously assumed at the plasma membrane, offers new opportunities for hormonal cross talk, as numerous other plant receptor proteins, including the structurally related ethylene receptors (Chen *et al.,* 2002), auxin signalling-related proteins and specific metabolic enzymes, such as cytokinin oxidases are also located at the ER (Werner *et al.,* 2003; Geldner & Robatzek, 2008; Irani & Russinova, 2009; Friml & Jones, 2010; Wulfetange *et al.,* 2011a). In *Arabidopsis*, cytokinins are perceived by the three membrane-bound sensor histidine kinases AHK2, AHK3 and AHK4 (Inoue *et al.,* 2001; Suzuki *et al.,* 2001; Ueguchi *et al.,* 2001; Yamada *et al.,* 2001). Although genetic studies have shown a considerable degree of functional redundancy among the three receptors, individual receptors were reported to possess distinct functions and to mediate specific cytokinin activities (Higuchi *et al.,* 2004; Nishimura *et al.,* 2004; Riefler *et al.,* 2006). AHK3 has been identified as the cytokinin receptor that plays a major role in mediating senescence (Kim *et al.,* 2006). As cytokinin-mediated defense responses are associated with altered senescence phenotypes (Walters & McRoberts, 2006), an AHK3 receptor-deficient *Arabidopsis* T-DNA insertion line was chosen as a candidate to analyse cytokinin-related effects in pathogen interaction. To this end, leaves of *ahk3* KO mutant were infiltrated with the hemibiotrophic pathogen *Pseudomonas syringae* pv*. tomato* DC3000 (*Pst*), a non-cytokinin-producing pathogen (Choi *et al.,* 2010) and the outcome of interaction was analysed. The analyses revealed that the AHK3 receptor-deficient mutant exhibited enhanced susceptibility to *Pst*, which was reflected in faster development of disease symptoms (Figure 20 A) and faster proliferation of bacteria (Figure 20 B). This is in accordance with Choi and co-workers (2010), who reported that plant-derived cytokinins positively affect plant immunity to *Pst* by showing that elevated levels of endogenous cytokinin in *Isopentenyltransferase* (IPT) overexpressing plants enhance plant resistance against *Pst*, while *ahk2ahk3* cytokinin receptor-double knockout plants

displayed enhanced susceptibility. Based on these findings, Choi and co-workers (2010) proposed a model in which cytokinin perception through the receptors AHK2 and AHK3 in *Arabidopsis* elicits a defense response against non-cytokinin producing pathogens by modulating defense signalling. They suggested that mainly AHK3 is responsible for eliciting the defense response. There is no clear evidence for AHK3 being the main receptor mediating plant defense responses, as the results by Choi and co-workers (2010) were obtained from *ahk2ahk3* double knockout plants. The results obtained in this study clearly show an enhanced susceptibility phenotype in the single *ahk3* loss-of-function mutant. This phenotype is similar to the *ahk2ahk3* phenotype and supports a predominant role of AHK3 in defense signalling.

4.3.3 Loss-of-function of AHK3 cytokinin receptor leads to constitutive ROS production in *Arabidopsis*

As described in detail in Section 4.2.4, reactive oxygen species (ROS) are continuously generated as toxic byproducts of photosynthetic and respiratory electron transport (Tichy & Vermaas, 1999; Apel & Hirt, 2004; Pérez-Pérez *et al.,* 2009). In plants, also mitochondria and the plasmamembrane NADPH oxidase can be a source of ROS (Torres *et al.,* 2010). To cope with the cytotoxic properties of ROS, the cells hold efficient mechanisms for scavenging and detoxification of ROS. The equilibrium between generation and removal of ROS can be perturbed by environmental stress stimuli, leading to disturbances in cellular integrity and the metabolic balance (Apel & Hirt, 2004 and references therein). These external stress factors leading to redox imbalances within the plant cells can be of abiotic or biotic origin. In plants, ROS are known to play an important role in defense reactions against pathogen attacks. In addition of being toxic to microorganisms, ROS are involved in various defense-related processes, such as cross-linking of cell wall components during the formation of papillae, in the hypersensitive reaction, in defense gene expression and also as signalling molecules in defense-related signal transduction (Lamb & Dixon, 1997).

A luminol-based assay was conducted in this study to analyse the ROS production in the *Arabidopsis ahk3*-loss-of-function mutant. *Ahk3* KO showed a constitutive ROS production, while the WT displayed no ROS production under the conditions tested (Figure 21). Environmental stress factors, such as high light, which might cause redox imbalances leading to the production of ROS, can be excluded as the measurement took place in darkness. The addition of exogenous glucose prior to the measurement did not affect the observed ROS production, neither in *ahk3* KO nor in

the WT (Figure 21). Glucose was added to check for electron imbalances in the respiratory chain. Due to the non-affected ROS production in presence or absence of glucose, redox imbalances in the electron transport chain and/or the PQ pool are rather unlikely to cause the constitutive ROS production in *ahk3* KO. These results rather point to defects in scavenging or possibly reduced activities of ROS-scavenging enzymes, such as superoxide dismutases, catalase-peroxidases and peroxiredoxins (Jeanjean *et al.,* 2007; Pérez-Pérez *et al.,* 2009, Bernroitner *et al.,* 2009), causing the constitutive ROS production in *ahk3* KO. However, as ROS production in plant cells can have various causes, further research is required to elucidate the cause for the constitutive ROS production in *ahk3* KO. Moreover, especially with regard to the fact that the cyanobacterial *hik12* loss-of-function mutant shows a similar phenotype of constitutive ROS production (Figure 18), it will be interesting for future work to clarify the underlying mechanisms.

5 Summary

The ability to perceive environmental changes and to respond by adapting appropriately is indispensable for the survival and successful competition of all living organisms. Sophisticated signal transduction systems confer the ability to mediate these adaptive responses. In the present work, two signalling components, the phytochrome photoreceptor CPH2 and the histidine kinase 12 (HIK12) of the cyanobacterium *Synechocystis* sp. PCC 6803 were investigated with a special focus on the central carbon metabolism.

The phytochrome photoreceptor CPH2 of *Synechocystis* is known to be involved in phototaxis and motility. In the present work, a new function of CPH2 as a regulator of the glucose metabolism was shown. The knockout of *cph2* results in a strongly retarded growth phenotype under biomatforming conditions in darkness and presence of glucose as sole energy source for heterotrophic growth. This phenotype correlates with a reduced glucose-6-phosphate dehydrogenase (G6PDH) enzyme activity in the knockout and a strongly down-regulated transcript level of cytochrome *c* oxidase encoding *CtaDI* gene. These phenotypes can be complemented by over-expression of CPH2 in the knockout background.

The second signalling component HIK12, a histidine kinase of *Synechocystis*, displays homology to the cytokinin receptor family in *Arabidopsis thaliana.* The knockout of *hik12* results in a strongly retarded growth phenotype under biomat-forming conditions in the light and in the presence of glucose. This phenotype correlates with a reduced G6PDH enzyme activity, increased glycogen content and the incapability to upregulate the transcript level of cytochrome *c* oxidase encoding *CtaDI* gene. These phenotypes can be complemented by overexpression of HIK12 in the knockout background, confirming a new regulatory function of HIK12 on the central carbon metabolism. Interestingly, *hik12* KO displayed constitutive production of reactive oxygen species (ROS).

The obtained results show a clear regulatory function of the phytochrome photo-receptor CPH2 and the histidine kinase HIK12 on the central carbon metabolism of *Synechocystis* sp. PCC 6803. These phenotypes manifest under biomatforming conditions, which implies the transition from fast exponential to slowed down growth.

Cytokinins are a class of phytohormones that regulate various physiological and developmental processes in higher plants, including cell division and differentiation,

chloroplast development, seed germination, delay of leaf senescence, nutrient mobilization and stress responses. Recently, cytokinins have emerged to be involved in processes related to defense mechanisms during plant-pathogen interaction. In the present work, the role of cytokinins during the interaction with biotrophic/hemi-biotrophic pathogens was investigated. Transiently transformed barley cells, over-expressing cytokinin-degrading enzymes, were analysed during the interaction with the biotrophic powdery mildew fungus *Blumeria graminis* f.sp. *hordei* (*Bgh*). The simultaneous overexpression of cytokinin oxidases 1 and 2 resulted in reduced penetration success of *Bgh*, indicating that a lowered cytokinin level in the cells positively affects resistance against *Bgh* spores. An AHK3-cytokinin-receptor deficient *Arabidopsis* T-DNA-insertion line was analysed during the interaction with the hemibiotrophic pathogen *Pseudomonas syringae* pv. *tomato* (*Pst*). The AHK3 cytokinin receptor-deficient T-DNA insertion line exhibited enhanced susceptibility to *Pst*, which is reflected in faster development of disease symptoms, indicating that cytokinins promote resistance of *Arabidopsis* to *Pst*. Interestingly, a constitutive ROS production in the *ahk3* KO mutant in the absence of any elicitors was shown. Together, the results obtained in the present work further support an essential function of cytokinins in plant-pathogen interactions by confirming that cytokinins affect plant immunity.

6 Zusammenfassung

Die Fähigkeit Veränderungen der Umwelt wahrzunehmen und durch entsprechende Anpassung darauf zu reagieren ist unverzichtbar für das Überleben und den erfolgreichen Wettbewerb aller Lebewesen. Die Fähigkeit zur Anpassung wird durch ausgeklügelte Signaltransduktions-Systeme verliehen. Die vorliegende Arbeit untersucht zwei Signaltransduktions-Komponenten des Cyanobakteriums *Synechocystis* sp. PCC 6803, den Phytochrom-Photorezeptor CPH2 und die Histidin-Kinase 12 (HIK12), in Bezug auf ihre Funktion auf den zentralen Kohlenstoff-Metabolismus.

Über den Phytochrom-Photorezeptor CPH2 in *Synechocystis* ist bereits bekannt, dass dieser in Phototaxis und Motilität involviert ist. Diese Arbeit zeigt nun eine neue Funktion von CPH2, als Regulator des Glukose-Metabolismus. Der Knockout von *cph2* führt zu einem stark verlangsamten Wachstums-Phänotyp unter Biofilm-bildenden Bedingungen, in Dunkelheit und in Anwesenheit von Glukose als einziger Energiequelle für heterotrophes Wachstum. Dieser Phänotyp korreliert mit einer reduzierten Glukose-6-Phosphat Dehydrogenase (G6PDH) Enzym-Aktivität und einem stark herunter-regulierten Transkript-Niveau des für Cytochrom-*c*-Oxidase codierenden Gens *CtaDI*. Diese Phänotypen können durch die Überexpression von CPH2 im Knockout-Hintergrund komplementiert werden.

Die zweite Signaltransduktions-Komponente, HIK12, eine Histidin-Kinase in *Synechocystis*, weist Homologien zur Cytokinin-Rezeptor-Familie in *Arabidopsis thaliana* auf. Der Knockout von *hik12* hat einen stark verlangsamten Wachstums-Phänotyp unter Biomat-bildenden Bedingungen, im Licht und in der Anwesenheit von Glukose zur Folge. Dieser Phänotyp korreliert mit einer reduzierten G6PDH Enzym-Aktivität, erhöhtem Glykogengehalt und der Unfähigkeit, das Transkript-Niveau des für Cytochrom-*c*-Oxidase codierenden Gens *CtaDI*, hochzuregulieren. Diese Phänotypen können durch die Überexpression von HIK12 im Knockout-Hintergrund komplementiert werden, was eine neue regulatorische Funktion von HIK12 auf den zentralen Kohlenstoff-Metabolismus bestätigt. Interessanterweise zeigt *hik12* KO zudem eine konstitutive Produktion von reaktiven Sauerstoff-Spezies (ROS).

Die Ergebnisse dieser Arbeit zeigen eine klare regulatorische Funktion des Phytochrom-Photorezeptors CPH2 und der Histidin-Kinase HIK12 auf den zentralen Kohlenstoff-Metabolismus von *Synechocystis* sp. PCC 6803. Diese Phänotypen

manifestieren sich unter Biofilm-bildenden Bedingungen, die einen Wechsel von schnellem, exponentiellem zu verlangsamtem Wachstum einschliessen.

Cytokinine sind eine Klasse von Phytohormonen, die eine Vielzahl von physiologischen und entwicklungsspezifischen Prozessen in höheren Pflanzen, wie Zellteilung und -differenzierung, Chloroplastenbildung, Samenkeimung, Verzögerung der Seneszenz, Mobilisierung von Nährstoffen und Stress-Antworten, regulieren. Erst in letzter Zeit zeichnet sich ab, dass Cytokinine auch in Prozesse involviert sind, die an Abwehrmechanismen während der Pflanze-Pathogen-Interaktion beteiligt sind. Diese Arbeit untersucht die Rolle von Cytokininen während der Interaktion mit biotrophen/hemibiotrophen Pathogenen. Transient-transformierte Gerstenzellen, die Cytokinin-abbauende Enzyme überexprimieren, wurden während der Interaktion mit dem biotrophen Echten Mehltaupilz *Blumeria graminis* f.sp. *hordei* (*Bgh*), untersucht. Die gleichzeitige Überexpression der Cytokinin Oxidasen 1 und 2 führte zu einem reduzierten Penetrationserfolg der *Bgh*-Sporen, was darauf hindeutet, dass sich ein gesenkter Cytokinin-Spiegel in der Zelle positiv auf die Resistenz gegen *Bgh* auswirkt. Eine AHK3-Cytokinin-Rezeptor-defiziente *Arabidopsis* T-DNA-Insertionsmutante wurde während der Interaktion mit dem hemibiotrophen Pathogen *Pseudomonas syringae* pv. *tomato* (*Pst*) untersucht. Die AHK3-defiziente T-DNA Insertionsmutante zeigte eine verstärkte Suszeptibilität gegenüber *Pst*, die sich in schnellerer Entwicklung der Krankheitssymptome widerspiegelt. Dies wiederum deutet darauf hin, dass Cytokinine die Resistenz von *Arabidopsis* gegen *Pst* fördern. Interessanterweise zeigte die AHK3-defiziente T-DNA Insertionsmutante in Abwesenheit jeglicher Elicitoren eine konstitutive ROS-Produktion. Zusammengefasst unterstützen die Ergebnisse dieser Arbeit eine essentielle Funktion von Cytokininen in Pflanze-Pathogen-Interaktionen durch die Bestätigung, dass Cytokinine die pflanzliche Immunität beeinflussen.

7 References

Aiba, H., Nakasai, F., Mizushima, S. & Mizuno, T. (1989) Phosphorylation of a bacterial activator protein, OmpR, by a protein kinase, EnvZ, results in stimulation of its DNA-binding ability. *J. Biochem.* **106:**5-7.

Alex, L.A. & Simon, M.I. (1994) Protein histidine kinases and signal transduction in prokaryotes and eukaryotes. *Trends Genet.* **10:**133-138.

Alfonso, M., Perewoska, I., Constant, S. & Kirilovsky, D. (1999) Redox control of psbA expression in cyanobacterium *Synechocystis* strains. *J Photochem Photobiol B Biol.* **48:**104-113.

Alfonso, M., Perewoska, I. & Kirilovsky, D. (2000) Redox control of psbA gene expression in the cyanobacterium Synechocystis PCC 6803. Involvement of the cytochrome b(6)/f complex. *Plant Physiol.* **122:**505-516.

Allen, J.F., Sanders, C.E. & Holmes, N.G. (1985) Correlation of membrane protein phosphorylation with excitation energy distribution in the cyanobacterium *Synechococcus* 6301. *FEBS Lett.***193:**271-275.

Allen, J.F. (2003) Botany. State transitions-a question of balance. *Science* **299:** 1530-1532.

Amasino, R. (1955) Kinetin arrives: the 50th anniversary of a new plant hormone. *Plant Physiol.* **138**(3):1177-84.

Anantharaman, V. & Aravind, L. (2001) The CHASE domain: a predicted ligand-binding module in plant cytokinin receptors and other eukaryotic and bacterial receptors. *Trends Biochem Sci.* **26:**579–82.

Anders, K., von Stetten, D., Mailliet, J., Kiontke, S., Sineshchekov, V., Hildebrandt, P., Hughes, J. & Essen, L.O. (2011) Spectroscopic and photochemical characterization of the red-light sensitive photosensory module of CPH2 from *Synechocystis* PCC 6803. *Photochem Photobiol.* **87**:160-73.

Anderson, L. & McIntosh, L. (1991) Light-activated heterotrophic growth of the cyanobacterium *Synechocystis* sp. strain PCC 6803: a blue-light-requiring process. *J Bacteriol.* **173:**2761-2767.

Anderson, J.M., Chow, W.S. & Park, Y.I. (1995) The grand design of photosynthesis: acclimation of the photosynthetic apparatus to environmental cues. *Photosynth Res.* **46:**129-139.

Apel, K. & Hirt, H. (2004) Reactive oxygen species: metabolism, oxidative stress, and signal transduction. *Annu Rev Plant Biol.* **55:**373-399.

Appleby, J.L., Parkinson, J.S. & Bourret, R.B. (1996) Signal transduction via the multi-step phosphorelay: not necessarily a road less traveled. *Cell.* **86:**845-848.

Argueso, C., Ferreira, F. & Kieber, J. (2009) Environmental perception avenues: the interaction of cytokinin and environmental response pathways. *Plant Cell Environ.* **32:**1147-1160.

Argueso, C., Raines, T. & Kieber, J. (2010) Cytokinin signaling and transcriptional networks. *Curr Opin Plant Biol.* **13***:*533-539.

Argyros, R.D., Mathews, D.E., Chiang, Y.-H., Palmer, C.M., Thibault, D.M., Etheridge, N., Argyros, D.A., Mason, M.G., Kieber, J.J. & Schaller, G.E. (2008) Type B response regulators of *Arabidopsis* play key roles in cytokinin signaling and plant development. *Plant Cell.* **20:**2102-2116.

Ashby, A.M. (2000) Biotrophy and the cytokinin conundrum. *Physiol Mol Plant Pathol.* **57:**147-158.

Badger, M., Dean Price, G., Long, B. & Woodger, F. (2006) The environmental plasticity and ecological genomics of the cyanobacterial CO_2 concentrating mechanism. *J Exp Bot.* **57:**249-65.

Balibrea Lara, M.E., Gonzalez Garcia, M.C., Fatima, T., Ehneß, R., Lee, T.K., Proels, R., Tanner, W. & Roitsch, T. (2004) Extracellular invertase is an essential component of cytokinin-mediated delay of senescence. *Plant Cell.* **16:**1276-1287.

Barends, T.R.M., Hartmann, E., Griese, J., Beitlich, T., Kirienko, N.V., Ryjenkov, D.A., Reinstein, J., Shoeman, R.L., Gomelsky, M. & Schlichtung, I. (2009) Structure and mechanism of a bacterial light-regulated cyclic nucleotide phosphodiesterase. *Nature.* **459:**1015-1018.

Bari, J. & Jones, J.D.G. (2009) Role of plant hormones in plant defense responses. *Plant Mol Biol.* **69:**473-488.

Battchikova, N. & Aro, E.M. (2007) Cyanobacterial NDH-1 complexes: multiplicity in function and subunit composition. *Physiol Plant.* **131:**22-32.

Battchikova, N., Eisenhut, M. & Aro, E.M. (2010) Cyanobacterial NDH-1 complexes: Novel insights and remaining puzzles. *Biochim Biophys Acta.* **1807:**935-944.

Bhaya, D., Watanabe, N., Ogawa, T. & Grossman, A.R. (1999) The role of an alternative sigma factor in motility and pilus formation in the cyanobacterium *Synechocystis* sp. PCC 6803. *Proc Natl Acad Sci USA* **96**:3188-3193.

Bendall, D. & Manasse, R. (1995) Cyclic photophosphorylation and electron transport. *Biochim Biophys Acta* **1229:**23-38.

Bernát, G., Waschewski, N. & Rögner, M. (2009) Towards efficient hydrogen production: the impact of antenna size and external factors on electron transport dynamics in *Synechocystis* PCC 6803. *Photosynth Res.* **99:**205-216.

Bernroitner, M., Zamocky, M., Furtmüller, P.G., Peschek, G.A. & Obinger, C. (2009) Occurrence, phylogeny, structure, and function of catalases and peroxidases in cyanobacteria. *J Exp Bot.* **60:**423-440.

Berry, S., Schneider, D., Vermaas, W.F.J. & Rögner, M. (2002) Electron transport in whole cells of *Synechocystis* sp. strain PCC 6803: the role of the cytochrome *bd*-type oxidase. *Biochemistry* **41:** 3422-3429.

Bhoo, S.H., Davis, S.J., Walker, J., Karniol, B. & Vierstra, R.D. (2001) Bacteriophytochromes are photochromic histidine kinases using a biliverdin chromophore. *Nature* **414:**776-779.

Bishopp, A., Mähönen, A.P. & Helariutta, Y. (2006) Signs of change: hormone receptors that regulate plant development. *Development.* **133:**1857-1869.

Blumenstein, A., Vienken, K., Tasler, R., Purschwitz, J., Veith, D., Frankenberg-Dinkel, N. & Fischer, R. (2005) The *Aspergillus nidulans* phytochrome FphA represses sexual development in red light, *Curr Biol.* **15:**1833-1838.

Bonaventura, C. & Myers, J. (1969) Fluorescence and oxygen evolution from *Chlorella pyrrenoidosa. Biochim Biophys Acta* **189:**366-383.

Bourret, R.B. & Silversmith, R. (2010) Two-component signal transduction. *Curr Opin Microbiol.* **13:**113-115.

Bradford, M.M. (1976) A rapid and sensitive method for the quantitation of microgram quantities of protein utilizing the principle of protein-dye binding. *Anal Biochem.* **72:**248-254.

Braun, U., Cook, R.T.A., Imman, A.J. & Shin, H.D. (2002) The taxonomy of the powdery mildew fungi. In: The Powdery Mildews – A Comprehensive Treatise (Bélanger, R.R., Bushnell, W.R., Dik, A.J. and Carver, T.L.W. Eds.), St. Paul, Minnesota, pp. 13-55.

Bukhov, N. & Carpentier, R. (2004) Alternative photosystem I - driven electron transport routes: mechanisms and functions. *Photosynth Res.* **82:**17-33.

Butler, W.L., Norris, K.H., Siegelman, H.W. & Hendricks, S.B. (1959) Detection, assay, and preliminary purification of the pigment controlling photoresponsive development of plants. *Proc Natl Acad Sci USA* **45:**1703-1708.

Caesar, K., Thamm, A.M.K., Witthöft, J., Elgass, K., Huppenberger, P., Grefen, C., Horak, J. & Harter, K. (2011) Evidence for the localization of the *Arabidopsis* cytokinin receptors AHK3 and AHK4 in the endoplasmic reticulum. *J Exp Bot.* **62:**5571-5580.

Campbell, D., Hurry, V., Clarke, A. Gustafsson, P. & Öquist, G. (1998) Chlorophyll fluorescence analysis of cyanobacterial photosynthesis and acclimation. *Microbiol Mol Biol Rev.* **62:**667-683.

Chang, C. & Stewart, R.C. (1998) The two-component system: regulation of diverse signaling pathways in prokaryotes and eukaryotes. *Plant Physiol.* **117:**1043-1051.

Chen, Y.F., Randlett, M.D., Findell, J.L. & Schaller, G.E. (2002) Localization of the ethylene receptor ETR1 to the endoplasmic reticulum of *Arabidopsis. J Biol Chem.* **277:**19861-19866.

Chen, M. & Chory, J. (2011) Phytochrome signalling mechanisms and the control of plant development. *Trends Cell Biol.* **21:**664-671.

Cheng, X., Jiang, H., Zhang, J., Qian, Y., Zhu, S. & Cheng, B. (2010) Overexpression of type-A rice response regulators, OsRR3 and OsRR5, results in lower sensitivity to cytokinins. *Genet Mol Res.* **9:**348-359.

Choi, J., Huh, S.U., Kojima, M., Sakakibara, H., Paek, K.H. & Hwang, I. (2010) The cytokinin-activated transcription factor ARR2 promotes plant immunity via TGA3/NPR1-dependent salicylic acid signaling in *Arabidopsis. Dev Cell* **19:**284-295.

Choi, J., Choi, D., Lee, S., Ryu, C.M. & Hwang, I. (2011) Cytokinins and plant immunity: old foes or new friends? *Trends Plant Sci* **16:**388-394.

Chow, W.S., Melis, A. & Anderson, J.M. (1990) Adjustments of photosystem stoichiometry in chloroplasts improve the quantum efficiency of photosynthesis. *Proc Natl Acad Sci USA* **87:** 7502-7506.

Cooley, J.W., Howitt, C.A. & Vermaas, W.F.J. (2000) Succinate: quinol oxidoreductase in the cyanobacterium *Synechocystis* sp. strain PCC 6803: presence and function in metabolism and electron transport. *J Bacteriol.* **182:**714-722.

Cooley, J.W. & Vermaas, W.F.J. (2001) Succinate dehydrogenase and other respiratory pathways in thylakoid membranes of *Synechocystis* sp. strain PCC 6803: capacity comparisons and physiological function. *J Bacteriol.* **183**:4251-4258.

Cossar, J.D., Rowell, P. Stewart, W.D.P. (1984) Thioredoxin as a modulator of glucose-6-phosphate dehydrogenase in a N_2-fixing cyanobacterium. *J Gen Microbiol.* **130:** 991-998.

Costerton, J.W., Cheng, K.J., Geesey, G.G., Ladd, T.I., Nickel, J.G., Dasgupta, M. & Marrie, T.J. (1987) Bacterial biofilms in nature and disease. *Annu Rev Microbiol.* **41:**435-464.

Costerton, J.W., Lewandowski, Z., De Beer, D., Caldwell, D.E., Korber, D. & James, G. (1994) Biofilms, the customized microniche. *J Bacteriol.* **176:**2137-2142.

Cotter, P. & Stibitz, S. (2007) c-di-GMP-mediated regulation of virulence and biofilm formation. *Curr Opin Microbiol.***10:**17-23.

Crawford, N.A., Sutton, C.W., Yee, B.C., Johnson, T.C., Carlson, D.C. & Buchanan, B.B. (1984) Contrasting modes of photosynthetic enzyme regulation in oxygenic and anoxygenic prokaryotes. *Arch Microbiol.***139**:124-129.

Cyanobase (2012), www.genome.kazusa.or.jp/cyanobase.

Davis, S.J., Vener, A.V & Vierstra, R.D. (1999) Bacteriophytochromes: phytochrome-like photoreceptors from nonphotosynthetic eubacteria. *Science.* 286:2517-2520.

Dello Ioio, R., Linhares, F.S., Scacchi, E., Casamitjana-Martinez, E., Heidstra, R., Costantino, P. & Sabatini, S. (2007) Cytokinins determine *Arabidopsis* root-meristem size by controlling cell differentiation. *Curr Biol.* **17:**678-82.

Dello Ioio, R., Nakamura, K., Moubayidin, L., Perilli, S., Taniguchi, M., Morita, M.T., Aoyama, T., Costantino, P. & Sabatini, S. (2008) A genetic framework for the control of cell diviosn and differentiation in the root meristem. *Science.* **322:**1380-1384.

Dietzel, L., Brautigam, K. & Pfannschmidt, T. (2008) Photosynthetic acclimation: state transitions and adjustment of photosystem stoichiometry. Functional relationships between short-term and long-term light quality acclimation in plants. *FEBS J* **275:**1080-1088.

El Bissati, K. & Kirilovsky, D. (2001) Regulation of psbA and psaE expression by light quality in *Synechocystis* species PCC 6803. A redox control mechanism. *Plant Physiol.* **125:**1988-2000.

Elich, T.D. & Chory, J. (1997) Phytochrome: if it looks and smells like a histidine kinase, is it a histidine kinase? *Cell.* **91:**713-716.

Endo, T. (1997) Cytochrome b/f complex is not involved in respiration in the cyanobacterium *Synechocystis* PCC 6803 grown photoautotrophically. *Biosci Biotechnol Biochem.* **61:**1770-1771.

Fankhauser, C. (2001) The phytochromes, a family of red/far-red absorbing photoreceptors. *J Biol Chem.* **276:**1453-11456.

Ferreira, F.J. & Kieber, J.J. (2005) Cytokinin signaling. *Curr Opin Plant Biol.* **8:**518-525.

Fiedler, B., Broc, D., Schubert, H., Rediger, A., Börner, T. & Wilde, A. (2004) Involvement of cyanobacterial phytochromes in growth under different light qualities and quantities. *Photochem Photobiol.* **79:**551-555.

Fiedler, B., Börner, T. & Wilde, A. (2005) Phototaxis in the cyanobacterium *Synechocystis* sp. PCC 6803: role of different photoreceptors. *Photochem Photobiol.* **81:**1481-1488.

Finer, J.J., Vain, P., Jones, M.W. & McMullen, M.D. (1992) Development of the particle inflow gun for DNA delivery to plant cells. *Plant Cell Rep.* **11:**323-328.

Forchhammer, K. (2004) Global carbon/nitrogen control by PII signal transduction in cyanobacteria: from signals to targets. *FEMS Microbiol Rev* **28:**319-333.

Fork, D.C. & Herbert, S.K. (1993) Electron transport and photophosphorylation by Photosystem I *in vivo* in plants and cyanobacteria. *Photosynth Res.* **36:**149-168.

Franco-Zorrilla, J.M., Martin, A.C., Solano, R., Rubio, V., Leyva, A. & Paz-Ares, J. (2002) Mutations at CRE1 impair cytokinin-induced repression of phosphate starvation responses in *Arabidopsis. Plant J.* **32:**353-360.

Franco-Zorrilla, J.M., Martin, A.C., Leyva, A. & Paz-Ares, J. (2005) Interaction between phosphate-starvation, sugar, and cytokinin signaling in *Arabidopsis* and the roles of cytokinin receptors CRE1/AHK4 and AHK3. *Plant Physiol.* **138:**847-857.

Frébort, I., Kowalska, M., Hluska, T., Frébortová & Galuszka, P. (2011) Evolution of cytokinin biosynthesis and degradation. *J Exp Bot.* **62:**2431-2452.

Friml, J. & Jones, A.R. (2010) Endoplasmic reticulum: the rising compartment in auxin biology. *Plant Physiol.* **154:**458-462.

Fujita, Y. (1997) A study on the dynamic features of photosystem stoichiometry: accomplishments and problems for future studies. *Photosynth Res* **53:**83-93.

Furuya, M. (1993) Phytochromes: their molecular species, gene family and functions. *Annu Rev Plant Physiol Plant Mol Biol 44:*617-645.

Gajdosová, S., Spíchal, L., Kamínek, M., Hoyerová, K., Novák, O., Dobrev, P.I., Galuszka, P., Klíma, P., Gaudinová, A., Ziková, E., Hanus, J., Dancák, M., Trávnícek, B., Pesek, B., Krupicka, M., Vankóva, R., Strnad, M. & Motyka, V. (2010) Distribution, biological activities, metabolism, and the conceivable function of *cis*-zeatin-type cytokinins in plants. *J Exp Bot.* **62:**2827-2840.

Gan, S. & Amasino, R.M. (1995) Inhibition of leaf senescence by autoregulated production of cytokinin. *Science.* **270:**1986-1988.

Galperin, M.Y., Nikolskaya, A.N. & Koonin, E.V. (2001) Novel domains of the prokaryotic two-component signal transduction systems. *FEMS Microbiol Lett.* **203:** 11-21.

Galperin, M.Y. (2006) Structural classification of bacterial response regulators: diversity of output domains and domain combinations. *J Bacteriol.* **188:**4169-4182.

Galperin, M.Y. (2010) Diversity of structure and function of response regulator output domains. *Curr Opin Microbiol.* **13:**150-159.

Galuszka, P., Frébortová, J., Werner, T., Yamada, M., Strnad, M., Schmülling, T. & Frébort, I. (2004) Cytokinin oxidase/dehydrogenase genes in barley and wheat: cloning and heterologous expression. *Eur J Biochem*. **271:**3990-4002.

Gao, R. & Stock, A.M. (2009) Biological insights from structures of two-component proteins. *Annu Rev Microbiol.* **63:**133-154.

Geldner, N. & Robatzek, S. (2008) Plant receptors go endosomal: a moving view on signal transduction. *Plant Physiol.* **147:**1565-1574.

Giordano, M., Beardall, J. & Raven, J.A. (2005) CO_2 concentrating mechanisms in algae: Mechanisms, environmental modulation, and evolution. *Annu Rev Plant Biol* **56:**99-131.

Glazer, A.N. (1977) Structure and molecular organization of the photosynthetic accessory pigments of cyanobacteria and red algae. *Mol Cell Biochem*. **18:**125-140.

Gleason, F. (1996) Glucose-6-phosphate dehydrogenase from the cyanobacterium, *Anabaena* sp. PCC 7120: purification and kinetics of redox modulation. *Arch Biochem Biophys* **334:**277-283.

Goetz, M., Godt, D.E., Guivarch, A., Kahmann, U., Chriqui, D. & Roitsch, T. (2001) Induction of male sterility in plants by metabolic engineering of the carbohydrate supply. *Proc Natl Acad Sci USA.* **98:**6522-6527.

Golden, S.S. & Canales, S.R. (2003) Cyanobacterial circadian clocks-timing is everything. *Nat Rev Microbiol.* **1:**191-199.

Gomez-Baena, G., Lopez-Lozano, A., Gil-Martinez, J., Lucena, J.M., Diez, J., Candau, P., & Garcia-Fernandez, J.M. (2008) Glucose uptake and its effect on gene expression in *Prochlorococcus*. *PLoS ONE* **3:**e3416.

Goulian, M. (2010) Two-component signaling circuit structure and properties. *Curr Opin Microbiol.* **13:**184-189.

Grant, M. & Lamb, C. (2006) Systemic immunity. *Curr Opin Plant Biol* **9:**414-420.

Grigorieva, G. & Shestakov, S. (1982) Transformation in the cyanobacterium *Synechocystis* sp. 6803. *FEMS Microbiol Lett*. **13:**367-370.

Großkinsky, D.K., Naseem, M., Abdelmohsen, U.S., Plickert, N., Engelke, T., Griebel, T., Zeier, J., Novák, O., Strnad, M., Pfeifhofer, H., van der Graaf, E., Simon, U. & Roitsch, T. (2011) Cytokinins mediate resistance against *Pseudomonas syringae* in tobacco through increased antimicrobial phytoalexin synthesis independent of salicylic acid signaling. *Plant Physiol*. **157:**815-830.

Grossman, A.R., Schaefer, M.R., Chiang, G.G., & Collier, J.L. (1993) The phycobilisome, a light-harvesting complex responsive to environmental conditions. *Microbiol Rev*. **57:**725-749.

Gutierrez, R.A., Lejay, L.V., Dean, A., Chiaromonte, F., Shasha, D.E. & Coruzzi, G.M. (2007) Qualitative network models and genome-wide expression data define carbon/nitrogen-responsive molecular machines in *Arabidopsis. Genome Biol* **8:**R7.

Hagen, K.D. & Meeks, J.C. (2001) The unique cyanobacterial protein OpcA is an allosteric effector of glucose-6-phosphate dehydrogenase in *Nostoc punctiforme* ATCC 29133. *J Biol Chem* **276:**11477–11486.

Haimovich-Dayan, M., Kahlon, S., Hihara, Y., Hagemann, M., Ogawa, T., Ohad, I., Lieman-Hurwitz, J. & Kaplan, A. (2011) Cross talk between photomixotrophic growth and CO_2-concentrating mechanism in *Synechocystis* sp. strain PCC 6803. *Environ Microbiol.* **13:**1767-1777.

Hart, S.E., Schlarb-Ridley, B.G., Bendall, D.S. & Howe, C.J. (2005) Terminal oxidases of cyanobacteria. *Biochem Soc Trans.* **33:**832-835.

Hengge, R. (2009) Proteolysis of sigmaS (RpoS) and the general stress response in *Escherichia coli. Res Microbiol.* **160:**667-76.

Herbert, S., Martin, R.E. & Fork, D.C. (1995) Light adaptation of cyclic electron transport through photosystem I in the cyanobacterium *Synechococcus* sp. PCC7942. *Photosynth Res*. **46:**277-285.

Heyl, A. & Schmülling, T. (2003) Cytokinin signal perception and transduction. *Curr Op Plant Biol.* **6:**480-488.

Heyl, A., Werner, T. & Schmülling, T. (2006) Cytokinin metabolism and signal transduction. In *Plant Hormone signaling* Edited by: Hedden, P., Thomas, S. Oxford: Blackwell Publishing; 2006:93-123.

Heyl, A., Wulfetange, K., Pils, B., Nielsen, N., Romanov, G.A. & Schmülling, T. (2007) Evolutionary proteomics identifies amino acids essential for ligand-binding of the cytokinin receptor CHASE domain. *BMC Evol Biol.* **7:**62.

Herreiro, A. & Flores, E. (2008) The Cyanobacteria. Molecular Biology, Genomics and Evolution. Norfolk, UK. Caister Academic Press.

Higuchi, M., Pischke, M.S., Mähönen, A.P., Miyawaki, K., Hashimoto, Y., Seki, M., Kobayashi, M., Shinozaki, K., Kato, T., Tabata, S., Helariutta, Y., Sussmann, M.R. & Kakimoto, T. (2004) *In planta* functions of the *Arabidopsis* cytokinin receptor family. *PNAS.* **101:**8821-8826.

Hihara, Y., Kamei, A., Kanehisa, M., Kaplan, A. & Ikeuchi, M. (2003) DNA microarray analysis of redox-responsive genes in the genome of the cyanobacterium *Synechocystis* sp. strain PCC 6803. *J Bacteriol.* **185:**1719-1725.

Hirani, T.A., Suzuki, I., Murata, N., Hayashi, H. & Eaton-Rye, J.J. (2001) Characterization of a two-component signal transduction system involved in the induction of alkaline phosphatase under phosphate-limiting conditions in *Synechocystis* sp. PCC 6803. *Plant Mol Biol* **45:**133-144.

Hirose, N., Makita, N., Kojima, M., Kamada-Nobusada, T. & Sakakibara, H. (2007) Overexpression of a type-A response regulator alters rice morphology and cytokinin metabolism. *Plant Cell Physiol.* **48:**523-539.

Hirose, Y., Shimada, T., Narikawa, R., Katayama, M. & Ikeuchi, M. (2008) Cyanobacteriochrome CcaS is the green light receptor that induces the expression of phycobilisome linker protein. *Proc Natl Acad Sci.* **105:**9528- 9533.

Hirose, Y., Narikawa, R., Katayama, M. & Ikeuchi, M. (2010) Cyanobacteriochrome CcaS regulates phycoerythrin accumulation in *Nostoc punctiforme*, a group II chromatic adapter. *Proc Natl Acad Sci.* **107:**8854-8859.

Hsiao, H.Y., He, Q., Van Waasbergen, L.G. & Grossman, A.R. (2004) Control of photosynthetic and high-light-responsive genes by the histidine kinase DspA: negative and positive regulation and interactions between signal transduction pathways. *J Bacteriol* **186:**3882-3888.

Howitt, C.A., Cooley, J.W., Wiskich, J.T. & Vermaas, W.F. (2001) A strain of *Synechocystis* sp. PCC 6803 without photosynthetic oxygen evolution and respiratory oxygen consumption: implications for the study of cyclic photosynthetic electron transport. *Planta.* **214:**46-56.

Howitt, C.A. & Vermaas, W.F.J. (1998) Quinol and cytochrome oxidases in the cyanobacterium *Synechocystis* sp. PCC 6803. *Biochemistry* **37**:17944-17951.

Hughes, J., Lamparter, T., Mittmann, F., Hartmann, E., Girtner, W., Wilde A. & Börner, T. (1997) A prokaryotic phytochrome. *Nature.* **386:**663.

Hübschmann, T., Börner, T., Hartmann, E. & Lamparter, T. (2001) Characterization of the CphI holo-phytochrome from *Synechocystis* sp. PCC 6803. *Eur J Biochem.* **268:**2055-2063.

Hückelhoven, R., Dechert, C. & Kogel, K.-H. (2003) Overexpression of barley BAX inhibitor 1 induces breakdown of mlo-mediated penetration resistance to *Blumeria graminis. Proc Natl Acad Sci USA.* **100:**5555-5560.

Hückelhoven, R. (2007) Transport and secretion in plant-microbe interactions. *Curr Opin Plant Biol.* **10:**573-579.

Hunter, T. (1995) Protein kinases and phosphatases: the yin and yang of protein phosphorylation and signaling. *Cell.* **80**:225-236.

Hunter, T. & Plowman, G.D. (1997) The protein kinase s of budding yeast: six score and more. *Trends Biochem Sci.* **22:**18-22.

Hwang, I. & Sheen, J. (2001) Two-component circuitry in *Arabidopsis* cytokinin signal transduction. *Nature* **413:**383-389.

Hwang, D., Chen, H.C. & Sheen, J. (2002) Two-component signal transduction pathways in *Arabidopsis. Plant Physiol.* **129:**500-515.

Hwang, I. & Sakakibara, H. (2006) Cytokinin biosynthesis and perception. *Planta.***126:**528-538.

Hwang, I., Sheen, J. & Müller, B. (2012) Cytokinn signaling networks. *Annu Rev Plant Biol.* **63:**353-380.

Ikeuchi, M. & Ishizuka, T. (2008) Cyanobacteriochromes: A new superfamily of tetrapyrrole-binding photoreceptors in cyanobacteria. *Photochem Photobiol Sci.* **7:**1159-1167.

Inoue, T., Higuchi, M., Hashimoto, Y., Seki, M., Kobayashi, M. Kato, T. Tabata, S., Shinozaki, K. & Kakimoto, T. (2001) Identification of CRE1 as a cytokinin receptor from *Arabidopsis. Nature.* **409:**1060-1063.

Irani, N.G. & Russinova, E. (2009) Receptor endocytosis and signaling in plants. *Curr Opin Plant Biol.* **12:**653-659.

Ishida, K., Yamashino, T. & Mizuno, T. (2008) Expression of the cytokinin-induced type-A response regulator gene ARR9 is regulated by the circadian clock in *Arabidopsis thaliana. Biosci Biotechnol Biochem.* **72:**3025-3029.

Ishizuka, T., Shimada, T., Okajima, K., Yoshihara, S., Ochiai, Y., Katayama, M., & Ikeuchi, M. (2006) Characterization of cyanobacteriochrome TePixJ from a thermophilic cyanobacterium *Thermosynechococcus elongatus* strain BP-1. *Plant Cell Physiol.* **47:**1251-1261.

Ishizuka, T., Narikawa, R., Kohchi, T., Katayama, M. & Ikeuchi, M. (2007) Cyanobacteriochrome TePixJ of *Thermosynechococcus elongatus* harbors phycoviolobilin as a chromophore. *Plant Cell Physiol.* **48:**1385-1390.

Ishizuka, T., Kamlya, A., Suzuki, H., Narikawa, R., Noguchi, T., Inomata, K. & Ikeuchi, M. (2011) The cyanobacteriochrome, TePixJ, isomerizes its own chromophore by converting phycocyanobilin to phycoviolobilin. *Biochemistry.* **50:***953-961.*

Iwai, M., Takizawa, K., Tokutsu, R., Okamuro, A., Takahashi, Y. & Minagawa, J. (2010) Isolation of the elusive supercomplex that drives cyclic electron flow in photosynthesis. *Nature.* **464:**1210-1213.

Iwasaki, H., Williams, S.B., Kitayama, Y., Ishiura, M., Golden, S.S. & Kondo. T. (2000) A KaiC-interacting sensory histidine kinase, SasA, necessary to sustain robust circadian oscillation in cyanobacteria. *Cell.* **101:**223-233.

Jeanjean, R., Latifi, A., Matthijs, H.C.P. & Havaux, M. (2007) The PsaE subunit of photosystem I prevents light-induced formation of reduced oxygen species in the cyanobacterium *Synechocystis* sp. PCC 6803. *Biochim Biophys Acta.* **1777:**308-316.

Jenal, U. & Malone, J. (2006) Mechanisms of cyclic-di-GMP signaling in bacteria. *Annu Rev Genet.* **40:**385-407.

Jiang, Z.Y., Swem, L.R., Rushing, B.G., Devanathan, S., Tollin, G. & Bauer, C.E. (1999) Bacterial photoreceptor with similarity to photoactive yellow protein and plant phytochromes. *Science* **285:**406-409.

Joliot, P. & Joliot, A. (2006) Cyclic electron flow in C3 plants. *Biochim Biophys Acta* **1757:**362-368.

Joshua, S. & Mullineaux, C.W. (2004) Phycobilisome diffusion is required for light-state transitions in cyanobacteria. *Plant Physiol.***135:**2112-2119.

Jung, K., Fried, L., Behr, S. & Heermann, R. (2012) Histidine kinases and response regulators in networks. *Curr Opin Microbiol.* **15:**118-124.

Kahlon, S., Beeri, K., Ohkawa, H., Hihara, Y., Murik, O., Suzuki, I., Ogawa, T. & Kaplan, A. (2006) A putative sensor kinase, Hik31, is involved in the response of *Synechocystis* sp. PCC 6803 to the presence of glucose. *Microbiology.***152:**47-55.

Kakimoto, T. (2003) Biosynthesis of cytokinins. *J Plant Res* **116:**233-239.

Kamada-Nobusada, T. & Sakakibara, H. (2009) Molecular basis for cytokinin biosynthesis. *Phytochem.* **70:**444-449.

Kaneko, T., Sato, S., Kotani, H., Tanaka, A., Asamizu, E., Nakamura, Y., Miyajima, N., Hirosawa, M., Sugiura, M., Sasamoto, S., Kimura, T., Hosouchi, T., Matsuno, A., Muraki, A., Nakazaki, N., Naruo, K., Okumura, S., Shimpo, S., Takeuchi, C., Wada, T., Watanabe, A., Yamada, M., Yasuda, M. & Tabata, S. (1996) Sequence analysis of the genome of the unicellular cyanobacterium *Synechocystis* sp. strain PCC 6803. II. Sequence determination of the entire genome and assignment of potential protein-coding regions (supplement). *DNA Res.* **3:**109-136.

Kaneko, T., Nakamura, Y., Sasamoto, S., Watanabe, A., Kohara, M., Matsumoto, M., Shimpo, S., Yamada, M. & Tabata, S. (2003) Structural analysis of four large plasmids harboring in a unicellular cyanobacterium, *Synechocystis* sp. PCC 6803. *DNA Res.* **10:**221-228.

Kanesaki, Y., Yamamoto, H., Paithoonrangsarid, K., Shoumskaya, M., Suzuki, I., Hayashi, H. & Murata, N. (2007). Histidine kinases play important roles in the perception and signal transduction of hydrogen peroxide in the cyanobacterium, *Synechocystis* sp. PCC 6803. *Plant J.* **49:**313-324.

Kaplan, A. & Reinhold, L. (1999) The CO_2 concentrating mechanisms in photosynthetic microorganisms. *Annu Rev Plant Physiol Plant Mol Biol* **50:**539-570.

Kaplan, A., Hagemann, M., Bauwe, H., Kahlon, S. & Ogawa, T. (2008) Carbon acquisition by cyanobacteria: mechanisms, comparative genomics and evolution. In: Herrero A, Flores E (eds) The cyanobacteria: molecular biology, genomics and evolution, Caister Academic Press, Norfork, pp. 305–334.

Karniol, B. & Vierstra, R.D. (2003) The pair of bacteriophytochromes from *Agrobacterium tumefaciens* are histidine kinases with opposing photobiological properties. *Proc Natl Acad Sci USA.* **100:**2807-2812.

Karniol, B., Wagner, J.R., Walker, J.M. & Vierstra, R.D. (2005) Phylogenetic analysis of the phytochrome superfamily reveals distinct microbiol subfamilies of photoreceptors. *Biochem J.* **392:**103-116.

Kato, M., Mizuno, T., Shimizu, T. & Hakoshima, T. (1997) Insights into multistep phosphorelay from the crystal structure of the C-terminal HPt domain of ArcB. *Cell* **88:**717-723.

Keener, J. & Kustu, S. (1988) Protein kinase and phosphoprotein phosphatase activities of nitrogen regulatory proteins NTRB and NTRC of enteric bacteria: roles of the conserved amino-terminal domain of NTRC. *Proc Natl Acad Sci USA.* **85:**4976-4980.

Kehoe, D.M. & Grossman, R. (1996) Similarity of a chromatic adaptation sensor to phytochrome and ethylene receptors. *Science.* **273:**1409-1412.

Kieber, J.J. & Schaller, G.E. (2010) The perception of cytokinin: a story50 years in the making. *Plant Physiol.* **154***:*487-492.

Kim, J.H., Johannes, L., Goud, B., Antony, C., Lingwood, C.A., Daneman, R. & Grinstein, S. (1998) Noninvasive measurement of the pH of the endoplasmatic reticulum at rest and during calcium release. *Proc Natl Acad Sci USA.* **95:**2997-3002.

Kim, H.J., Ryu, H., Hong, S.H., Woo, H.R., Lim, P.O., Lee, I.C., Sheen, J., Nam, H.G. & Hwang, I. (2006) Cytokinin-mediated control of leaf longevity by AHK3 through phosphorylation of ARR2 in *Arabidopsis. PNAS*. **103:**814-819.

Knowles, V.L. & Plaxton, W.C. (2003) From genome to enzyme: analysis of key glycolytic and oxidative pentose-phosphate pathway enzymes in the cyanobacterium *Synechocystis* sp. PCC 6803. *Plant Cell Physiol.* **44:**758-763.

Knoop, H., Zilliges, Y., Lockau, W. & Steuer, R. (2010) The metabolic network of *Synechocystis* sp. PCC 6803: systemic properties of autotrophic growth. *Plant Physiol.* **154:**410-422.

Koksharova, O.A. (2009) Application of genetic tools to cyanobacterial biotechnology and ecology. In. Gault, P.M. & Marler, H.J. (Eds.) Handbook on cyanobacteria. Nova science Publishers, New York, USA, pp. 211-232.

Köllmer, I. (2009) Funktionelle Charakterisierung von CKX7 und cytokininregulierten Transkriptionsfaktorgenen in *Arabidopsis thaliana*. Doctoral thesis. Freie Universität Berlin, Berlin.

Kruger, N.J. & von Schaewen, A. (2003) The oxidative pentose phosphate pathway: structure and organization. *Curr Opin Plant Biol.* **6:**236-246.

Kufryk, G.I. & Vermaas, W.F.J. (2006) Sll1717 affects the redox state of the plastoquinone pool by modulating quinol oxidase activity in thylakoids. *J Bacteriol.* **188:**1286-1294.

Kurian, D., Jansèn, T. & Mäenpää, P. (2006) Proteomic analysis of heterotrophy in *Synechocystis* sp. PCC 6803. *Proteomincs.* **5:**1483-1494.

Lamb, C. & Dixon, R.A. (1997) The oxidative burst in plant disease resistance. *Annu. Rev. Plant Physiol. Plant Mol. Biol.* **48:**251-275.

Lamparter, J., Mittmann, F., Gärtner, W., Börner, T., Hartmann, E. & Hughes, J. (1997) Characterization of recombinant phytochrome from the cyanobacterium. *Synechocystis. Proc Natl Acad Sci USA* **94:**11792-11797.

Lamparter, T., Michael, N., Mittmann, F. & Esteban, B. (2002) Phytochrome from *Agrobacterium tumefaciens* has unusual spectral properties and reveals an N-terminal chromophore attachment site. *Proc Natl Acad Sci USA.* **99**:11628-11633.

Latifi, A., Ruiz, M. & Zhang, C.C. (2009) Oxidative stress in cyanobacteria. *FEMS Microbiol Rev.* **33:**258-278.

Laub, M.T. & Goulian, M. (2007) Specificity in two-component signal transduction pathways. *Annu Rev Genet.* **41:**121-145.

Lee, J.M., Ryu, J.Y., Kim, H.H., Choi, S.B., Tandeau de Marsac, N. & Park, Y.-I. (2005) Identification of a glucokinase that generates a major glucose phosphorylation activity in the cyanobacterium Synechocystis sp. PCC6803. *Mol Cells* **19:**256-261.

Lee, S., Ryu, J.Y., Kim, S.Y., Jeon, J.H., Song, J.Y, Cho, H.T., Choi, S.B., Choi, D., de Marsac, N.T, Park, Y.I. (2007) Transcriptional regulation of the respiratory genes in the cyanobacterium *Synechocystis* sp. PCC 6803 during the early response to glucose feeding. *Plant Physiol.* **145:**1018-1030.

Li, H. & Sherman, L.A. (2000) A redox-responsive regulator of photosynthesis gene expression in the cyanobacterium *Synechocystis* sp. strain PCC 6803. *J Bacteriol.* **182:**4268-4277.

Li, J., Yang, H., Peer, W.A., Richter, G., Blakeslee, J.J., Bandyopadhyay, A., Titapiwatanakun, B., Undurraga, S., Khodakovskaya, M., Richards, E.L., Krizek, B., Murphy, A.S., Gilroy, S. & Gaxiola, R. (2005) *Arabidopsis* H$^+$-PPase AVP1 regulates auxin-mediated organ development. *Science.* **310:**121-125.

Lois, A.F., Weinstein, M., Ditta, G.S. & Helinski, D.R. (1993) Autophosphorylation and phosphatase activities of the oxygen-sensing protein fixL of *Rhizobium meliloti* are coordinately regulated by oxygen. *J Biol Chem.* **268:**4370-4375.

Lomin, S.N., Yonekura-Sakakibara, K., Romanov, G.A. & Sakakibara, H. (2011) Ligand-binding properties and subcellular localization of maize cytokinin receptors. *J Exp Bot.* **62:**5149-5159.

Loomis, W.F., Shaulsky, G. & Wang, N. (1997) Histidine kinases in signal transduction pathways of eukaryotes. *J Cell Sci.* **110:**1141-1145.

Loomis, W.F., Kuspa, A. & Shaulsky, G. (1998) Two-component signal transduction systems in eukaryotic microorganisms. *Curr Opin Microbiol.* **1:**643-648.

Lopez-Carbonell, M., Moret, A. & Nadal, M. (1998) Changes in cell ultrastructure and zeatin riboside concentrations in *Hedera helix*, *Pelargonium zonale*, *Prunus avium*, and *Rubus ulmifolius* leaves infected by fungi. *Plant Dis.* **82:**914-918.

Los, D.A., Suzuki, I., Zinchenko, V.V. & Murata, N. (2008) Stress responses in *Synechocystis:* regulated genes and regulatory systems. In The Cyanobacteria:

Molecular Biology, Genomics and Evolution, pp. 117–157. Edited by A. Herrero & E. Flores. Norfolk: Caister Academic Press.

Ma, W.M. & Mi, H.L. (2008) Effect of exogenous glucose on the expression and activity of NADPH dehydrogenase complexes in the cyanobacterium *Synechocystis* sp. strain PCC 6803. *Plant Physiol Biochem.* **46:**775-779.

MacColl, R. (1998) Cyanobacterial phycobilisomes *J Struct Biol.* **124:**311-334.

Mähönen, A.P., Bonke, M., Kauppinen, L., Riikonen, M., Benfey, P.N. & Helariutta, Y. (2000) A novel two-component hybrid molecule regulates vascular morphogenesis of the *Arabidopsis* root. *Genes Dev.* **14:**2938-2943.

Mähönen, A.P., Higuchi, M., Tormakangas, K., Miyawaki, K., Pischke, M.S., Sussman, M.R., Helariutta, Y. & Kakimoto, T. (2006) Cytokinins regulate a bidirectional phosphorelay network in *Arabidopsis. Curr Biol.* **16:**1116-1122.

Manodori, A. & Melis, A. (1986) Cyanobacterial acclimation to photosystem I or photosystem II light. *Plant Physiol* **82:**185-189.

Mao, H.B., Li, G.F., Ruan, X., Wu, Q.Y., Gong, Y.D., Zhang, X.F., & Zhao, N.M. (2002) The redox state of plastoquinone pool regulates state transitions via cytochrome b_6f complex in *Synechocystis* sp. PCC 6803. *FEBS Lett*. **519:**82-86.

Margulis, L. (1970) Origin of eukaryotic cells. Yale University Press. New Haven, Conneticut.

Maruyama-Nakashita, A., Nakamura, Y., Yamaya, T. & Takahashi, H. (2004) A novel regulatory pathway of sulfate uptake in *Arabidopsis* roots: implication of CRE1/WOL/AHK4-mediated cytokinin-dependent regulation. *Plant J.* **38:**779-789.

Muramatsu, M. & Hihara, Y. (2012) Acclimation to high-light conditions in cyanobacteria: from gene espression to physiological responses. *J Plant Res.* **125:**11-39.

Mason, M.G., Mathews, D.E., Argyros, D.A., Maxwell, B.B., Kieber, J.J., Alonso, J.M., Ecker, J.R. & Schaller, G.E. (2005) Multiple type-B response regulators mediate cytokinin signal transduction in *Arabidopsis. Plant Cell.* **17:** 3007-3018.

Mathews, S. & Sharrock, R.A. (1997) Phytochrome gene diversity. *Plant Cell Environ.* **20:**666–671.

Maxwell, B.B. & Kieber, J.J. (2005) Cytokinin signal transduction. In Plant Hormones: Biosynthesis, Signal Transduction, Action! P.J. Davies, ed (Dordrecht, The Netherlands: Kluwer Academic Publishers), pp.321-349.

McConnell, M.D., Koop, R., Vasilev, S. & Bruce, D. (2002) Regulation of the distribution of chlorophyll and phycobilin-absorbed excitation energy in cyanobacteria. A structure-based model for the light state transition. *Plant Physiol* **130:**1201-1212.

McGinn, P.J., Price, G.D., Maleszka, R. & Badger, M.R. (2003) Inorganic carbon limitation and light control the expression of transcripts related to the CO_2-concentrating mechanism in the cyanobacterium *Synechocystis* sp. strain PCC6803. *Plant Physiol* **132:**218-229.

Mi, H., Endo, T., Schreiber, U., Ogawa, T. & Asada, K. (1992) Electron donation from cyclic and respiratory flow to the phytosynthetic intersystem chain is mediated by pyridine nucleotide dehydrogenase in the cyanobacterium *Synechocystis* PCC6803. *Plant Cell Physiol.* **33:**1233-1238.

Mi, H., Endo, T., Schreiber, U., Ogawa, T. & Asada, K. (1995) Thylakoid membrane-bound, NADPH-specific pyridine nucleotide dehydrogenase complex mediated cyclic electron transport in the cyanobacterium *Synechocystis* sp. PCC6803. *Plant Cell Physiol.* **36:**661-668.

Miyawaki, K., Tarkowski, P., Matsumoto-Kitano, M., Kato, T., Sato, S., Tarkowska, D., Tabata, S., Sandberg, G. & Kakimoto, T. (2006) Roles of *Arabidopsis* ATP/ADP isopentenyltransferases and tRNA isopentenyltransferases in cytokinin biosynthesis. *Proc Natl Acad Sci USA*. **103:**16598-16603.

Miller, C.O., Skoog, F., von Saltza, M.H. & Strong, F. (1955) Kinetin, a cell division factor from desoxyribonucleic acid. *J Am Chem Soc.* **77:**1392-1293.

Mikami, K., Kanesaki, Y., Suzuki, I. & Murata, N. (2002) The histidine kinase Hik33 perceives osmotic stress and cold stress in *Synechocystis* sp. PCC 6803. *Mol Microbiol.* **46:**905-915.

Min, H.T. & Golden, S.S. (2000) A new circadian class 2 gene, opcA, whose product is important for reductant production at night in *Synechococcus elongatus* PCC 7942. *J Bacteriol.* **182:**6214-6221.

Mizuno, T., Kaneko, T. & Tabata, S. (1996) Compilation of all genes encoding bacterial two-component signal transducers in the genome of the cyanobacterium, *Synechocystis* sp. strain PCC 6803. *DNA Res*. **3:**407-414.

Mizuno, T. (1997) Compilation of all genes encoding two-component phosphotransfer signal transducers in the genome of *Escherichia coli. DNA Res.* **4:**161-168.

Mizuno, T. (2004) Plant response regulators implicated in signal transduction and circadian rhythm. *Curr. Opin. Plant Biol.* **7:**499-505.

Mogi, T. & Miyoshi, H. (2009) Properties of cytochrome *bd* plastoquinol oxidase from the cyanobacterium *Synechocystis* sp. PCC 6803. *J Biochem.* **145:**3395-401.

Mok, M.C. (1994) Cytokinins and plant development-an overview. In Mok, D.W.S.& Mok, M.C., eds. (1994) Cytokinins-Chemistry, activity and function. Boca Raton: CRC Press, pp. 155-166.

Mok, D.W. & Mok, M.C. (2001) Cytokinin metabolism and action. *Annu Rev Plant Biol.* **52**:89-118.

Montgomery, B.L. & Lagarias, J.C. (2002) Phytochrome ancestry: sensors of bilins and light. *Trends Plant Sci.* **7:**357-366.

Montgomery, B.L. (2007) Sensing the light: photoreceptive systems and signal transduction in cyanobacteria. *Mol Microbiol.* **64:**16-27.

Moon, Y.J., Kim, S.Y., Jung, K.H., Choi, J.S., Park, Y.M. & Chung, Y.H. (2011) Cyanobacterial phytochrome CPH2 is a negative regulator in phototaxis towards UV-A. *FEBS Lett.* **585:**335-340.

Motyka, V., Faiss, M., Strand, M., Kaminek, M. & Schmülling, T. (1996) Changes in Cytokinin Content and Cytokinin Oxidase Activity in Response to Derepression of ipt Gene Transcription in Transgenic Tobacco Calli and Plants. *Plant Physiol.* **112:**1035-1043.

Mougel, C. & Zhulin, I.B. (2001) CHASE: an extracellular sensing domain common to transmembrane receptors from prokaryotes, lower eukaryotes and plants. *Trends Biochem Sci.* **26:**582-584.

Müller, B. (2011) Generic signal-specific responses: cytokinin and context-dependent cellular responses. *J Exp Bot.* **62:**3273-3288.

Müller, B. & Sheen, J. (2007) *Arabidopsis* cytokinin signaling pathway. *Sci STKE 2007.* **407:**cm4.

Mullineaux, C.W. & Allen, J.F. (1986) The state 2 transition in the cyanobacterium *Synechococcus* 6301 can be driven by respiratory electron flow into the plastoquinone pool. *FEBS Lett.* **205:**155-160.

Mullineaux, C.W. & Allen, F. (1990) State 1-State 2 transitions in the cyanobacterium *Synechococcus* 6301 are controlled by the redox state of electron carriers between photosystem I and II. *Photosynth Res.* **23:**297-311**.**

Mullineaux, C.W. (2008a) Phycobilisome-reaction centre interaction in cyanobacteria. *Photosynth Res*. **95:**175-182.

Mullineaux, C.W. (2008b) Biogenesis and dynamics of thylakoid membranes and the photosynthetic apparatus. The Cyanobacteria (Herrero A & Flores E, eds), pp. 289–304. *Caister Academic Press, Norfolk, UK*.

Munekage, Y., Hashimoto, M., Miyake, C., Tomizawa, K., Endo, T., Tasaka, M., & Shikanai, T. (2004) Cyclic electron flow around photosystem I is essential for photosynthesis. *Nature.* **429:**579-582.

Munekage, Y. & Shikanai, T. (2005) Cyclic electron transport though photosystem I. *Plant Biotechnol.* **22:**361-369.

Murata, N. (1969) Control of excitation transfer in photosynthesis. I. Light-induced change of chlorophyll a fluorescence in *Porphyridium cruentum*. *Biochim Biophys Acta* **172:**242-251.

Murata, N. & Suzuki, I. (2006) Exploitation of genomic sequences in a systematic analysis to access how cyanobacteria sense environmental stress. *J Exp Bot.* **57:**235-247. Epub 2005 Nov 29.

Murphy, A.M., Pryce-Jones, E., Johnstone, K. & Ashby, A.M. (1997) Comparison of cytokinin production *in vitro* by *Pyrenopeziza brassicae* with other plant pathogens. *Physiol Mol Plant Pathol*. **50:** 53-65.

Nagatani, A. (2010) Phytochrome: structural basis for its function. *Curr Opin Plant Biol.* **13:**565-570.

Nakamura, Y., Kaneko, T. & Tabata, S. (2000) CyanoBase, the genome database for *Synechohcystis* sp. strain PCC6803: status for the year 2000. *Nucleic Acids Res*. 28:72.

Nakamura, Y., Takahashi, J., Sakurai, A., Inaba, Y., Suzuki, E., Nihei, S., Fujiwara, S., Tsuzuki, M., Miyashita, H., Ikemoto, H., Kawachi, M., Sekiguchi, H. & Kurano, N. (2005) Some Cyanobacteria synthesize semi-amylopectin type alpha-polyglucans instead of glycogen. *Plant Cell Physiol*. **46:**539-545.

Nakao, M., Okamoto, S., Kohara, M., Fujishiro, T., Fujisawa, T., Sato, S., Tabata, S., Kaneko, T. & Nakamura, Y. (2010) CyanoBase: the cyanobacteria genome database update 2010. *Nucleic Acids Res.* **38:**2009-2011.

Narikawa, R., Fukushima, Y., Ishizuka, T., Itoh, S. & Ikeuchi, M. (2008) A novel photoactive GAF domain of cyanobacteriochrome AnPixJ shows reversible green/red photoconversion. *J Mol Biol.* **380:**844-855.

Nickelsen, J., Rengstl, B., Stengel, A., Schottkowski, M., Soll, J. & Ankele, E. (2010) Biogenesis of the cyanobacterial thylakoid membrane system-an update. *FEMS Microbiol Lett.* **315:**1-5.

Nishimura, C., Ohashi, Y., Sato, S., Kato, T., Tabata, S. & Ueguchi, C. (2004) Histidine kinase homologs that act as cytokinin receptors possess overlapping functions in the regulation of shoot and root growth in *Arabidopsis. Plant Cell.* **16:**1365-1377.

Ogawa, T. & Mi, H. (2007) Cyanobacterial NADPH dehydrogenase complexes. *Photosynth Res.* **93:**69-77.

Okhawa, H., Dean Price, G., Badger, M. R. & Ogawa, T., (2000) Mutation of *ndh* genes leads to inhibition of CO_2 uptake rather than HCO_3^- uptake in *Synechocystis* sp. strain PCC 6803. *J Bacteriol.* **182**:2591-2596.

Osanai, T., Kanesaki, Y., Nakano, T., Takahashi, H., Asayama, M., Shirai, M., Kanehisa. M., Suzuki, I., Murata, N. & Tanaka, K. (2005) Positive regulation of sugar catabolic pathways in the cyanobacterium *Synechocystis* sp. PCC 6803 by the group 2 sigma factor sigE. *J Biol Chem.* **280:**30653-30659.

Osanai, T., Azuma, M. & Tanaka, K. (2007) Sugar catabolism regulated by light- and nitrogen-status in the cyanobacterium *Synechocystis* sp. PCC 6803. *Photochem Photobiol Sci.* **6:**508-514.

Paget, M.S.B. & Helmann, J.D. (2003) The r70 family of sigma factors, *Genome Biol.* **4:**203.

Paithoonrangsarid, K., Shoumskaya, M.A., Kanesaki, Y., Satoh, S., Tabata, S., Los, D.A., Zinchenko, V.V., Hayashi, H., Tanticharoen, M., Suzuki, I. & Murata, N. (2004) Five histidine kinases perceive osmotic stress and regulate distinct sets of genes in *Synechocystis. J Biol Chem*. **279:**53078-53086.

Pakrasi, H.B. (1995) Genetic analysis of the form and function of photosystem I and photosystem II. *Annu Rev Genet*. **29:**755-776.

Panstruga, R. (2004) Establishing compatibility between plants and obligate biotrophic pathogens. *Curr Opin Plant Biol.* **6:**320-326.

Park, C.M., Kim, J.I., Yang, S.S., Kang, J.G., Kang, J.H., Shim, J.Y., Chung, Y.H., Park, Y.M. & Song, P.S. (2000) A second photochromic bacteriophytochrome from *Synechocystis* sp. PCC 6803: spectral analysis and down-regulation by light. *Biochemistry* **39:**10840-10847.

Parkinson, J.S. & Kofoid, E.C. (1992) Communication modules in bacterial signaling proteins. *Annu Rev Genet.* **26:**71-112.

Pearce, J., Leach, C.K. & Carr, N.G. (1969) The incomplete tricarboxylic acid cycle in the blue-green alga *Anabaena variabilis. J Gen Microbiol.* **55:** 371-378.

Pelroy, R.A., Kirk, M.R. & Bassham, J.A. (1976) Photosystem II regulation of macromolecule synthesis in the blue-green alga *Aphanocapsa* 6714. *J Bacteriol* **128:**623-632.

Pérez-Pérez, M.E., Mata-Cabana, A., Sánchez-Riego, A.M., Lindahl, M. & Florencio, F.J. (2009) A comprehensive analysis of the peroxiredoxin reduction system in the cyanobacterium *Synechocystis* sp. PCC 6803 reveals that all five peroxiredoxins are thioredoxin dependent. *J Bacteriol.* **191:**7477-7489.

Perilli, S., Moubayidin, L. & Sabatini, S. (2010) The molecular basis of cytokinin function. *Curr Opin Plant Biol.* **13:**21-26.

Perry, J., Koteva, K. & Wright, G. (2011) Receptor domains of two-component signal transduction systems. *Mol Biosyst.* **7:**1388-1398.

Pesavento, C. & Hengge, R. (2009) Bacterial nucleotide-based second messengers. *Curr Opin Microbiol.* **12:**170-176.

Pertry, I. Václavíková, K., Depuydt, S., Galuszka, P., Spíchal, L., Temmermann, W., Stes, E., Schmülling, T. Kakimoto, T., Van Montagu, M.C., Strnad, M., Holsters, M., Tarkowski, P. & Vereecke, D. (2009) Identification of *Rhodococcus fascians* cytokinins and their modus operandi to reshape the plant. *Proc Natl Acad Sci USA.* **106:**929-934.

Pfannschmidt, T., Nilsson, A. & Allen, J.F. (1999) Photosynthetic control of chloroplast gene expression. *Nature.* **397:**625-628.

Pils, D. & Schmetterer, G. (2001) Characterization of three bioenergetically active respiratory terminal oxidases in the cyanobacterium *Synechocystis* sp. strain PCC 6803. *FEMS Microbiol Lett.* **203:**217-222.

Pils, D. & Heyl, A. (2009) Unraveling the evolution of cytokinin signaling. *Plant Physiol.* **151:**782-791.

Plaxton, W.C. & Podesta, F.E. (2006) The functional organization and control of plant respiration. *Crit Rev Plant Sci.* **25:**159-198.

Plowman, G.D., Sudarsanam, S., Bingham, J., Whyte, D. & Hunter, T. (1999) The protein kinases of *Caenorhabditis elegans*: a model for signal transduction in multicellular organisms. *Proc Natl Acad Sci USA.* **96:**13603-13610.

Preiss, J. (1984) Bacterial glycogen synthesis and its regulation. *Annu. Rev. Microbiol.* **38:**419-458.

Preiss, J. & Sivak, M.N. (1998a) Biochemistry, molecular biology and regulation of starch synthesis. *Genet Eng.* **20:**177-223.

Preiss, J. & Sivak, M.N. (1998b) Starch and glycogen biosynthesis. In: Pinto BM (ed) Comprehensive natural products chemistry. Pergamon, Oxford, pp. 441–495.

Price, G.D., Badger, M.R., Woodger, F.J. & Long, B.M. (2008) Advances in understanding the cyanobacterial CO2-concentrating-mechanism (CCM): functional components, Ci transporters, diversity, genetic regulation and prospects for engineering into plants. *J Exp Bot.* **59:**1441-1461.

Punwani, J.A., Hutchison, C.E., Schaller, G.E. & Kieber, J.J. (2010) The subcellular distribution of the *Arabidopsis* histidine phosphotransfer proteins is independent of cytokinin signaling. *Plant J.* **62:**473-482.

Quail, P.H. (1994) Photosensory perception and signal transduction in plants. *Curr Opin Genet Dev*. **4:**652-661.

Quail, P.H., Boylan, M.T., Parks, B.M., Short, T.W., Xu, Y. & Wagner, D. (1995) Phytochromes: photosensory perception and signal transduction. *Science.* **268:**675-680.

Quail, P.H. (1997) An emerging molecular map of the phytochromes. *Plant Cell Environ.* **20:**657-665.

Quail, P.H. (2002) Phytochrome photosensory networks. *Nat Rev Mol Cell Biol.* **14:**180-188.

Reiser, V., Raitt, D.C. & Saito, H. (2003) Yeast osmosensor Sln1 and plant cytokinin receptor Cre1 respond to changes in turgor pressure. *J Cell Biol.* **161:**1035-1040.

Riefler, M., Novak, O., Strnad, M. & Schmülling, T. (2006) *Arabidopsis* cytokinin receptor mutants reveal functions in shoot growth, leaf senescence, seed size, germination, root development and cytokinin metabolism. *Plant Cell.* **18:**40-54.

Rippka, R., Deruelles, J., Waterbury, J.B., Herdman, M. & Stanier, R.Y. (1979) Generic assignments, strain histories and properties of pure cultures of cyanobacteria. *Journal of General Microbiology.* **111:**1-61.

Robert-Seilaniantz, A., Navarro, L., Bari, R. & Jones, J.D. (2007) Pathological hormone imbalances. *Curr Opin Plant Biol.* **10:**372-379.

Robinson, V.L., Buckler, D.R. & Stock, A.M. (2000) A tale of two components: a novel kinase and a regulatory switch. *Nat Struct Biol.* **7:**626-633.

Rockwell, N.C., Su, Y.S. & Lagarias, J.C. (2006) Phytochrome structure and signaling mechanisms. *Annu Rev Plant Biol.* **57:**837-858.

Rockwell, N.C., Njuguna, S.L., Roberts, L., Castillo, E., Parson, V.L., Dwojak, S., Lagarias, J.C. & Spiller, S.C. (2008) A second conserved GAF-domain cysteine is required for the blue/green photoreversibility of cyanobacteriochrome Tlr0924 from *Thermosynechococcus elongatus. Biochemistry.* **47:**7304-7316.

Rockwell, N.C., Shang, L., Martin, S.S. & Lagarias, J.C. (2009) Distinct classes of red/far-red photochemistry within the phytochrome superfamily. *Proc Natl Acad Sci USA.* **106:**6123-6127.

Rockwell, N.C. & Lagarias, J.C. (2010) A brief history of phytochromes. *Chemphyschem.* **11:**1172-1180.

Rockwell, N.C., Martin, S.S., Feoktistova, K. & Lagarias, J.C. (2011) Diverse two-cysteine photocycles in phytochromes and cyanobacteriochromes. *Proc Natl Acad Sci.* **108:**11854-11859.

Roitsch, T. (1999) Source-sink regulation by sugars and stress. *Curr Opin Plant Biol.* **2:**198-206.

Roitsch, T., Balibrea Lara, M.E., Hofmann, M., Proels, R. & Sinha, A.K. (2003) Extracellular invertase: key metabolic enzyme and PR protein. *J Exp Bot.* **54:**513-524.

Romanov, G.A., Spichal, L., Lomin, S.N., Strnad, M. & Schmülling, T. (2005) A live cell hormone-binding assay on transgenic bacteria expressing a eukaryotic receptor protein. *Anal Biochem.* **347:**129-13.

Romanov, G.A., Lomin, S.N. & Schmülling, T. (2006) Biochemical characteristics and ligand-binding properties of *Arabidopsis* cytokinin receptor AHK3 compared to CRE/AHK4 as revealed by a direct binding assay. *J Exp Bot.* **57:**4051-4058.

Römling, U., Gomelsky, M. & Galperin, M.Y. (2005) C-di-GMP: The dawning of a novel bacterial signalling system. *Mol Microbiol.* **57:**629-639.

Rumeau, D., Peltier, G. & Cournac, L. (2007) Chlororespiration and cyclic electron flow around PSI during photosynthesis and plant stress response. *Plant Cell Environ.* **30:**1041-1051.

Ryan, R.P., Fouhy, Y., Lucey, J.F. & Dow, J.M. (2006) Cyclic Di-GMP signaling in bacteria: recent advances and new puzzles. *J Bacteriol.* **188:**8327-8334.

Ryu, J.Y., Suh, K.H., Chung, Y.H., Park, Y.M., Chow, W.S. & Park, Y.I. (2003) Cytochrome *c* oxidase of the cyanobacterium *Synechocystis* sp. PCC 6803 protects photosynthesis from salt stress. *Mol Cells.* **16:**74-77.

Ryu, J.Y., Song, J.Y., Lee, J.M., Jeong, S.W., Chow, W.S., Choi, S.B., Pogson, B.J. & Park, Y.I. (2004) Glucose-induced expression of carotenoid biosynthesis genes in the dark is mediated by cytosolic pH in the cyanobacterium *Synechocystis* sp. PCC 6803. *J Biol Chem.* **279:** 25320-25325.

Sakai, H., Honma, T., Aoyama, T., Sato, S., Kato, T., Tabata, S. & Oka, A. (2001) *Arabidopsis* ARR1 is a transcription factor for genes immediately responsive to cytokinins. *Science.* **294:**1519-1521.

Sakakibara, H. (2006) Cytokinins: activity, biosynthesis, and translocation. *Annu Rev Plant Biol.* **57:**431-449.

Sambrook, J., Fritsch, E.F. & Maniatis, T. (1989) Molecular cloning: a laboratory manual. 2nd ed. Cold Spring Harbor Laboratory Press, Cold Spring Harbor, N.Y.

Savakis, P., De Causmaecker, S., Angerer, V., Ruppert, U., Anders, K., Essen, L.-O. & Wilde, A. (2012) Light-induced alteration of c-di-GMP level controls motility in *Synechocystis* sp. PCC 6803. *Mol Microbiol.* **85:**239-251.

Schaeffer, F. & Stanier, R.Y. (1978) Glucose-6-phosphate dehydrogenase of *Anabaena* sp. Kinetic and molecular properties. *Arch Microbiol.* **116**:9-19.

Schaller, G.E., Ladd, A.N., Lanahan, M.B., Spanbauer, J.M. & Bleecker, A.B. (1995) The ethylene response mediator ETR1 from Arabidopsis forms a disulfide-linked dimer. *J Biol Chem*. **270:**12526-12530.

Schaller, G.E., Matthews, D.E., Gribskov, M. & Walker, J.C. (2002) Two-component signaling elements and hystidyl-aspaartyl phosphorelays. The *Arabidopsis* Book (C.Somerville, E.Meyerowitz, editors), 1-9.

Schaller, G.E., Kieber, J. & Shiu, S.H. (2008) Two-component signaling elements and histidyl-aspartyl phosphorelays. In The Arabidopsis Book, C. Somerville and E. Meyerowitz, eds. (Rockville, MD: American Society of Plant Biologists), DOI10.1199/tab.0086.

Schaller, E., Shiu, S.H. & Armitage, J.P. (2011) Two-component systems and their co-option for eukaryotic signal transduction. *Curr Biol.* **21:**320-330.

Scheibe, R., Backhausen, J.E., Emmerlich, V. & Holtgrefe, S. (2005) Strategies to maintain redox homeostasis during photosynthesis under changing conditions. *J Exp Bot.* **56:**1481-1489.

Scherer, S., Stürzl, E. & Böger, P. (1982) Interaction of respiratory and photosynthetic electron transport in *Anabaena variabilis. Kütz Arch Microbiol.* **132:**333-337.

Schirmer, T. & Jenal, U. (2009) Structural and mechanistic determinants of c-di-GMP signalling. *Nat Rev Microbiol.* **7:**724-735.

Schmülling, T., Werner, T., Riefler, M., Krupková, E. & Bartryna y Manns, I. (2003) Structure and function of cytokinin oxidase/dehydrogenase genes of maize, rice, *Arabidopsis* and other species. *J Plant Res.* **116:**241-252.

Schopf, J.W. (1993) Microfossils of the early archean apex chert: new evidence of the life antiquity. *Science.* **260:** 640-646.

Schweizer, P., Pokorny, J., Abderhalden, O. & Dudler, R. (1999) A transient assay system for the functional assessment of defense-related genes in wheat. *Mol Plant-Microbe Interact.* **12:**647-654.

Selivankina, S.Y., Zubkova, N.K., Kupriyanova, E.V., Lyukevich, T.V., Kusnetsov, V.V., Los, D.A. & Kulaeva, O.N. (2006) Cyanobacteria respond to cytokinin. *Russian Journal of Plant Physiology.* **53:**751-755.

Sharrock, R.A. (2008) The phytochrome red/far-red photoreceptor superfamily. *Genome Biol.* **9:**230.

Shastri, A.A. & Morgan, J.A. (2005) Flux balance analysis of photoautotrophic metabolism. *Biotechnol Prog.* **21:**1617-1626.

Shastri, A.A. & Morgan, J.A. (2007) A transient isotopic labeling methodology for C-13 metabolic flux analysis of photoautotrophic microorganisms. *Phytochemistry.* **68:**2302-2312.

Shi, L., Bischoff, K.M. & Kennelly, P.J. (1999) The icfG gene cluster of *Synechocystis* sp. strain PCC 6803 encodes an Rsb/Spo-like protein kinase, protein phosphatase, and two phosphoproteins. *J Bacteriol.* **181:**4761-4767.

Shi, X & Rashotte, A.M. (2012) Advances in upstream players of cytokinin phosphorelay: receptors and histidine phosphotransfer proteins. *Plant Cell Rep.* **31:**789-799.

Shikanai, T. (2007) Cyclic electron transport around photosystem I: genetic approaches. *Annu Rev Plant Biol.* **58:**199-217.

Shoumskaya, M.A., Paithoonrangsarid, K., Kanesaki, Y., Los, D.A., Zinchenko, V.V., Tanticharoen, M., Suzuki, I. & Murata, N. (2005) Identical Hik–Rre systems are involved in perception and transduction of salt signals and hyperosmotic signals but regulate the expression of individual genes to different extents in *Synechocystis. J Biol Chem.* **280:**21531-21538.

Singh, A.K., Hong, L. & Sherman, L.A. (2004) Microarray analysis and redox control of gene expression in the cyanobacterium *Synechocystis* sp. PCC 6803. *Physiol Plant.* **120:**27-35.

Singh, A.K. & Sherman, L.A. (2005) Pleiotropic effect of a histidine kinase on carbohydrate metabolism in *Synechocystis* sp. strain PCC 6803 and its requirement for heterotrophic growth. *J Bacteriol* **187:**2368-2376.

Singh, A.K., Elvitiglia, T., Bhattacharyya-Pakrasi, M., Aurora, R., Gosh, B. & Pakrasi, H.B. (2008) Integration of carbon and nitrogen metabolism with energy production is crucial to light acclimation in the cyanobacterium *Synechocystis. Plant Phys.* **148:**467-478.

Singh, A.K., Bhattacharyya-Pakrasi, M., Elvitiglia, T., Gosh, B., Aurora, R. & Pakrasi, H.B. (2009) A systems-level analysis of the effects of light quality on the metabolism of a cyanobacterium. *Plant Physiol.* **151:**1596-1608.

Singh, A.K., Elvitigala, T., Cameron, J.C., Gosh, B.K., Bhattacharyya-Pakrasi, M. & Pakrasi, H.B. (2010) Integrative analysis of large scale expression profiles reveals core transcriptional response and coordination between multiple cellular processes in a cyanobacterium. *BMC Syst Biol.* **4:**105.

Schirmer, T. & Jenal, U. (2009) Structural and mechanistic determinants of c-di-GMP signalling. *Nat Rev Microbiol.* **7:**724-735.

Schmetterer, G. (1994) Cyanobacterial respiration, p. 409-435. *In* D.A. Bryant (ed.), The molecular biology of cyanobacteria. Kluwer, Boston, Mass.

Schneegurt, M. A., Sherman, D. M., Nayar, S. & Sherman L. A. (1994) Oscillating behavior of carbohydrate granule formation and dinitrogen fixation in the cyanobacterium *Cyanothece* sp. strain ATCC 51142. *J Bacteriol.* **176:**1586-1597.

Schneider-Poetsch, H.A.W. (1992) Signal transduction by phytochrome: phytochromes have a module related to the transmitter modules of bacterial sensor proteins. *Photochem Photobiol.* **56:**839-846.

Smith, H. (1994) Phytochrome transgenics: functional, ecological and biotechnological applications. *Semin Cell Biol.* **5:**315-325.

Smith, H. (2000) Phytochromes and light signal perception by plants-an emerging synthesis. *Nature.* **407:**585-591.

Spíchal, L., Rakova, N.Y., Riefler, M., Romanov, G.A., Strnad, M. & Schmülling, T. (2004) Two cytokinin receptors of *Arabidopsis thaliana*, CRE1/AHK4 and AHK3, differ in their ligand specificity in a bacterial assay. *Plant Cell Physiol.* **45:**1299-1305.

Stal, L. & Moezelaar, R. (1997) Fermentation in cyanobacteria. *FEMS Microbiol. Rev.* **21:**179-211.

Stanier, R.Y., Kunisawa, R., Mandel, M. & Cohen-Bazire, G. (1971) Purification and properties of unicellular blue-green algae (order Chroococcales). *Bacterial Rev*. **35:**171-205.

Stanier, R.Y. & Cohen-Bazire, G. (1977) Phototrophic prokaryotes: the cyanobacteria. *Ann Rev Microbiol.* **31:**225-274.

Stock, J.B., Ninfa, A.J. & Stock, A.M. (1989) Protein phosphorylation and regulation of adaptive responses in bacteria. *Microbiol Rev.* **53:**450-490.

Stock, J.B., Surette, M.G., Levit, M. & Park, P. (1995) In Two-component signal transduction (eds, Hoch, J.A. & Silhavy, T.J.), 25–51 (American Society for Microbiology, Washington, DC).

Stock, A.M. (1999) A nonlinear stimulus-response relation in bacterial chemotaxis. *Proc Natl Acad Sci USA*. **96:**10945-10947.

Stock, A.M., Robinson, V.L. & Goudreau, P.N. (2000) Two-component signal transduction. *Annu Rev Biochem.* **69:**183-215.

Stock, J. & Da Re, S. (2000) Signal transduction: response regulators on and off. *Curr Biol.* **10:**420-424.

Stolz, A., Riefler, M., Lomin, S.N., Achazi, K., Romanov, G.A. & Schmülling, T. (2011) The specificity of cytokinin signalling in *Arabidopsis thaliana* is mediated by differing ligand affinities and expression profiles of the receptors. *Plant J.* **67:**157-168.

Summerfield, T.C., Nagarajan, S. & Sherman, L.A. (2011) Gene expression under low-oxygen conditions in the cyanobacterium *Synechocystis* sp. PCC 6803 demonstrates Hik31-dependent and -independent responses. *Microbiology.* **157:**301-312.

Sundaram, S., Karakaya, H., Scanlan, D.J. & Mann, N.H. (1998) Multiple oligomeric forms of glucose-6-phosphate dehydrogenase in cyanobacteria and the role of OpcA in the assembly process. *Microbiology.* **144:**1549-1556.

Suzuki, I., Los, D.A. & Murata, N. (2000) Perception and transduction of low-temperature signals to induce desaturation of fatty acids. *Biochem Soc Trans.* **28:**628-630.

Suzuki, T., Miwa, K., Ishikawa, K., Yamada, H., Aiba, H. & Mizuno, T. (2001) The *Arabidopsis* sensor His-kinase, AHK4, can respond to cytokinins. *Plant Cell Physiol.* **42:**107-113.

Suzuki, I., Kanesaki, Y., Hayashi, H., Hall, J. J., Simon, W. J., Slabas, A. R. & Murata, N. (2005). The histidine kinase Hik34 is involved in thermotolerance by regulating the expression of heat shock genes in *Synechocystis. Plant Physiol.* **138:** 1409-1421.

Suzuki, E., Okhawa, H., Moriya, K., Matsubara, T., Nagaike, Y., Iwasaki, I., Fujiwara, S., Tsuzuki, M. & Nakamura, Y. (2010) Carbohydrate metabolism in mutants of the cyanobacterium *Synechococcus elongatus* PCC 7942 defective in glycogen synthesis. *Appl Environ Microbiol.* **76:**3153-3159.

Tabei, Y., Okada, K., Makita, N. & Tsuzuki, M. (2009) Light-induced gene expression of fructose 1,6-bisphosphate aldolase during heterotrophic growth in a cyanobacterium *Synechocystis* sp. PCC 6803. *FEBS J.* **276:**187-198.

Takahashi, H., Uchimiya, H. & Hihara, Y. (2008) Difference in metabolite levels between photoautotrophic and photomixotrophic cultures of *Synechocystis* sp. PCC 6803 examined by capillary electrophoresis electrospray ionization mass spectrometry. *J Exp Bot.* **59:**3009-3018.

Takei, K., Sakakibara, H., Sugiyama, T. (2001) Identification of genes encoding adenylate isopentenyltransferase, a cytokinin biosynthesis enzyme, in *Arabidopsis thaliana. J Biol Chem*. **276:**26405-26410.

Tamayo, R., Pratt, J.T. & Camilli, A. (2007) Roles of cyclic diguanylate in the regulation of bacterial pathogenesis. *Annu Rev Microbiol.* **61:**131-148.

Tang, G.Q., Lüscher, M. & Sturm, A. (1999) Antisense repression and vacuolar and cell wall invertase in transgenic carrot alters early plant development and sucrose partitioning. *Plant Cell.* **11:**1-14.

Tamayo, R., Pratt, J.T. & Camilli, A. (2007) Roles of cyclic diguanylate in the regulation of bacterial pathogenesis. *Annu Rev Microbiol*. **61:**131-148.

Tanaka, Y., S. Katada, H. Ishikawa, T. Ogawa, & Takabe, T. (1997) Electron flow from NAD(P)H dehydrogenase to photosystem I is required for adaptation to salt shock in the cyanobacterium *Synechocystis* sp. PCC6803. *Plant Cell Phy*siol. **38:**1311-1318.

Terauchi, K., Montgomery, B.L., Grossman, A.R., Lagarias, J.C. & Kehoe, D.M. (2004) RcaE is a complementary chromatic adaptation photoreceptor required for green and red light responsiveness. *Mol Microbiol.* **51:** 567-577.

Tichy, M. & Vermaas, W. (1999) In vivo role of catalase-peroxidase in *Synechocystis* sp. strain PCC 6803. *J Bacteriol*. **181:**1875-1882.

Tischler, A.D. & Camilli, A. (2004) Cyclic diguanylate (c-di-GMP) regulates *Vibrio cholerae* biofilm formation. *Mol Microbiol.* **53:**857-869.

To, J.P.C., Haberer, G., Ferreira, F.J. Deruère, J., Mason, M.G., Schaller, G.E., Alonso, J.M., Ecker, J.R. & Kieber, J.J. (2004) Type-A ARRs are partially redundant negative regulators of cytokinin signaling in *Arabidopsis. Plant Cell*. **16:**658-671.

To, J.P., Deruère, J., Maxwell, B.B., Morris, V.F., Hutchison, C.E., Ferreira, F.J., Schaller, G.E. & Kieber, J.J. (2007) Cytokinin regulates type-A *Arabidopsis* Response Regulator activity and protein stability via two-component phosphorelay. *Plant Cell.* **19:**3901-3914.

To, J.P.C & Kieber, J.J. (2008) Cytokinin signaling: two-components and more. *Trends Plant Sci.* **13:**85-92.

Torres, M.A. (2010) ROS in biotic interactions. *Physiologia Plantarum.* **138:**414-429.

Tsai, Y.-C., Weir, N.R., Hill, K., Zhang, W., Kim, H.J., Shiu, S.-H., Schaller, G.E. & Kieber, J.J. (2012) Characterization of genes involved in cytokinin signaling and metabolism from rice. *Plant Phys.* **158:**1666-1684.

Tsunoyama, Y., Bernát, G., Dyczmons, N., Schneider, D. & Rögner, M. (2009) Multiple Rieske proteins enable short-and long-term light adaptation of *Synechocystis* sp. PCC 6803. *J Biol Chem.* **284:**27875-277883.

Tu, C.J., Shrager, J., Burnap, R.L., Postier, B.L. & Grossman, A.R. (2004) Consequences of a deletion in *dspA* on transcript accumulation in *Synechocystis* sp. strain PCC 6803. *J Bacteriol*. **186:**3889-3902.

Udvardy, J., Borbely, G., Juhasz, A., & Farkas, G.L. (1984) Thioredoxins and the redox modulation of glucose-6-phosphate dehydrogenase in *Anabaena* sp. strain PCC 7120 vegetative cells and heterocysts. *J Bacteriol.* **157:**681-683.

Ueguchi, C., Sato, S., Kato, T. & Tabata, S. (2001) The *AHK4* gene involved in the cytokinin-signaling pathway as a direct receptor molecule in *Arabidopsis thaliana*. *Plant Cell Physiol.* **42:**751-755.

Ulrich, L.E. & Zhulin, I.B. (2009) The MiST2 database: a comprehensive genomics resource on microbial signal transduction. *Nucleic Acids Res.* **38:**D401-D407.

Ulijasz, A.T., Cornilescu, G., von Stetten, D., Cornilescu, C.C., Velazquez Escobar, F., Zhang, J., Stankey, R.J., Rivera, M., Hildebrandt, P. & Vierstra, R.D. (2009) Cyanochromes are blue/green light photoreversible photoreceptors defined by a stable double cysteine linkage to a phycoviolobilin-type chromophore. *J Biol Chem*. **284:**29757-29772.

Ulijasz, A.T. & Vierstra, R.D. (2011) Phytochrome structure and photochemistry: recent advances toward a complete molecular picture. *Curr Opin Plant Biol.* **14:**498-506.

van den Hoek, C., Jahns, H.M. & Mann, D.G. (1993) Algen. Georg Thieme Verlag, Stuttgart, London.

van Thor, J.J., Hellingwerf, K.J. & Matthijs, H.C. (1998) Characterization and transcriptional regulation of the *Synechocystis* PCC 6803 petH gene, encoding ferredoxin-NADP+ oxidoreductase: involvement of a novel type of divergent operator. *Plant Mol Biol.* **36:**353-363.

Vermaas, W.F.J, Shen, G. & Styring, S. (1994) Electrons generated by photosystem II are utilised by an oxidase in the absence of photosystem I in the cyanobacterium *Synechocystis* sp. PCC 6803. *FEBS Letters.* **337:**103-108.

Vermaas, W.F. (2001) Photosynthesis and respiration in cyanobacteria. In: Encyclopedia of Life Sciences. Nature Publishing Group, London, p. 1-7.

Vioque, A. (1992) Analysis of the gene encoding the RNA subunit of ribonuclease P from cyanobacteria. *Nucleic Acids Res*. **20:**6331-6337.

Wadhams, G.H. & Armitage, J.P. (2004) Making sense o fit all: bacterial chemotaxis. *Nat Rev Mol Cell Biol.* **5:**1024-37.

Walters, D.R. & McRoberts, N. (2006) Plants and cytokinins: a pivotal role for cytokinins? *Trends Plant Sci.* **11:**5981-586.

Walters, D.R., McRoberts, N. & Fitt, B.D. (2008) Are green islands red herrings? Significance of green islands in plant interactions with pathogens and pests. *Biol Rev Camb Philos Soc.* **83:**79-102.

Wang, R., Okamoto, M., Xing, X. & Crawford, N.M. (2003) Microarray analysis of the nitrate response in *Arabidopsis* roots and shoots reveals over 1,000 rapidly responding genes and new linkages to glucose, trehalose-6-phosphate, iron, and sulfate metabolism. *Plant Physiol.* **132:**556-567.

Werner, T., Motyka, V., Laucou, V., Smets, R,, Van Onckelen, H. & Schmülling, T. (2003) Cytokinin-deficient transgenic *Arabidopsis* plants show multiple developmental alterations indicating opposite functions of cytokinins in the regulation of shoot and root meristem activity. *Plant Cell*. **15:**2532-2550.

Werner, T. & Schmülling, T. (2009) Cytokinin action in plant development. *Curr Opin Plant Biol.* **12:**527-538.

Wilde, A., Churin, Y., Schubert, H. & Börner T. (1997) Disruption of a *Synechocystis* sp. PCC 6803 gene with partial similarity to phytochrome genes alters growth under changing light qualities. *FEBS Lett.* **406**:89-92.

Wilde, A., Fiedler, B. & Börner, T. (2002) The cyanobacterial phytochrome Cph2 inhibits phototaxis towards blue light. *Mol Microbiol.* **44:**981-988.

Williams, J.G.K. (1988) Construction of Specific Mutation in Photosystem II Photosynthetic Reaction Center by Genetic Engineering Methods in *Synechocystis* 6803. *Methods in Enzymology*. **167:**766-778.

Whitton, B.A. & Potts, M. (2000) Introduction to the cyanobacteria. In: The Ecology of Cyanobacteria: Their Diversity in Time and Space. Whitton, B.A.; Potts, M. (ed.) Kluwer Academic Publishers, Dordrecht, London, Boston p. 1-11.

Wollman, F.A. (2001) State transitions reveal the dynamics and flexibility of the photosynthetic apparatus. *EMBOJ.* **20:**3623-3630.

Wood, A.P., Aurikko, J.P. & Kelly, D.P. (2004) A challenge for 21st century molecular biology and biochemistry: what are the causes of obligate autotrophy and methanotrophy? *FEMS Microbiol Rev.* **28:**335.

Wu, S.H. & Lagarias, J.C. (2000) Defining the bilin lyase domain: lessons from the extended phytochrome superfamily. *Biochemistry* **39:**13487-13495.

Wuichet, K., Cantwell, B.J. & Zhulin, I.B. (2010) Evolution and phyletic distribution of two-component signal transduction systems. *Curr Opin Microbiol.* **13:**219-225.

Wulfetange, K., Lomin, S.N., Romanov, G.A., Stolz, A., Heyl, A. & Schmülling, T. (2011a) The cytokinin receptors of *Arabidopsis thaliana* are locating mainly to the endoplasmatic reticulum. *Plant Physiol.* **156:**1808-1818.

Wulfetange, K., Saenger, W., Schmülling, T. & Heyl, A. (2011b) Cell-free expression, purification and characterization of the membrane-bound ligand-binding CHASE-TM domain of the cytokinin receptor CRE1/AHK4 of *Arabidopsis thaliana*. *Mol Biotechnol.* **47:**211-219.

Wurgler-Murphy, S.M. & Saito, H. (1997) Two-component signal transducers and MAPK cascades. *Trends Biochem Sci.* **22:**172-176.

Wurgler-Murphy, S.M., Maeda, T., Witten, E.A. & Saito, H. (1997) Regulation of the *Saccharomyces cerevisiae* HOG mitogen-activated protein kinase by the PTP2 and PTP3 protein tyrosine phosphatases. *Mol Cell Biol.* **17:**1289-1297.

Yamada, H., Suzuki, T., Terada, K., Takei, K., Ishikawa, K., Miwa, K., Yamashino, T. & Mizuno, T. (2001) The *Arabidopsis* AHK4 histidine kinase is a cytokinin binding receptor that transduces cytokinin signals across the membrane. *Plant Cell Physiol.* **42:**1017-1023.

Yan, H. & Chen, W. (2010) 3',5'-cyclic diguanylic acid: a small nucleotide that makes big impacts. *Chem Soc Rev.* **39:**2914-2924.

Yang, C., Hua, Q. & Shimizu, K. (2002) Metabolic flux analysis in *Synechocystis* using isotope distribution from ^{13}C-labeled glucose. *Metab Eng.* **4:**202-216.

Yeh, K. C., Wu, S.H., Murphy J. T. & Lagarias, J. C. (1997) A cyanobacterial phytochrome two-component light sensory system. *Science.* **277:**1505-1508.

Yeh, K.C. & Lagarias, J.C. (1998) Eukaryotic phytochromes: light-regulated serine/threonine protein kinases with histidine kinase ancestry. *Proc Natl Acad Sci USA.* **95:**13976-13981.

Yoshihara, S., Katayama, M., Geng, X. & Ikeuchi, M. (2004) Cyanobacterial phytochrome-like PixJ1 holoprotein shows novel reversible photoconversion between blue- and green-absorbing forms. *Plant Cell Physiol.* **45:**1729-1737.

Zhang, C.C. (1996) Bacterial signalling involving eukaryotic-type protein kinases. *Mol Microbiol.* **20:**9-15.

Zhang, S. & Bryant, D.A. (2011) The tricarboxylic acid cycle in cyanobacteria. *Science.* **334:**1551-1553.

Zhou, F., Zhang, Z., Gregersen, P.L., Mikkelsen, J.D., de Nergaard, E., Collinge, D.B. & Thordal-Christensen, H. (1998) Molecular characterization of the oxalate oxidase involved in the response of barley to the powdery mildew fungus. *Plant Physiol.* 117:33-41.
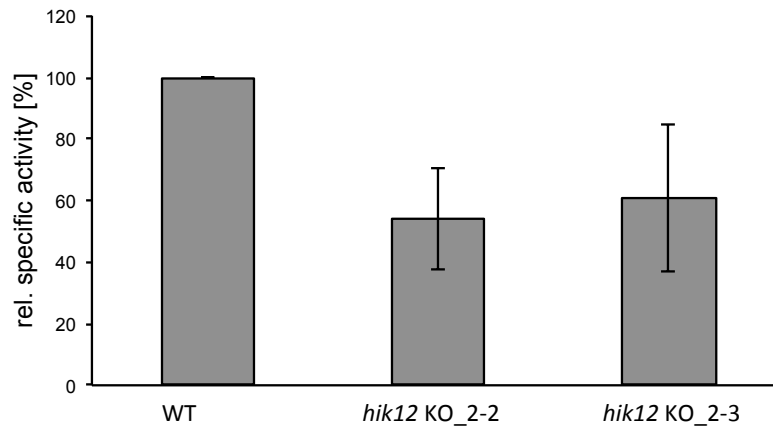
8 Supplement
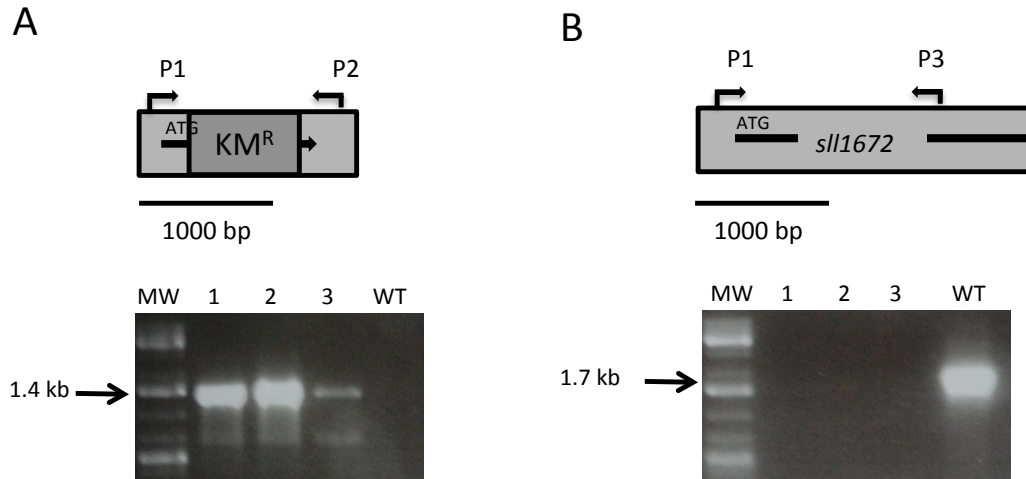
Supplementary figure 1: Verification of genomic integration of the kanamycine (KM[R]) resistance cassette in 3 transformants (designated 1, 2, 3) by PCR on genomic DNA.

A) Schematic illustration of *hik12* KO construct. Primer P1 (Hik12 KO Check fw_1241)/P2 (Hik12 KO Check rev_1242) bind within the flanking regions of *hik12* (*sll1672*), amplifying parts of the flanking regions and the inserted KM[R] (estimated fragment size: 1396 bp, black arrow).

B) Schematic illustration of wildtype *hik12* (*sll1672*). Primer P1 (Hik12 KO Check fw_1241, also used in A), primer P3 (Hik12 SDM-2) binds within *hik12* ORF (estimated fragment size in WT: 1744 bp, black arrow). MW, molecular mass standard.

Supplementary figure 2: Specific G6PDH activity in WT and *hik12 _2* KO mutants under photomixotrophic/biomatforming growth conditions.

Photoautotrophically grown, mid-exponential cell cultures (OD_{750} = 0.6-0.8) of WT and hik12_2 KO mutants (clone 2-2 and clone 2-3) were supplied with glucose at a final concentration of 10 mM and incubated without agitation for 96 h, 28°C, under continuous illumination with a light intensity of 20 µmol photons m^{-2} s^{-1}. 100 µg of crude protein were used in a total volume of 1 ml assay solution to determine G6PDH activity. Data are normalized to the WT (0.051 ± 0.001 U/µg protein, set as 100% for each individual experiment). Columns represent average values of 3 independent experiments. Bars represent standard errors.
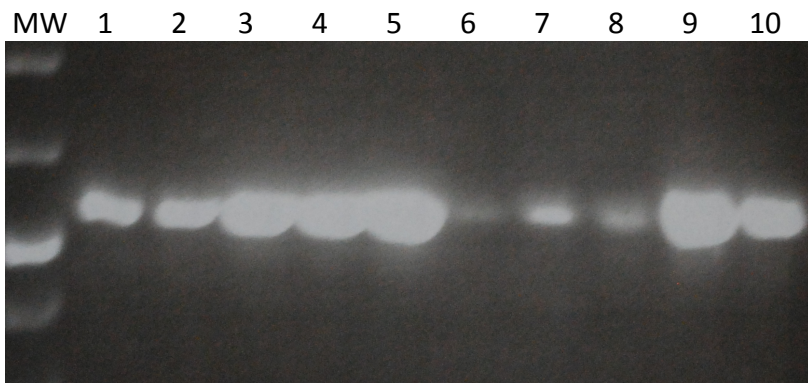
Supplementary figure 3: PCR-based verification of T-DNA insertion in AHK3-T-DNA insertion plants.

To verify the T-DNA insertion in AHK3-T-DNA insertion plants, genomic DNA was isolated as described in 2.1.1. To detect the presence of the T-DNA insertion in 10 transgenic AHK3-T-DNA insertion line plants (designated 1-10), a T-DNA-insert-specific primer (T-DNA, stocknumber: 356) and a genomic reverse primer (AHK3-7 rev, stocknumber: 907) were used for PCR. Primer sequences are given in Table 2. Estimated fragment size: 550 bp. MW, molecular mass standard.